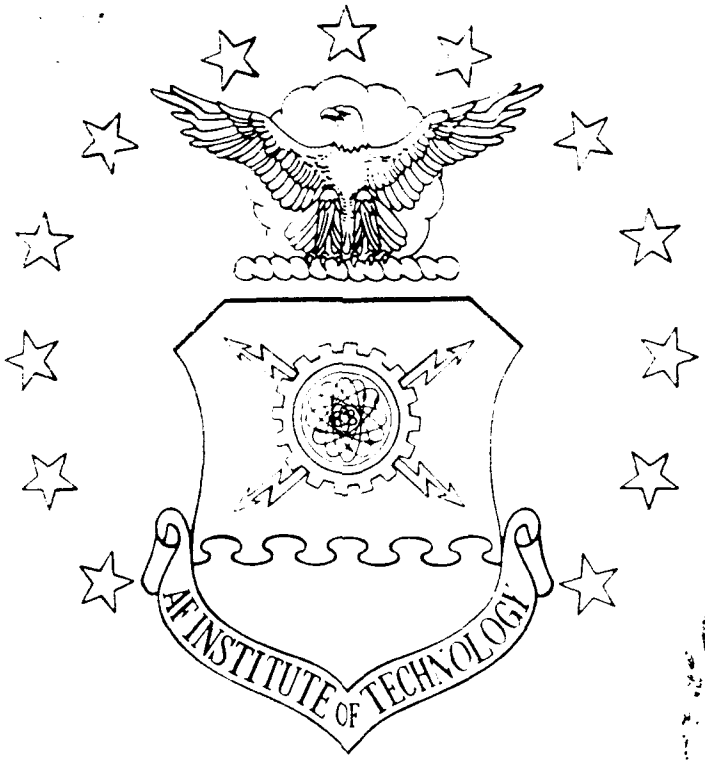

DYNAMIC ANALYSIS OF A COMBAT AIRCRAFT WITH CONTROL SURFACE FAILURE

Thesis

Captain Marc Roy
AFIT/GAE/ENY/90D-24

DEPARTMENT OF THE AIR FORCE
AIR UNIVERSITY
AIR FORCE INSTITUTE OF TECHNOLOGY

Wright-Patterson Air Force Base, Ohio

AFIT/GAE/ENY/90D-24

(1)

DYNAMIC ANALYSIS OF A COMBAT AIRCRAFT WITH CONTROL SURFACE FAILURE

Thesis
Captain Marc Roy
AFIT/GAE/ENY/90D-24

Approved for Public Release;Distribution unlimited

AFIT/GAE/ENY/90D-24

DYNAMIC ANALYSIS OF A COMBAT AIRCRAFT WITH CONTROL SURFACE FAILURE

Thesis

Presented to the Faculty of the School of Engineering

of the Air Force Institute of Technology

Air University

in Partial Fulfillment of the Requirements for the Degree of

Master of Science in Aeronautical Engineering

By

Marc Roy, B.S.

Captain, Canadian Armed Forces

November, 1990

ACKNOWLEDGMENTS

In completing the work associated with this thesis, there are several people who deserve thanks for providing guidance and expertise.

First to my committee. Thanks to Dr Spenney who provided me with the initial background to start with this research. Many thanks to Captain Ridgeley who provided me with the necessary background to perform the work related to the aircraft controller. I appreciated your input and support.

To my advisor, Major Mracek, I thank you for taking an active interest in this problem and encouraging me. I will always remember our discussion about transforming stability derivatives from one frame of reference to another. Please accept my thanks.

A mes deux garcons, Jean-Philippe et Marc-Antoine, j'aimerais vous remercier pour avoir su me faire rire et m'apporter beaucoup d'amour durand les moments difficiles.

A mon epouse Solange; Sans ta patience, ton amour et tes mots d'encouragements je n'aurais pu finir cette these. Je ne sais comment te remercier pour tout ce que tu as fait pour moi. J'espere qu'un jour je pourrais en faire autant pour toi. Merci encore cherie, je t'aime.

Marc Roy

DYNAMIC ANALYSIS OF COMBAT AIRCRAFT WITH CONTROL SURFACR FAILURE

Table of Contents

List of Figures

List of Tables

ABSTRACT

In this thesis, an investigation was performed to analyze the dynamic stability characteristic of an aircraft which has sustained damage to a primary control surface. The analysis was performed using the existing functional form of actual wind tunnel data taken on a F-16 model. Two control schemes are used for trimming an F-16 that has sustained damaged to its rudder. The First control scheme represent the basic aircraft, while the second allowed the Horizontal Tail Ailerons to move independently from the Flaperons.

The investigation was conducted for one flight condition representative of the aircraft at cruise speed. Region in α/β space where trim can be achieved was selected as input into a linearized aircraft model. This model took into account the failed control surface. The eigenvalues of the open and closed loop models were analyzed to determine the region in α/β space where the aircraft was dynamically stable. The migration of the eigenvalues for several trim conditions was also investigated to gain some insight on the aircraft behavior while in an unsymmetrical orientation.

For this study, the open loop eigenvalues for the trim area investigated gave a stable system. When the aircraft controller was added into the system, regions of dynamic instability appeared. For Rudder Failure less than -20

degrees, trim could be achieved but the aircraft was dynamically unstable.

DYNAMIC ANALYSIS OF COMBAT AIRCRAFT WITH CONTROL SURFACE FAILURE

I. INTRODUCTION

In modern high performance aircraft, Flight Control Systems (FCS) are critical in achieving the performance levels and operational utility required. Also, new designs which increase the performance make the aircraft more dependent on the FCS for stabilization. If a control surface is damaged or not operational, the control laws designed for the healthy aircraft cease to be valid since any signal going to the damaged control surface will be ignored. Studies showed that the FCS contributed up to 20% of the aircraft losses in combat [1:1]. The principal reasons were the physical damage, the loss of function, or seriously degraded flying qualities.

In recent years, several methods have been examined to address the problem of damaged or failed control surfaces. The development of techniques, like restructuring the FCS, to restore control may have major implications in aircraft flight safety , sortie generation in a combat environment, in reliability and maintainability, and in saving the pilot's life and the aircraft. Before considering applying any of these techniques, we must understand the dynamics of

the aircraft and evaluate whether stabilization is possible.

Problem Definition

If a control surface is damaged or inoperable, several negative effects will be encountered. First, any input going to the damaged control surface will be ignored. The FCS will have to rely on the other surfaces to control the aircraft attitude. Second, the coupling effect between the longitudinal and lateral modes of the aircraft may not be negligible. For example, if the rudder fails and is locked into a position other then zero, the aircraft is likely to experience unwanted lateral force as well as yaw.
The questions that arise when a control surface becomes inoperable are: could we maintain the aircraft in an equilibrium or trimmed state, and is the aircraft dynamically stable? Depending on the flight condition, many newer types of combat aircraft have to rely on the FCS to provide dynamic stability even in a trimmed state.

This research will deal with the latter question and will attempt to provide a better understanding of the problem and the means available to address it.

Previous Work

Eslinger [2] investigated a failure of the AFTI/F-16 right horizontal tail with all other surfaces operational.

The failed surface was left free floating. His model utilized constant aerodynamic derivatives at the selected flight conditions. In order to restructure the control laws for both the healthy and damaged aircraft, he used the multivariable design technique developed by Professor Porter. As he noted [1], the left horizontal tail assumes primary pitch control while the other surfaces deflect to counter the rolling and yawing moments produced by the left horizontal tail deflection. Weiss et al, [3], developed and solved an automatic trim problem for restructurable aircraft control. In their paper, the failure is treated as a disturbance from desired steady-state outputs. Using the observable part of those disturbances that exist after a control surface failure, they feed forward a control solution which is a function of the desired steady-state output and the observed disturbance. They also noted [3:405], that the most challenging single element failure is a stuck rudder since it is used extensively for damping the dutch roll mode, and little side force can be produced by the other control surfaces.

Thural, [4], conducted wind tunnel experiment to investigate the effect of various types of control surface failures on the aircraft stability derivatives. He conducted his test on a one-twentieth scale model F-16 in the AFIT five foot wind tunnel. He collected data for three different configurations, where each represented a potential failure

type. The data was collected by varying each control surface individually for a given angle of attack (α) and sideslip angle (β). Therefore, the data includes information about the coupling of the static aerodynamic stability derivatives. His experimental setup did not permit him to collect data for dynamic stability derivatives.

In 1989, Zaiser, [5], reduced the data collected by Thural for one particular failure. He employed a least square curve fitting technique to develop polynomial functions which describe the aircraft static stability derivatives. After deriving the equilibrium equations for rectilinear flight in terms of the static stability derivatives, he analyzed the impact of an actuator failure of the rudder for the F-16 aircraft. He also investigated different control implementations which allowed for greater independence of movement among the undamaged control surfaces. Region in the α/β space where equilibrium was achievable were investigated at two different flight conditions.

At the conclusion of his thesis, Zaiser made several recommendations for follow-on work, [5:66]. He stated that a dynamic analysis should be performed to evaluate how the aircraft would respond if trimmed in an unsymmetrical orientation.

Purpose

This research will investigate the dynamic stability characteristic of an F-16 aircraft that has sustained damage to its rudder actuator. Static aerodynamic coupling that results from unsymmetrical trim orientation will be included in deriving a linear state-space model of the aircraft. For a given flight condition, several trimmed conditions will be investigated for dynamic stability. The impact of the failure will also be investigated for the current aircraft control laws.

Approach

To accomplish the stated purposes of this research, specific tasks are accomplished and presented in the different sections of this thesis. The force and moment coefficients that Capt Zaiser reduced into functional form are used in conjunction with the equilibrium equations to find a trim condition for a specific control implementation. The static stability derivatives are linearized for each static equilibrium condition and included in the aircraft plant model.

The linearized equations of motion are derived and analyzed to relate the impact that the different stability derivatives have on the model. As Weiss pointed out, [5:405], the actuator failure of the rudder is assumed to be the most significant single primary control failure. This is

taken into account, and the actual control laws of the F-16 aircraft are modified.

Presentation

The analysis performed in this thesis is presented in the following chapters. Chapter II gives an overview of how the equilibrium regions are obtained for the different control implementations assumed. The derivation of the linearized equations of motion and the formulation of the F-16 plant will be included in Chapter III. Chapter IV will look at the dynamic stability of the aircraft for the different trimmed conditions. The results of this analysis are presented and discussed in Chapter V and Chapter VI contains a summary of the results of this research and recommendations for further study.

II. TRIM DETERMINATION

Introduction

The analysis performed in this thesis is based on data obtained by Zaiser, [5], in his Master's thesis in 1989. In this chapter, a short description of the F-16 is given along with a discussion of the results obtained by Zaiser. More specific trim conditions are also evaluated using techniques similar to those employed by Zaiser.

Aircraft Description

The F-16 is a single engine, low aspect ratio fighter aircraft currently in service with several countries. Seven control surfaces are employed on the aircraft. All seven control surfaces are of interest in this research. The location of each control surface can be found by referring to Appendix A.

The primary function of the Leading Edge Flaps (LEFs) is to vary the camber of the wing as the angle of attack (α) increases. This causes C_{Lmax} to occur at higher α, thus providing more lift. They are designed to deflect symmetrically and their deflection is scheduled as a function of α and Mach number. Therefore, the pilot has no direct control authority on their deflection.

The Flaperons (FLs) are used to provide both lift and

rolling moment. Below a specific dynamic pressure ($\bar{q}$), the FLs act as flaps to provide lift. Otherwise, they act as ailerons which are controlled by the pilot to provide rolling moment.

The Horizontal Tails (HTs) are employed as elevators to provide a pitching moment commanded by the pilot. The HTs also deflect asymmetrically to augment the rolling moment, and their deflection is scheduled as a function of altitude, $\bar{q}$, and Flaperons input.

The Rudder is the primary control surface for yawing the aircraft. On the F-16, the rudder is the dominant surface for generating side forces.

Table 2-1 F-16 Reference Data

Gross Weight	gw	21018 lbf
Wing Area	S	300 Ft^2
Span	b	29 Ft
MAC	$\bar{c}$	10.94 Ft
Center of Gravity	Cg	0.35 MAC
Moment of inertia in Body axis		
X Moment	I_{xx}	10033.43 Slug Ft^2
Y Moment	I_{yy}	53876.27 Slug Ft^2
Z Moment	I_{zz}	61278.45 Slug Ft^2
X-Z Moment	I_{xz}	282.13 Slug Ft^2
Control Surface Deflection Limits		
LEF	$-2^o \leq \delta \leq 25^o$	
FL	$-20^o \leq \delta \leq 20^o$	
HT	$-25^o \leq \delta \leq 25^o$	
Rudder	$-30^o \leq \delta \leq 30^o$	

The sign convention adopted in this thesis is shown in Figure A-2 of Appendix A. Basic aircraft data is presented in Thural thesis [4:27], and is summarized in Table 2-1.

Aerodynamic Coefficients

The data collected by Thural, [4], is presented as nondimensional force and moment coefficients for a given α and β. Each coefficient can be transformed into a force or moment using

$$F_s = C_F \bar{q} S$$
$$M_s = C_M \bar{q} S b \qquad (2\text{-}1)$$

where F_S and M_S represent the appropriate force or moment acting on the aircraft in the stability axis system. Figure A-2 gives a graphical representation of each axis system. For a rigorous definition, refer to Etkin work [7:106-112]. Since the data was taken at finite discrete points, it was transformed in functional form for analytical purpose. Using a Least Square curve fitting technique, Zaiser determined the contribution of each force and moment on the aircraft and its control surfaces as a function of α and β, [5:10-16]. The functional form of each force or moment coefficient are represented by equation 2-2 where the first term represents the contribution of the basic aircraft with no control surface deflections, and the second term represents

$$C_F = \sum_{j=0}^{J} \sum_{i=0}^{I} A_{ij}\, \alpha^i\, \beta^j + \sum_{l=1}^{7} \sum_{m=0}^{M} \sum_{n=0}^{N} B_{lmn}\, \alpha^n\, \beta^m\, \delta_l \qquad (2\text{-}2)$$

the contribution of each control surface. The functional form of each aircraft static stability derivative is presented in Appendix B and an example is shown in Figure 2-1.

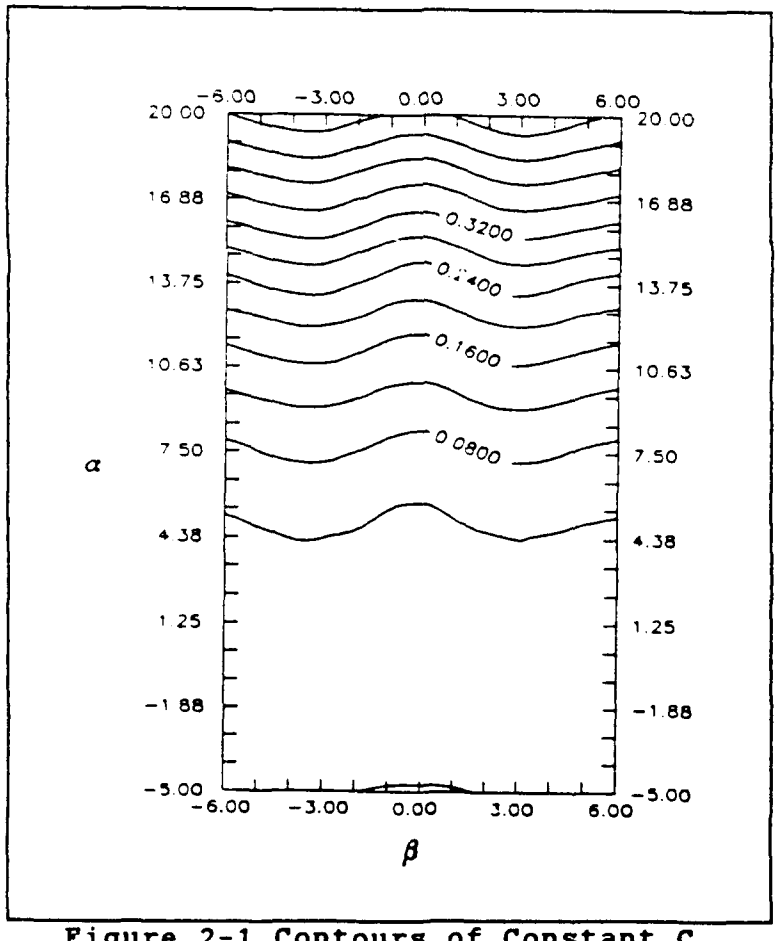

Figure 2-1 Contours of Constant C_D

Equilibrium State

The desired trim conditions that are investigated in this research have the aircraft flying a rectilinear trajectory at constant altitude. When the aircraft is in equilibrium, all external forces and moments acting on it equal zero. Therefore the equilibrium equations become

$$F_{A_X} + F_{T_X} - mg \sin\theta = 0 \qquad (2\text{-}3)$$

$$F_{A_Y} + mg \cos\theta \sin\phi = 0 \qquad (2\text{-}4)$$

$$F_{A_Z} + mg \cos\theta \sin\phi = 0 \qquad (2\text{-}5)$$

$$M_{A_X} = 0 \qquad (2\text{-}6)$$

$$M_{A_Y} = 0 \qquad (2\text{-}7)$$

$$M_{A_Z} = 0 \qquad (2\text{-}8)$$

where F_{Ai}, F_{TX}, and M_{Ai} represent the aerodynamic forces, the thrust force, and the aerodynamic moments in the i axis of the body axis reference system. θ and ϕ are the Euler angles that define the aircraft attitude with respect to earth inertial reference frame. The only other equation required in the trim analysis is an expression that defines the aircraft pitch angle for a constant altitude flight, which is

$$\theta = Tan^{-1}\left(Tan\alpha\ Cos\phi + \frac{Tan\beta}{Cos\alpha}\ Sin\phi \right) \qquad (2\text{-}9)$$

Since no restriction was placed on a wing level flight, coupling effects between the longitudinal and lateral modes are apparent in equations 2-4, 2-5 and 2-9. A complete derivation of the equilibrium equations can be found in [5:85-99].

Before solving the trim equations for a specific rudder failure, flight conditions need to be established. Table 2-2 gives the flight condition that is investigated in this research.

Table 2-2 Flight Condition

Mach	0.6
Altitude	15000 Ft
Velocity	375 KEAS
$\bar{q}$	300 psf

Problem Formulation

The desired equilibrium is a rectilinear flight at constant altitude. Although equilibrium states might be less difficult to achieve at other flight conditions, only rectilinear flight will be investigated. A failure of the rudder, which results in the rudder being locked into a specific deflection is the only failure mode that this thesis will study. The investigation will also be limited by the range of the test data that was collected by Thural [4]. Therefore the dimensions of the α/β space that will be

investigated are limited to $-6.0^{o} \leq \beta \leq 6.0^{o}$ and $0^{o} \leq \alpha \leq 20.0^{o}$.

Some assumptions still need to be stated before proceeding with the analysis. They are:

1. The aircraft is assumed to be a rigid frame.
2. The earth surface is assumed to be an inertial frame of reference.
3. The aircraft mass and mass distribution are assumed to be constant.
4. The X-Z plane of the aircraft is assumed to be a plane of symmetry.

These assumptions hold for both the equilibrium equations and the linearized equations of motion developed in Appendix D.

As discussed in the beginning of this chapter, the only control authority that the pilot has on a healthy aircraft is through the Horizontal Tail Elevator (HTE), the Rudder, and the Flaperons (FLs). The Horizontal Tail Ailerons (HTAs) deflection is proportional to the FLs deflection. For the flight conditions of Table 2-2, the HTAs deflect only a factor of 0.294 of the FLs [8].

The control schemes investigated in this thesis are derived by allowing successively greater independence. One point to note is that the control scheme discussed in this chapter does not refer to the control laws. The two control schemes investigated are shown in Table 2-3.

Table 2-3 Control schemes

Case A	Case B
δ_{FL}	δ_{FL}
δ_{HTE}	δ_{HTE}
	δ_{HTA}

Case A represents the basic aircraft. Case B allows the HTA to deflect independently from the FLs. It is assumed that an algorithm is present to trim the aircraft using these control surfaces without modifying the actual control laws. Also, the deflections of the individual control surfaces in both cases are related as follows:

$$\delta_{FL} = \frac{1}{2} (\delta_{RFL} - \delta_{LFL}) \qquad (2\text{-}10)$$

$$\delta_{HTE} = \frac{1}{2} (\delta_{RHT} + \delta_{LHT}) \qquad (2\text{-}11)$$

$$\delta_{HTA} = \frac{1}{2} (\delta_{RHT} - \delta_{LHT}) \qquad (2\text{-}12)$$

$$\delta_{LHF} = \frac{1}{2} (\delta_{RLE} + \delta_{LLE}) \qquad (2\text{-}13)$$

Before solving the trim problem, the external forces and moments acting on the aircraft still need to be determined. By specifying α, β, and the dynamic pressure $\bar{q}$,

the external forces and moments are evaluated using the polynomial listed in appendix B as a function of a specific control surface deflection. The total external force or moment acting on the aircraft can be written as

$$F_i = A_0 + B + \sum_{l=1}^{L} \sum_{m=0}^{1} \sum_{n=0}^{1} C_{lmn} \alpha^n \beta^m \delta_l \qquad (2\text{-}14)$$

where F_i is the total force or moment acting on the aircraft, A_0 is the contribution of the aircraft with all the control set to zero, B is the contribution of the failed rudder and the LEFs, and the last term is the force or moment that results from the unknown deflection of the control surfaces. The unknowns that remain to be evaluated are the deflection of the control surface.

Solving the trim problem

Assuming that the power available from the aircraft can compensate for the aerodynamic forces and the gravitational term in equation 2-3, the problem can be formulated as follows

$$-(A_Z + B_Z + mg\,Cos\theta\,Sin\phi) = \sum_{i=1}^{I} C_{Zi}\,\delta_i \qquad (2\text{-}15)$$

$$-(A_M + B_M) = \sum_{i=1}^{I} C_{Mi}\,\delta_i \qquad (2\text{-}16)$$

$$- (A_L + B_L) = \sum_{i=1}^{I} C_{Li}\, \delta_i \qquad (2\text{-}17)$$

$$- (A_N + B_N) = \sum_{i=1}^{I} C_{Ni}\, \delta_i \qquad (2\text{-}18)$$

Since the components on the left side of each equation are known, the problem can be reformulated as

$$b = [\, A \,]\, \delta \qquad (2\text{-}19)$$

where the vector b represents the known forces and moments, the A matrix contains the control derivatives, and δ is the unknown control deflection vector. Using equations 2-4, 2-9, and 2-15 to 2-18, the trim problem can be solved. For Case A, the I in equations 2-15 through 2-18 is two, since only the FLs and the HTE are directly controlled by the pilot. In case B, I equals three since the HTAs are assumed to be independent from the FLs.

Equation 2-4 and 2-9 are used first to estimate Φ and θ. For both cases, equation 2-19 represents an overdetermined system of equations that can be solved using Singular Value Decompositions (SVD) [9:59].

In his thesis, Zaiser wrote a computer code to solve for the trim conditions, where the A matrix in equation 2-19 was square [5:112]. The same code is modified and used to evaluate the trim conditions for each case at a given rudder

failure. Zaiser program was modified by the inclusion of a least square algorithm in the SVD routine. Since a least square solution can be obtained for any given set of initial conditions, a range of values that would be considered zero had to be established. Table 2-4 gives the limits that are incorporated into the code.

Table 2-4 Forces and Moments Limits

$\lvert F_{Az} \rvert$	<	50.0 lbf
$\lvert F_{Ay} \rvert$	<	50.0 lbf
$\lvert M_{Ax} \rvert$	<	500.0 lbf Ft
$\lvert M_{Ay} \rvert$	<	500.0 lbf Ft
$\lvert M_{Az} \rvert$	<	500.0 lbf Ft

Results from the Trim Analysis

The results from the trim analysis are presented in Figures 2-2 to 2-7. The area where equilibrium is possible is presented on the first graphic of each figure for a given case and rudder failure. The roll angle and the control surface deflections where the aircraft is in equilibrium are also presented. For each of the cases and rudder failures, if β is specified, only a very small variation in α is permitted for the aircraft to remain in equilibrium.

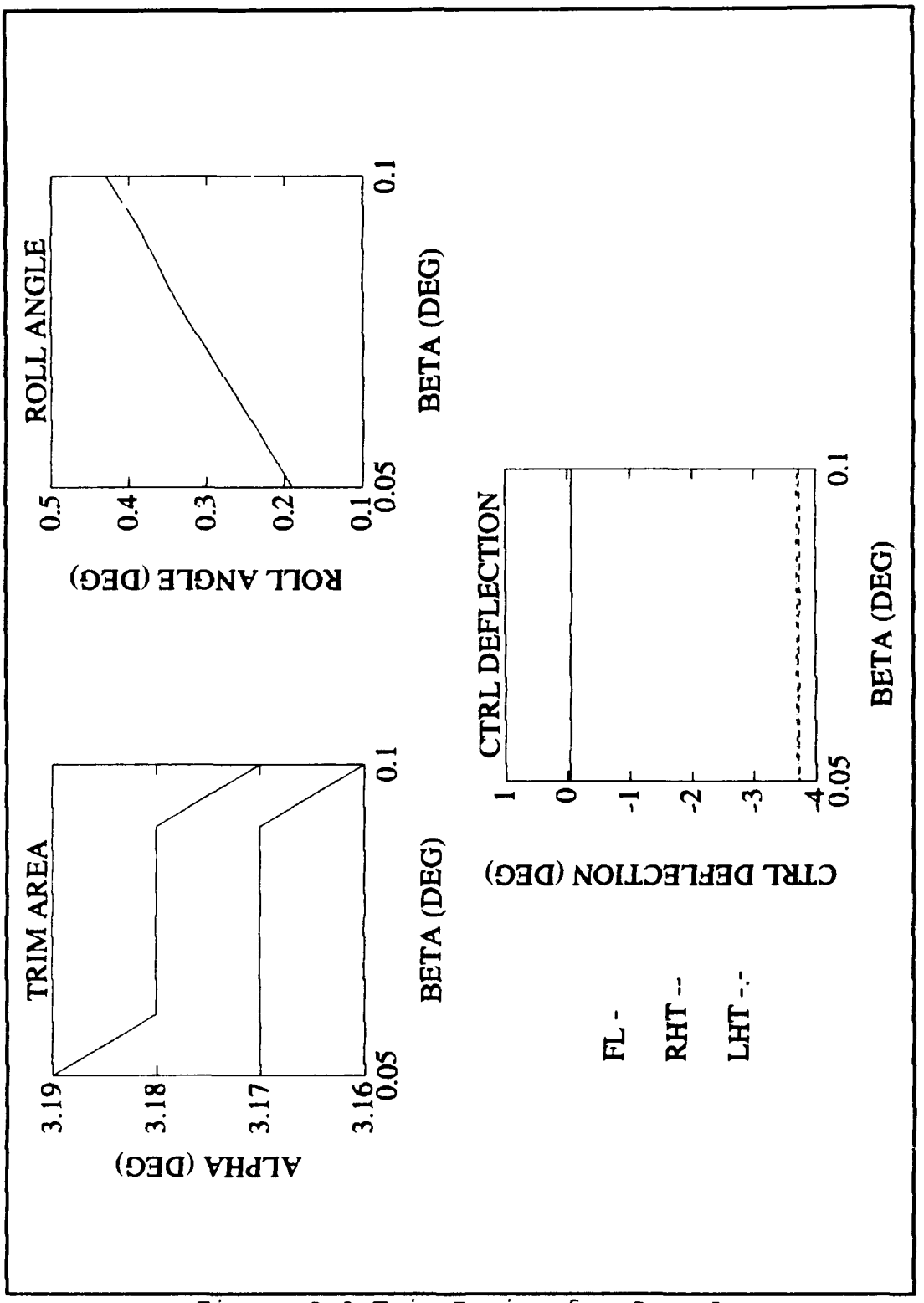

Figure 2-2 Trim Region for Case A
0 Degree Rudder Failure

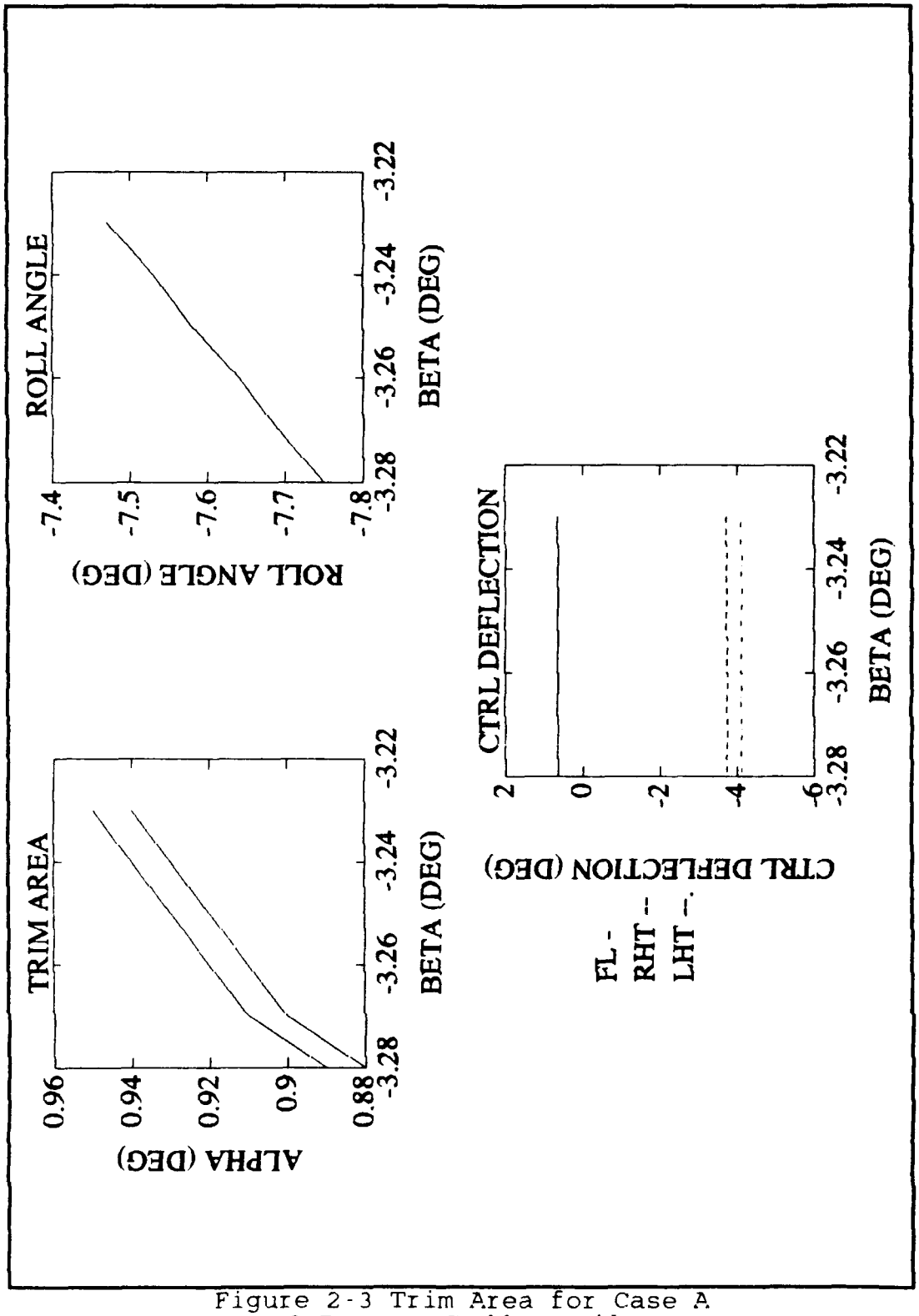

Figure 2-3 Trim Area for Case A
-10 Degrees Rudder Failure

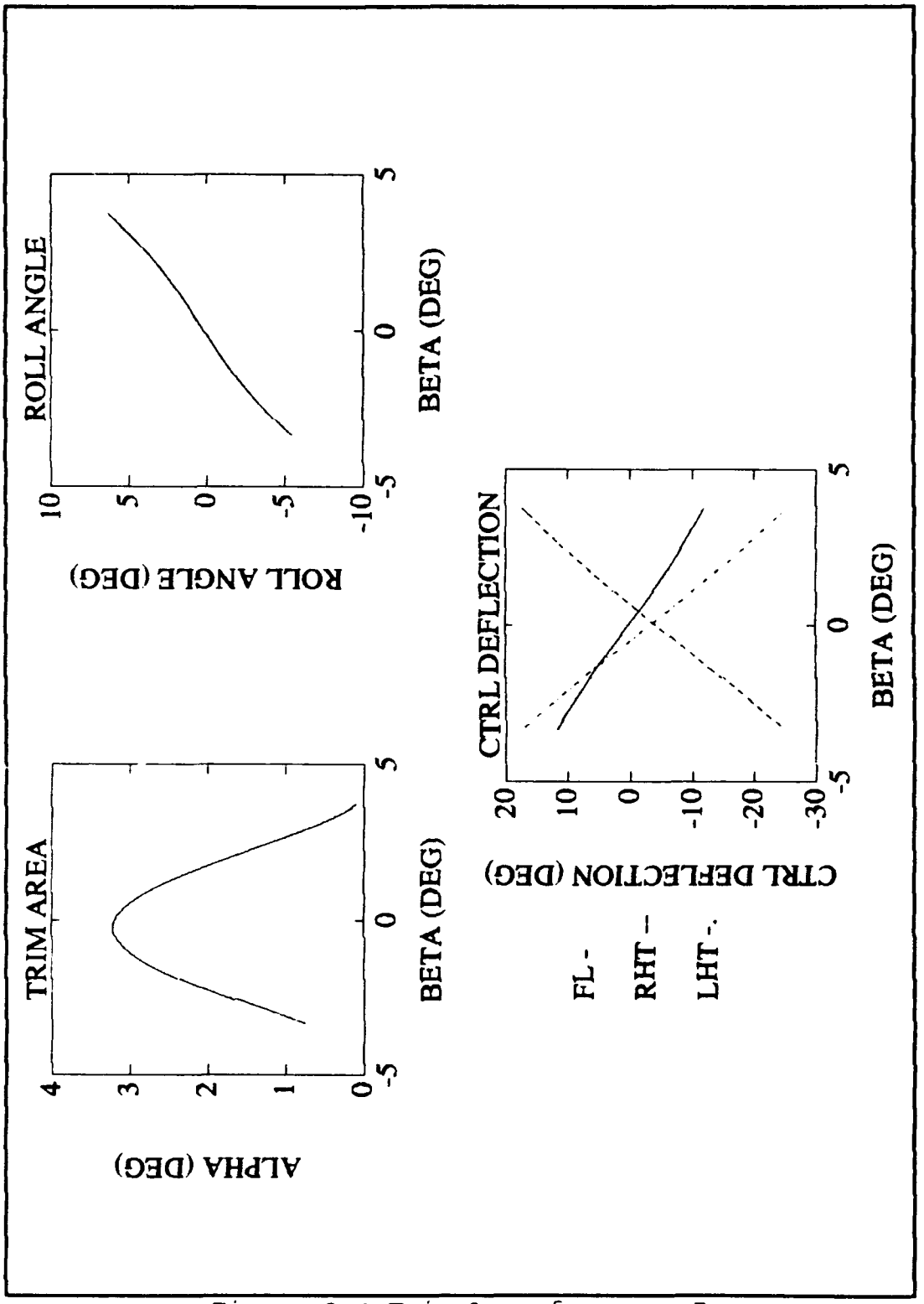

Figure 2-4 Trim Area for case B
0 Degrees Rudder Failure

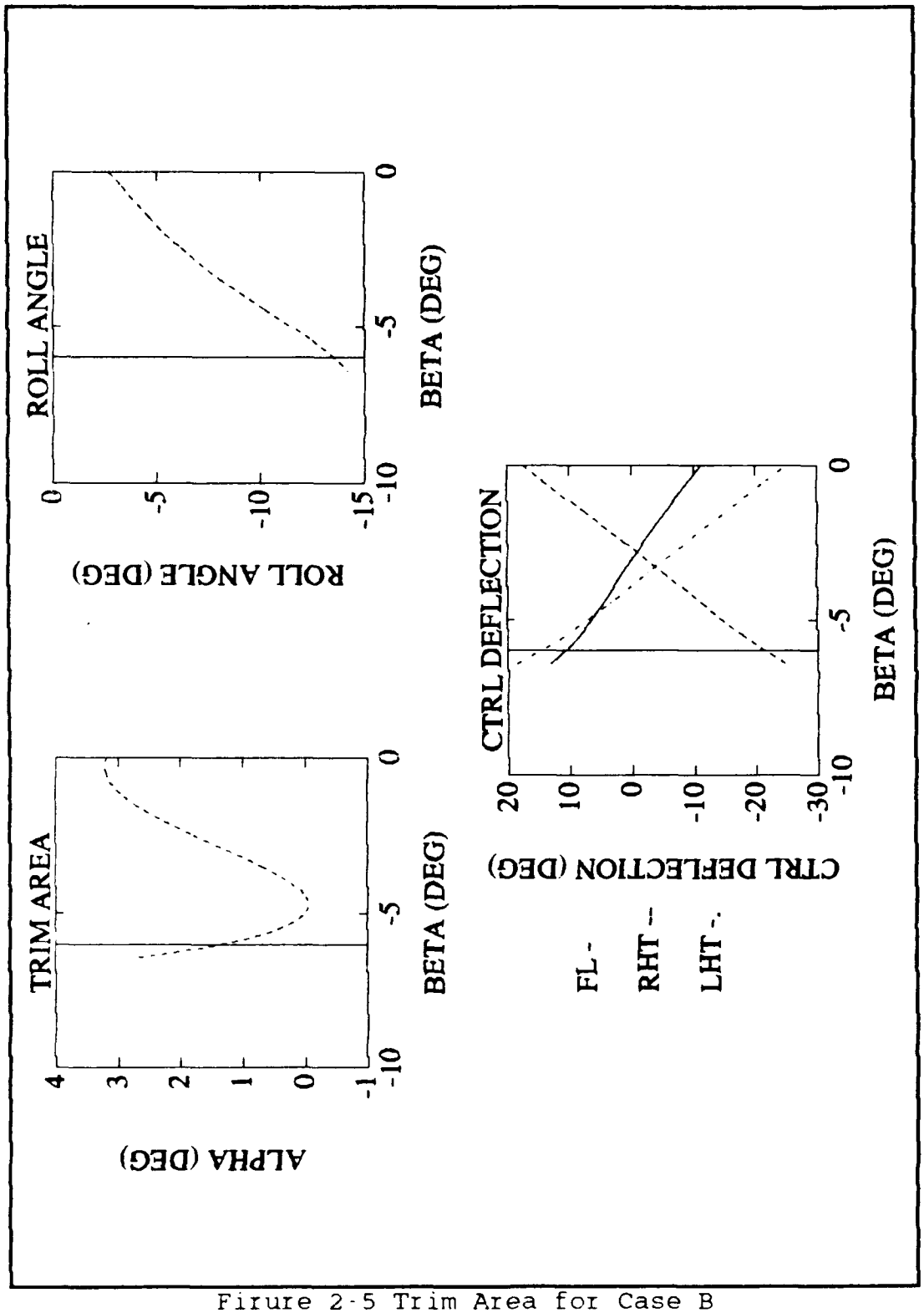

Firure 2-5 Trim Area for Case B
-10 Degrees Rudder Failure

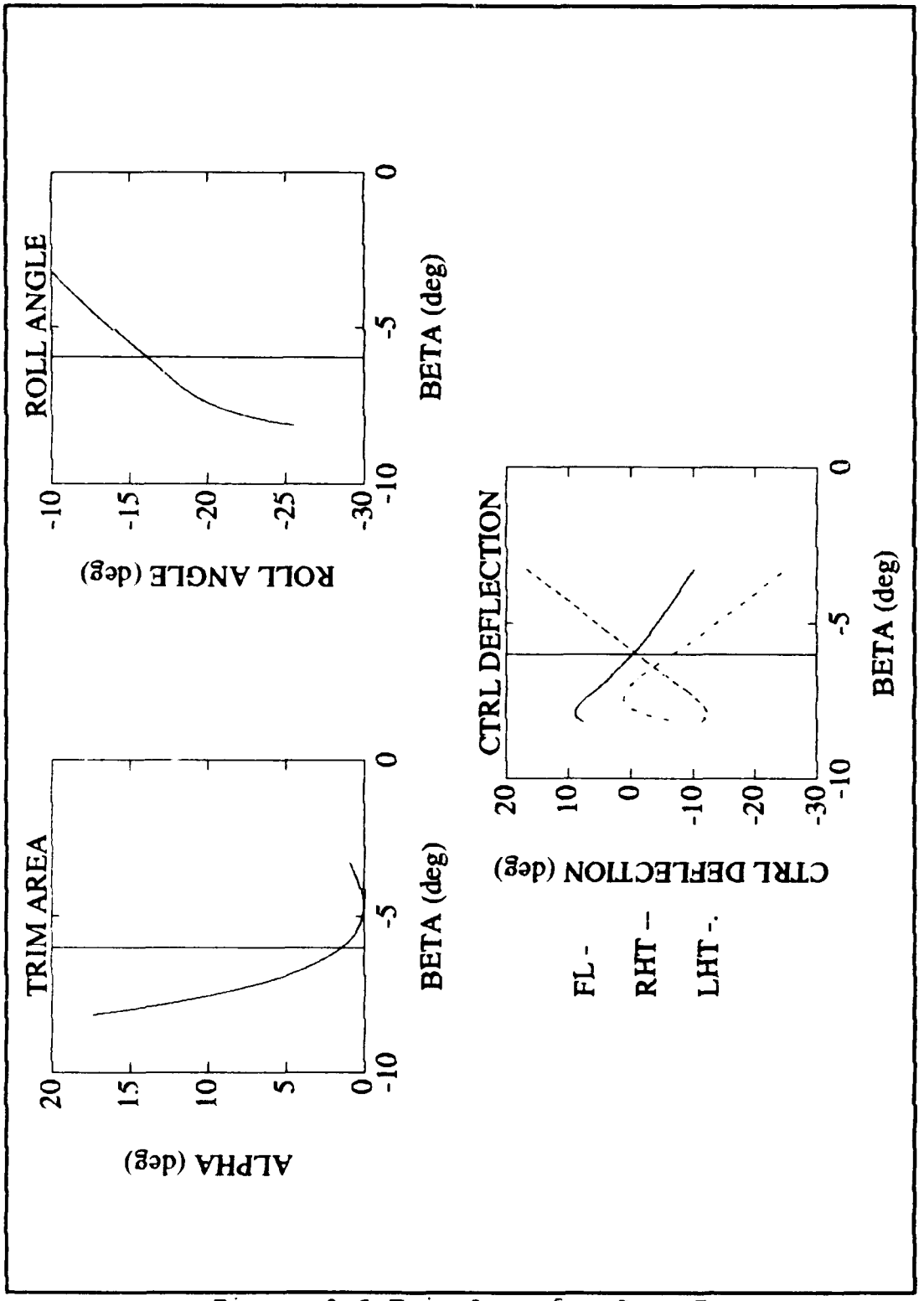

Figure 2-6 Trim Area for Case B
-20 Degrees Rudder Failure

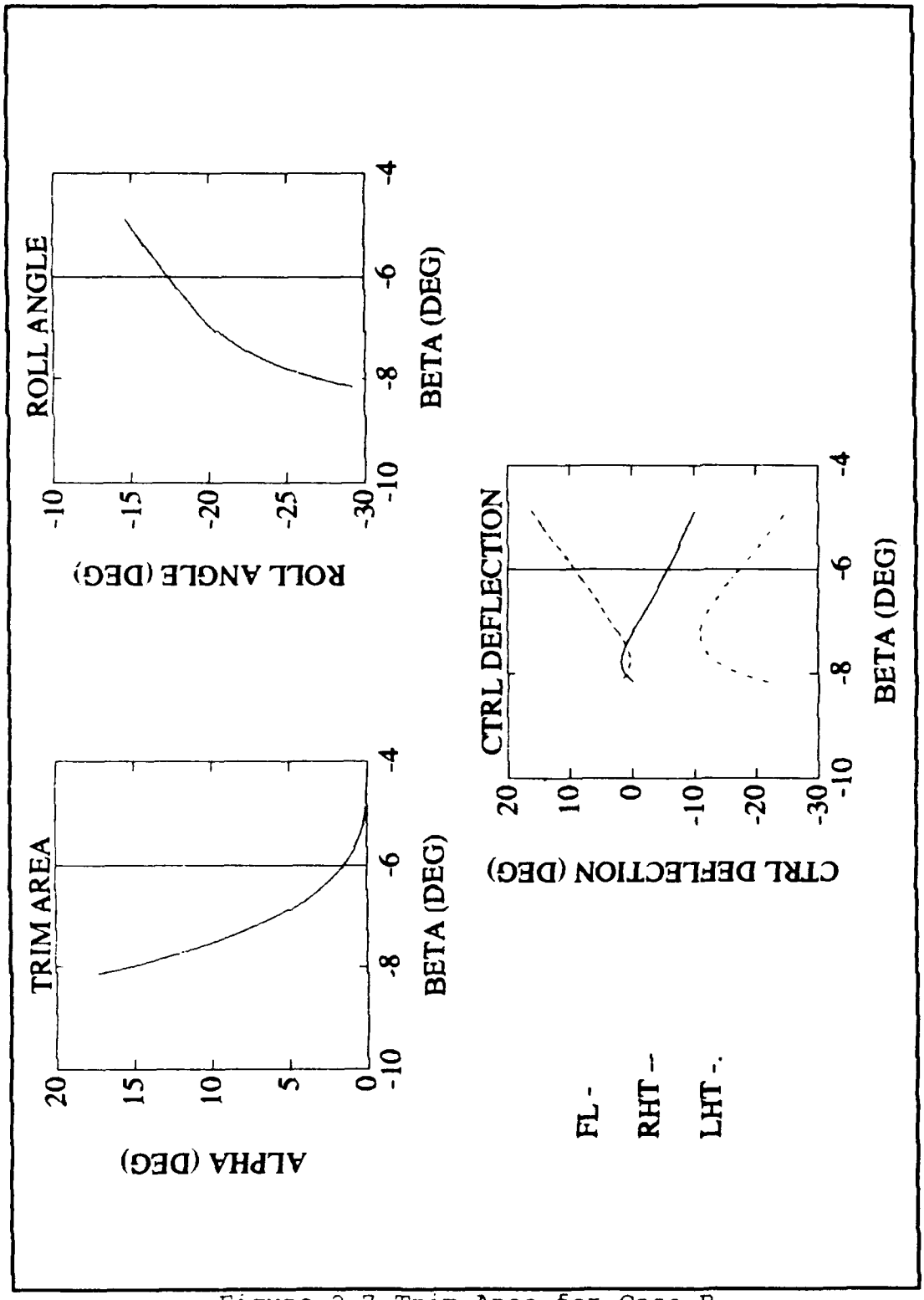

Figure 2-7 Trim Area for Case B
-25 Degrees Rudder Failure

For a zero degree rudder failure, both cases show some asymmetry. This results from the limits of Table 2-4 that needed to be included in the code to calculate the trim area. For a rudder failure other than zero degrees, a vertical line is included in each graphic at β=-6° since the functional representation of the stability derivative is only valid for $-6^{\circ} < \beta < 6^{\circ}$ and $0^{\circ} < \alpha < 20^{\circ}$, [5:30]. Data points to the left of that line are not analyzed, since for $\beta < -6^{\circ}$, the results are obtained by extrapolating the functional form of the stability derivatives.

One of the interesting features displayed in the results is the attitude of the aircraft for a specific condition. For a 25° rudder failure, case B, it might be preferable to trim the aircraft at β=-6°, α=1.8° and Φ=-18° since this is the trim condition that gives the most control authority to each control surface. This will be taken into consideration in the following chapters.

Summary

In this chapter, different rudder failure are presented for a given control scheme and flight condition. The aircraft controls are also presented with their limitations. Assumptions are made regarding the control scheme implementation for both cases. Data required to analyze the aircraft dynamic response for a specific failure conditions is presented.

III. AIRCRAFT PLANT MODEL

Introduction

In this chapter, the linearized F-16 plant model is derived using the functional representation of the static stability derivatives of Appendix B for several trim conditions. The eigenvalues of the open loop plant are analyzed to determine the dynamic characteristics of the aircraft for a specific rudder failure.

Linearized equations of motion

The mathematical model is presented in Appendix D. The sign convention for the axes and control deflections are shown in Figure A-2 of Appendix A. The simplifying assumptions made during the derivation of the equations of motion are:

Assumption 1. The aircraft is assumed to be a rigid body.

Assumption 2. The earth surface is assumed to be an inertial reference frame.

Assumption 3. The mass and mass distribution of the aircraft is assumed constant.

Assumption 4. Disturbances from steady flight conditions are small, implying a small angle approximation. Higher order terms

of the disturbance quantities are negligible.

Assumption 5. The flow surrounding the aircraft is assumed quasi-steady.

Assumption 6. Variation of the atmosphere, including density and speed of sound, are negligible for small altitude perturbations.

Even if these assumptions are made, the equations still include coupling effects. The complexity can be reduced by linearizing the equations of motion about a steady state flight. For this investigation, the only restriction is for the aircraft to fly a rectilinear trajectory at constant altitude which implies:

1. Initial side velocity may exist: V_0
2. Initial bank angle may exist : Φ_0
3. Initial pitch angle exists : θ_0
4. No initial angular velocities exist which results in

$$P_0 = Q_0 = R_0 = \dot{\psi} = \dot{\theta} = \dot{\phi} = 0 \qquad (3\text{-}1)$$

Equation 3-1 considerably simplifies the linearized equations of motion shown in Appendix D, but they still include coupling effects produced by the roll angle and the side velocity. In this research, the effects of unsteady atmospheric disturbances were neglected.

Aerodynamic Forces and Moments

Assuming that the aircraft has enough thrust so that steady state flight can be maintained, the thrust setting will balance the remaining forces in the corresponding axis. Also, the direct thrust contributions to the stability derivatives is generally negligible for conventional aircraft and is assumed to be zero for this aircraft [6:267]. The only part of the linearized equations of motion that still need development are the aerodynamic forces and moments .

The representation of the aerodynamic forces and moments is usually made in the stability axis system. Since the perturbed equations of motion are written in the body axis system, the aerodynamic forces and moments need to be transformed into that axis system. Each stability axis can be transformed into the body axis system using the stability to body axis transformation matrix ([BS]) presented in Appendix D. Once the transformation is made, the aerodynamic forces and moments are given in the same axis system as the equations of motion.

Each of the forces and moments need to be expanded to determine their dependence on the perturbed motion. The expansion is done using a Taylor series expansion at a given trim condition, denoted by the subscript $()_0$. The expansion of the forces and moments can be represented as

$$F = F_0 + \left(\frac{\partial F}{\partial \Lambda_1}\right)|_0 \lambda_1 + \left(\frac{\partial F}{\partial \Lambda_2}\right)|_0 \lambda_2 + \ldots + \left(\frac{\partial F}{\partial \Lambda_n}\right)|_0 \lambda_n \qquad (3\text{-}2)$$

$$M = M_0 + \left(\frac{\partial M}{\partial \Lambda_1}\right)|_0 \lambda_1 + \left(\frac{\partial M}{\partial \Lambda_2}\right)|_0 \lambda_2 + \ldots + \left(\frac{\partial M}{\partial \Lambda_n}\right)|_0 \lambda_n \qquad (3\text{-}3)$$

where the variable Λ represent the perturbed velocities and accelerations, and λ the perturbation from the $()_0$ condition. The higher order terms have been eliminated from the expansion in accordance with assumption 4. The results of this expansion is shown in Appendix D. The analysis of the aircraft motion is performed at different trim conditions where the aircraft attitude preclude the separation of the longitudinal and lateral mode. Therefore, all cross-coupling derivatives are included in the perturbed equations of motion.

State Space Form

In order to analyze the system, the perturbed equations of motion are put into matrix form. This form is used to determined the dynamic stability and control for various rudder failure and trim conditions. The matrix form of the perturbed equations of motion may be written as:

$$\dot{x} = A x + B u \qquad (3\text{-}4)$$

where x represent the aircraft states, A the plant matrix, u the control variables, and B the matrix of coefficients associated with the control. To determine the stability of the system, the eigenvalues of the plant matrix are computed using a control analysis program (Pro-Matlab [10]). If an eigenvalue has a positive real part, then this state is unstable. Dynamic stability still might be recovered with the controller. This aspect will be discussed in the next chapter. Each of the eigenvalues are also presented graphically to gain some insight on the plant behavior. It is also possible to analyze the controllability of the system. Equation 3-5 is one method to determine the controllability of the system. In this equation, A is the

$$M_c = [\, B \vdots AB \vdots A^2B \vdots \ldots \vdots A^{n-1}B \,] \qquad (3\text{-}5)$$

plant matrix, B the control matrix, M_c the controllability matrix, and n the number of states. If M_c is full rank, rank(M_c) = n, then that particular trim condition is completely controllable with the available inputs using state feedback. If the system is completely controllable then it is possible to reach any state [11:2-42].

Results

In order to facilitate the data handling, a computer code was written to determine the plant matrix, A, and the

control matrix, B, for different trim conditions. The computer code is presented in Appendix E. The static stability derivatives of Appendix B are linearized and included into the code. For specific α and β the static stability derivatives are evaluated and included in the linearized equations of motion. Table 3-1 lists the static

Table 3-1 Static stability Derivatives

Drag	:	C_D, $C_{D\alpha}$, $C_{D\beta}$
Lift	:	C_L, $C_{L\alpha}$, $C_{L\beta}$
Side	:	C_Y, $C_{Y\alpha}$, $C_{Y\beta}$
Pitch	:	C_m, $C_{m\alpha}$, $C_{m\beta}$
Roll	:	C_l, $C_{l\alpha}$, $C_{l\beta}$
Yaw	:	C_n, $C_{n\alpha}$, $C_{n\beta}$

stability derivatives that are linearized. The remaining stability derivatives were taken from data collected by the Flight Dynamics Laboratory for the AFTIF-16 flying at Mach 0.6 for three different altitudes (0, 5000, and 30000 FT). Since the altitude of interest in this research is 15000 feet, the stability derivatives were estimated using a second order polynomial fit of the three data point available. Table 3-2 list the value of the derivatives that are included in the computer code.

Since no data on the dynamic cross-coupling derivatives were available for the F-16, they were assumed to be zero. This is a reasonable assumption, since for low α their contribution to aircraft motion is relatively small according to Orlik-Rukemann, [12:1-1]. For each of the cases

Table 3-2 control derivatives

	C_D	C_L	C_m
u	0.000059	0.00002	-0.0000638
α	0.0	-0.99333	-0.77776
q	0.0	2.3989	-2.6761
	C_Y	C_l	C_n
β	0.0	0.0	0.0
p	0.080111	-0.23708	-0.0079264
r	0.53755	0.025172	-0.48192

and rudder failures, the eigenvalues are represented graphically in Figures 3-1 to 3-8. The vertical line at x=0.0 on most figures is a reference line. The eigenvalues for case A do not change much over the trim area for both rudder failures (less than are 2%) therefore an average value of each of them is considered appropriate. They are presented in Table 3-3.

Table 3-3 Eigenvalues for Case A

0 Degree rudder failure		-10 Degree Rudder Failure
$3.16 \leq \alpha \leq 3.19$		$0.88 \leq \alpha \leq 0.95$
$0.05 \leq \beta \leq 0.10$		$-3.28 \leq \beta \leq -3.22$
$0.19 \leq \Phi \leq 0.42$		$-7.75 \leq \Phi \leq -7.48$
-0.0023 ± 0.0676i	Phugoid	-0.0022 ± 0.0682i
-0.7275 ± 4.6301i	Short Period	-0.6499 ± 4.6773i
-.3624 ± 4.0805i	Dutch Roll	-0.4097 ± 3.8549i
-1.4703	Roll	-1.5711
-0.0309	Spiral	-0.0199

The legend that describes each figure is in Table 3-4.

Table 3-4 Legend for Figures 3-1 to 3-8

a: Dutch Roll
b: Short Period
c: Roll
d: Phugoid & Spiral

	RUDDER FAILURES DEGREES			
	0	-10	-20	-25
β_1	0.0°	0.0°	-4.4°	-5.0°
β_2	-3.3°	-6.0°	-6.0°	-6.0°

The functional form of the static stability derivatives was derived from data, where $-6.0^\circ < \beta < 6.0^\circ$ and $0.0^\circ < \alpha < 20.0^\circ$. Therefore the curve fitting used for points outside the β limits may show odd behavior. This is the reason why the eigenvalues have a strong departure for $\beta < -6.0^\circ$ and for rudder failures greater than -10°. One other interesting point is the dynamic stability of the open loop system. Since all the real parts of the eigenvalues are negative, the open loop plant is dynamically stable. Equation 3-5 was used to look at the controllability of the system. Boundary points as well as some intermediate points were evaluated for controllability. All the points that were checked yielded a controllable system. This means that with an

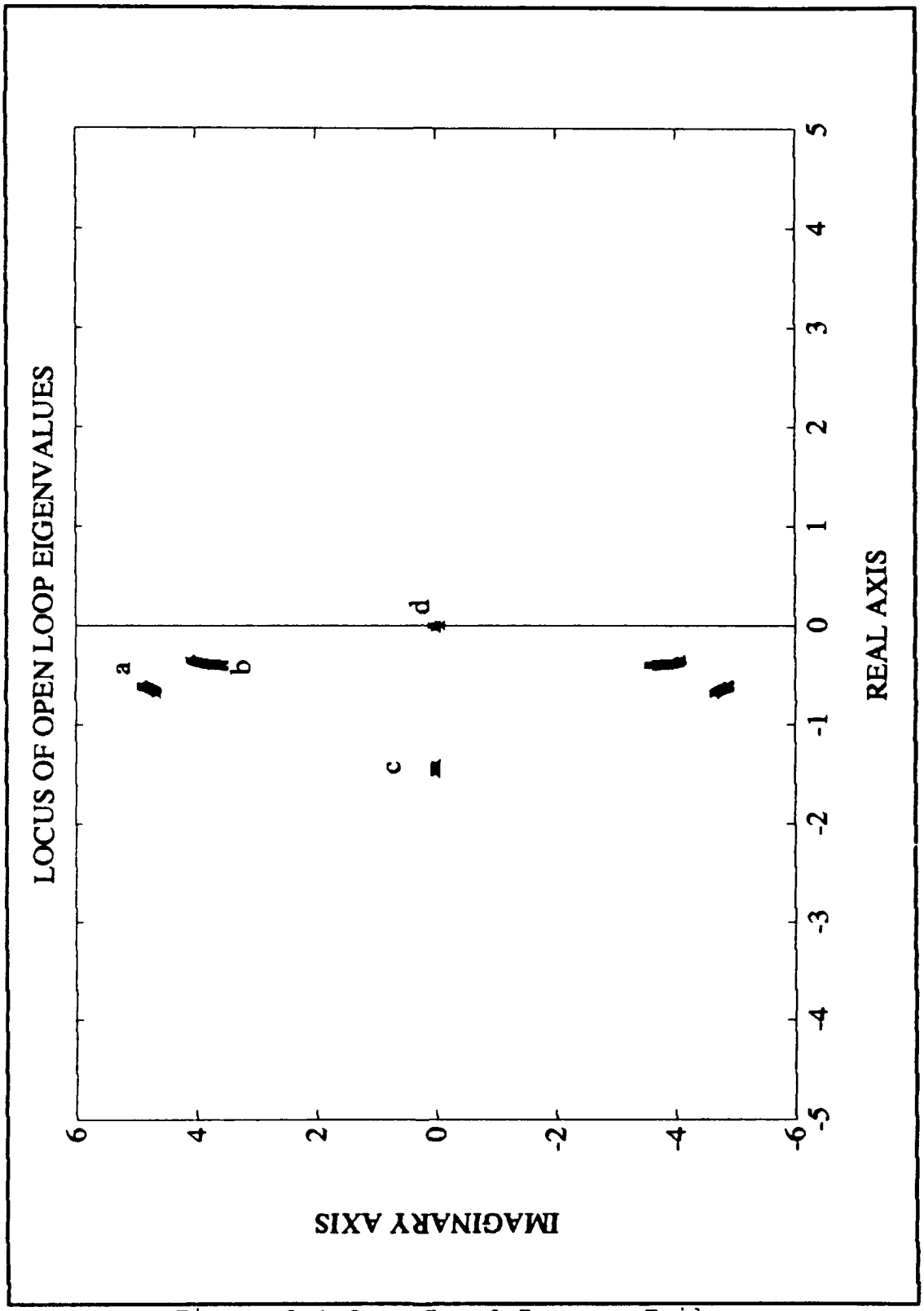

Figure 3-1 Case B 0 Degrees Failure

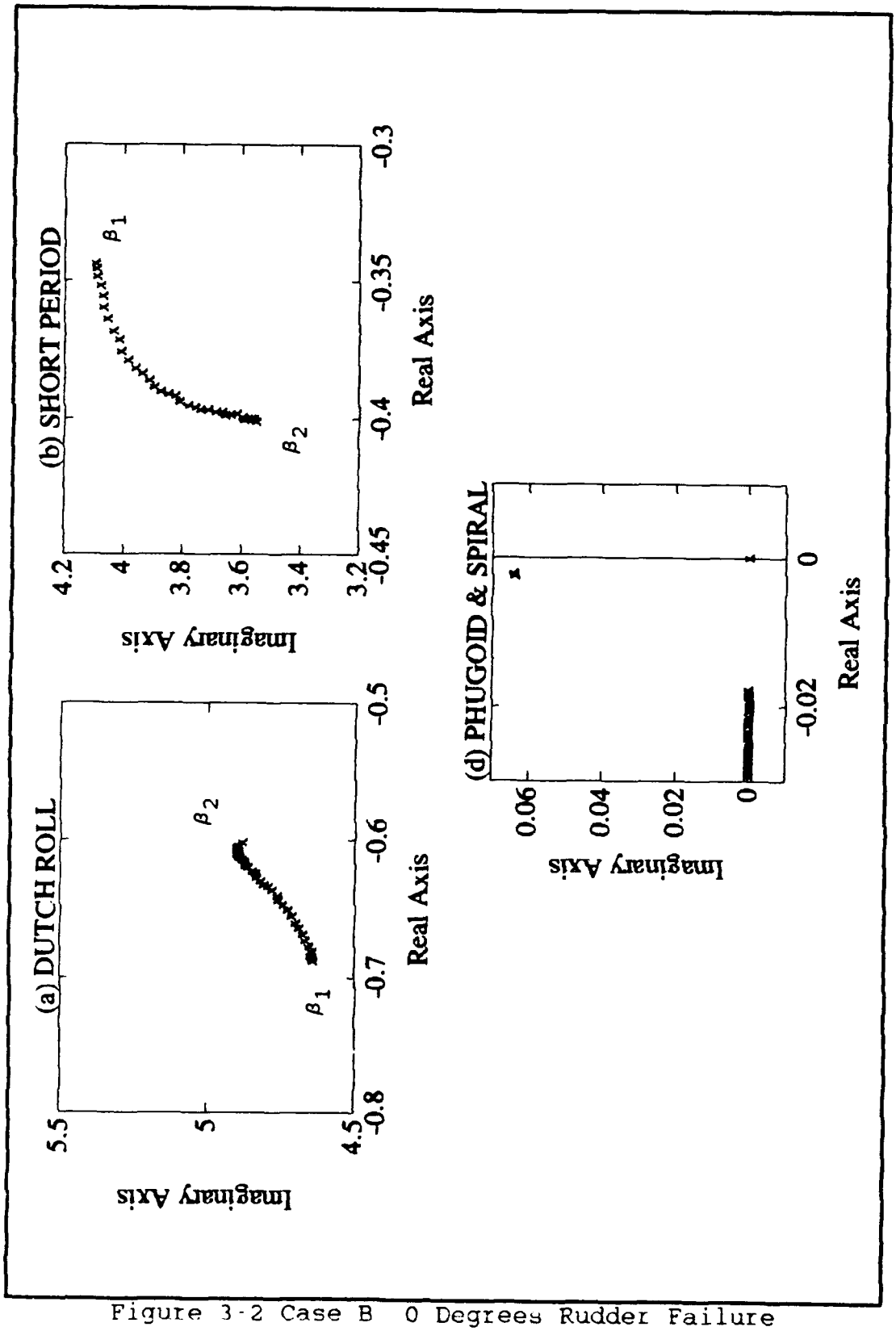

Figure 3-2 Case B 0 Degrees Rudder Failure

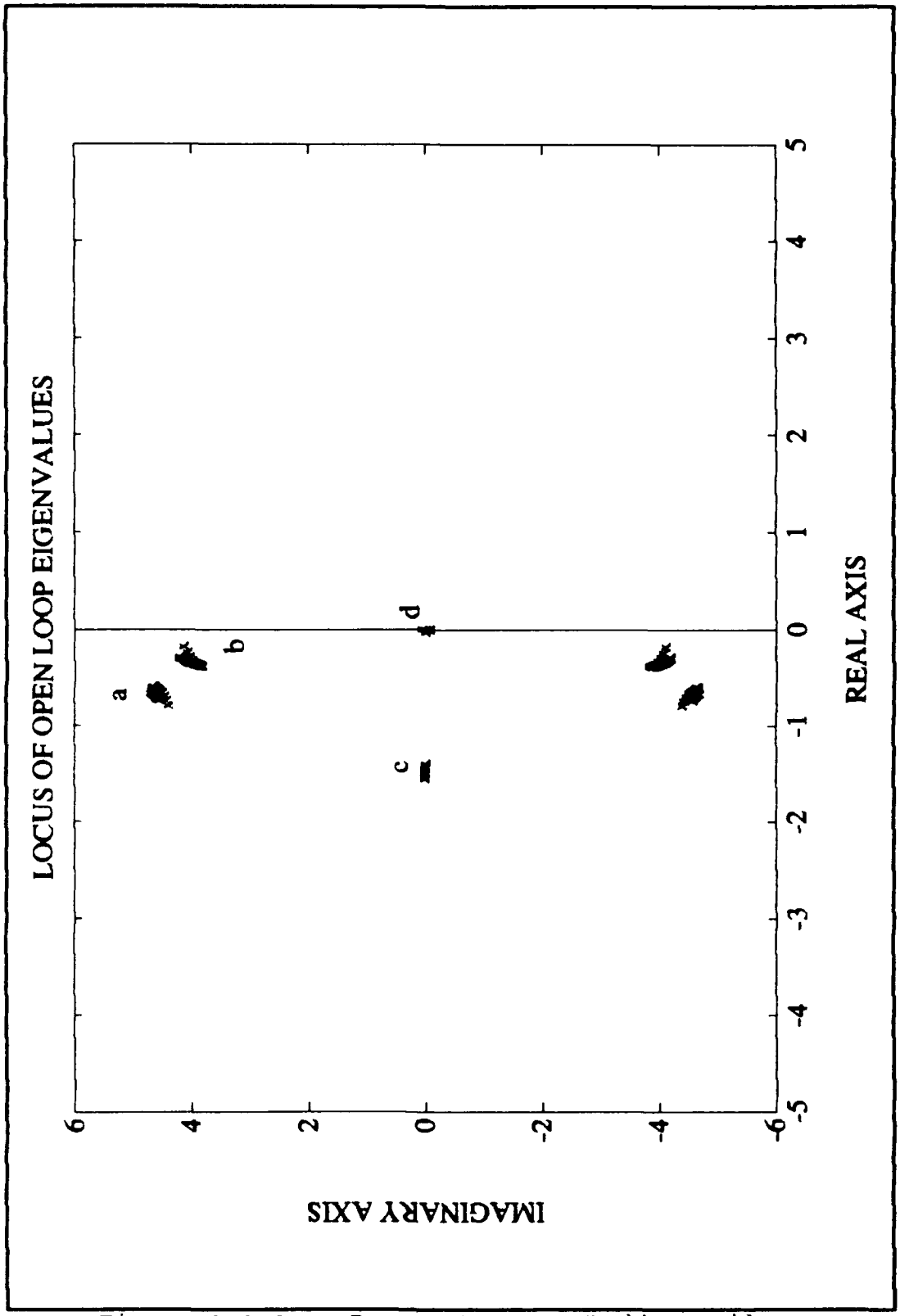

Figure 3-3 Case B -10 Degrees Rudder Failure

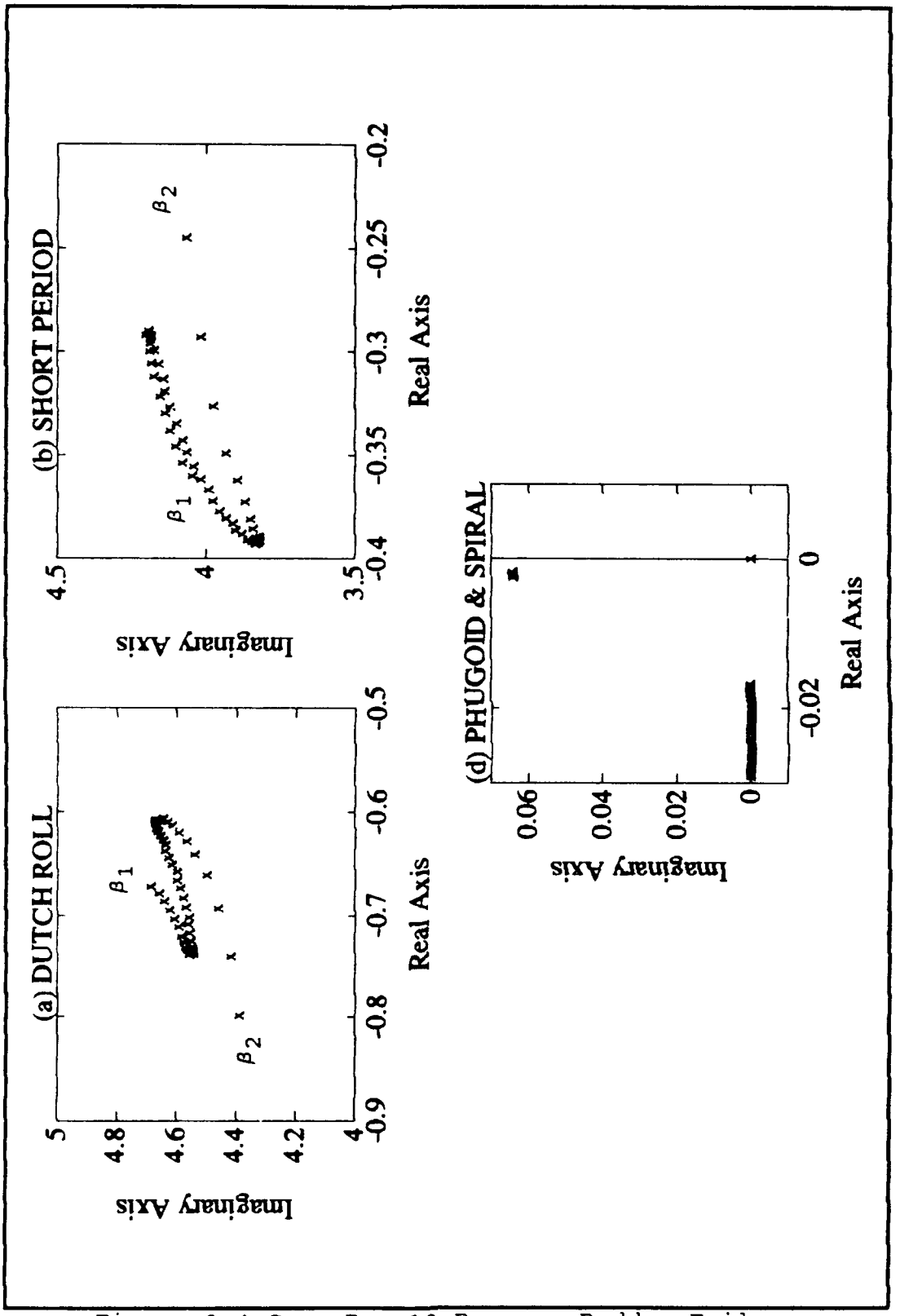

Figure 3-4 Case B -10 Degrees Rudder Failure

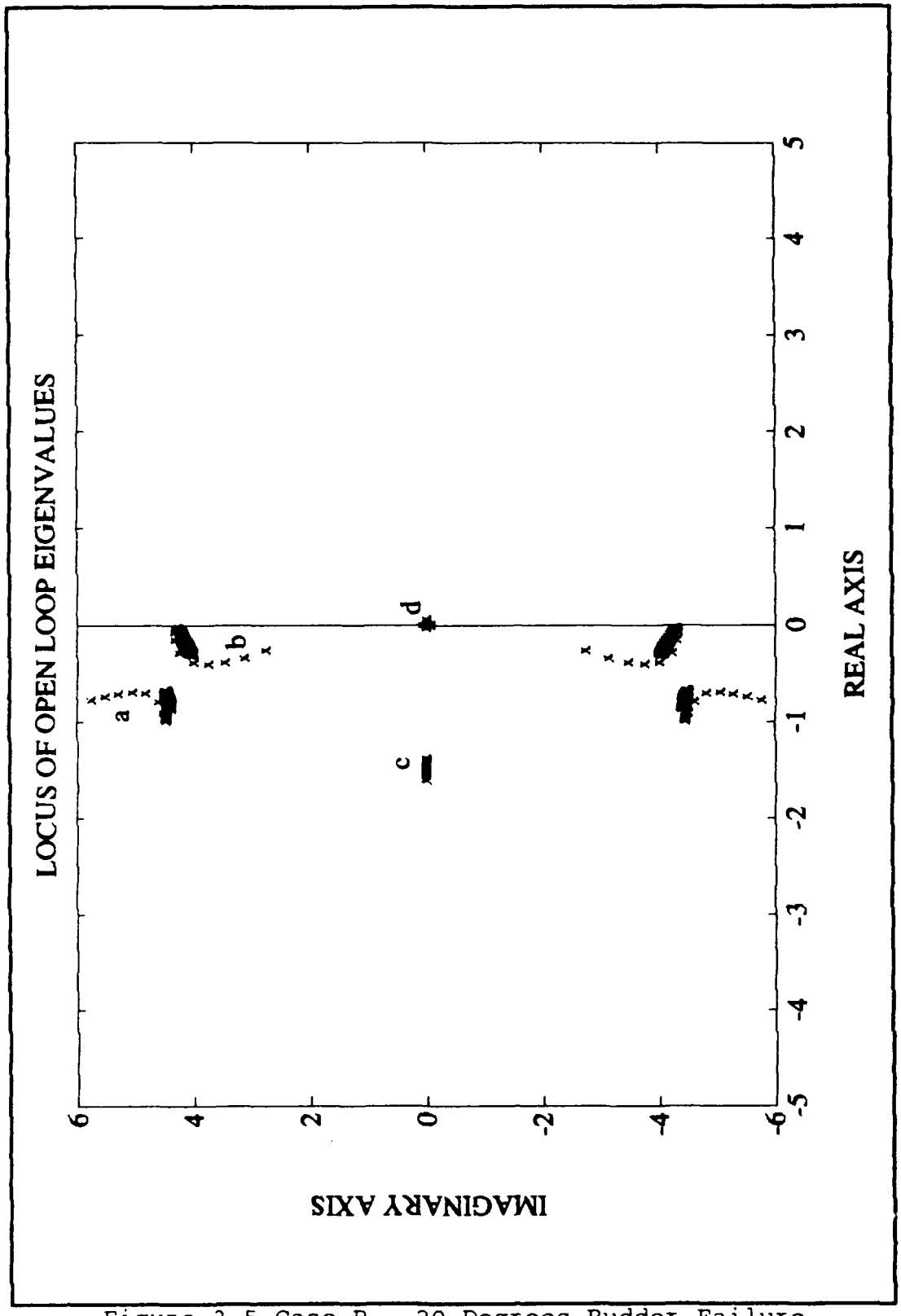

Figure 3-5 Case B -20 Degrees Rudder Failure

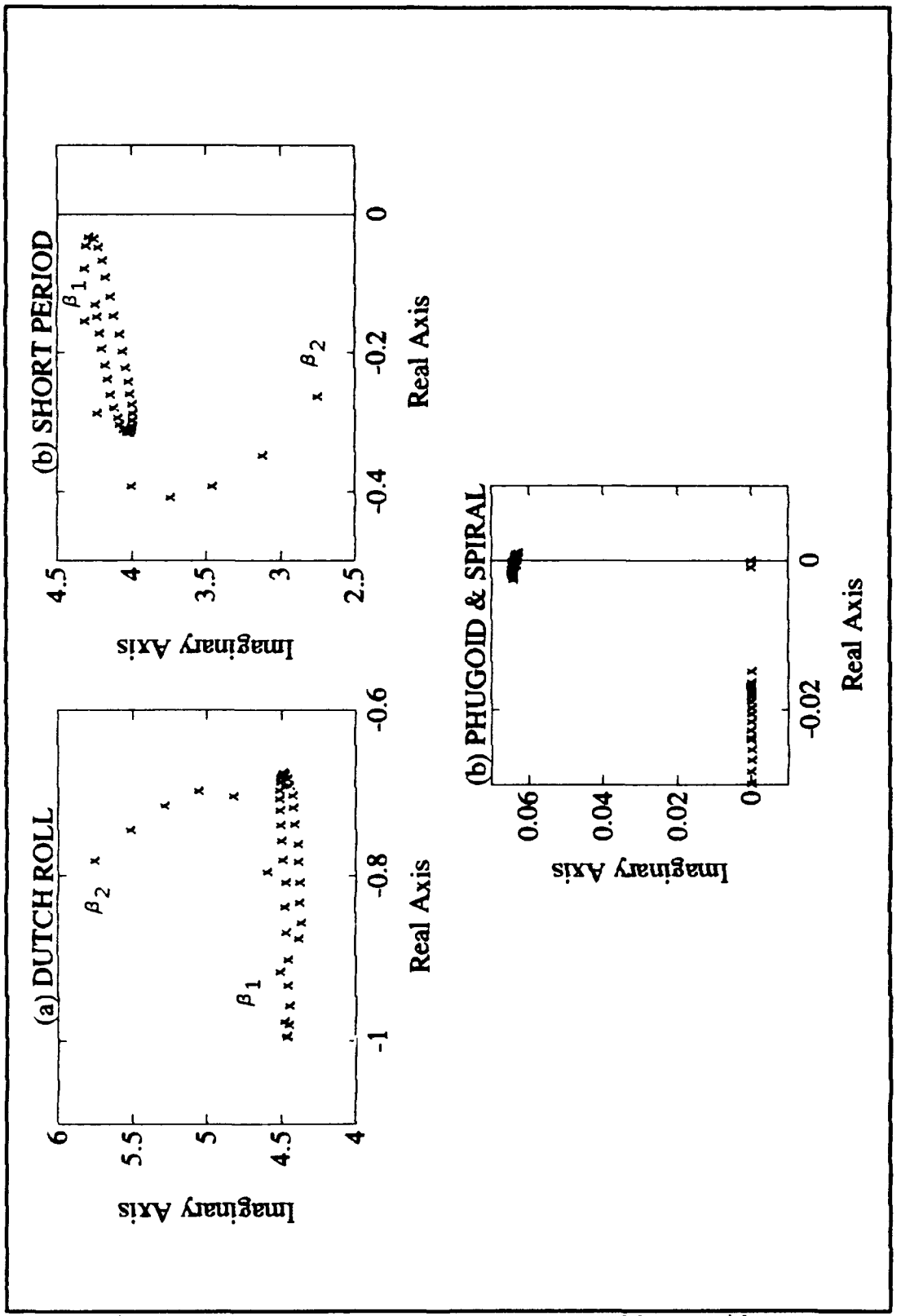

Figure 3-6 Case B -20 Degrees Rudder Failure

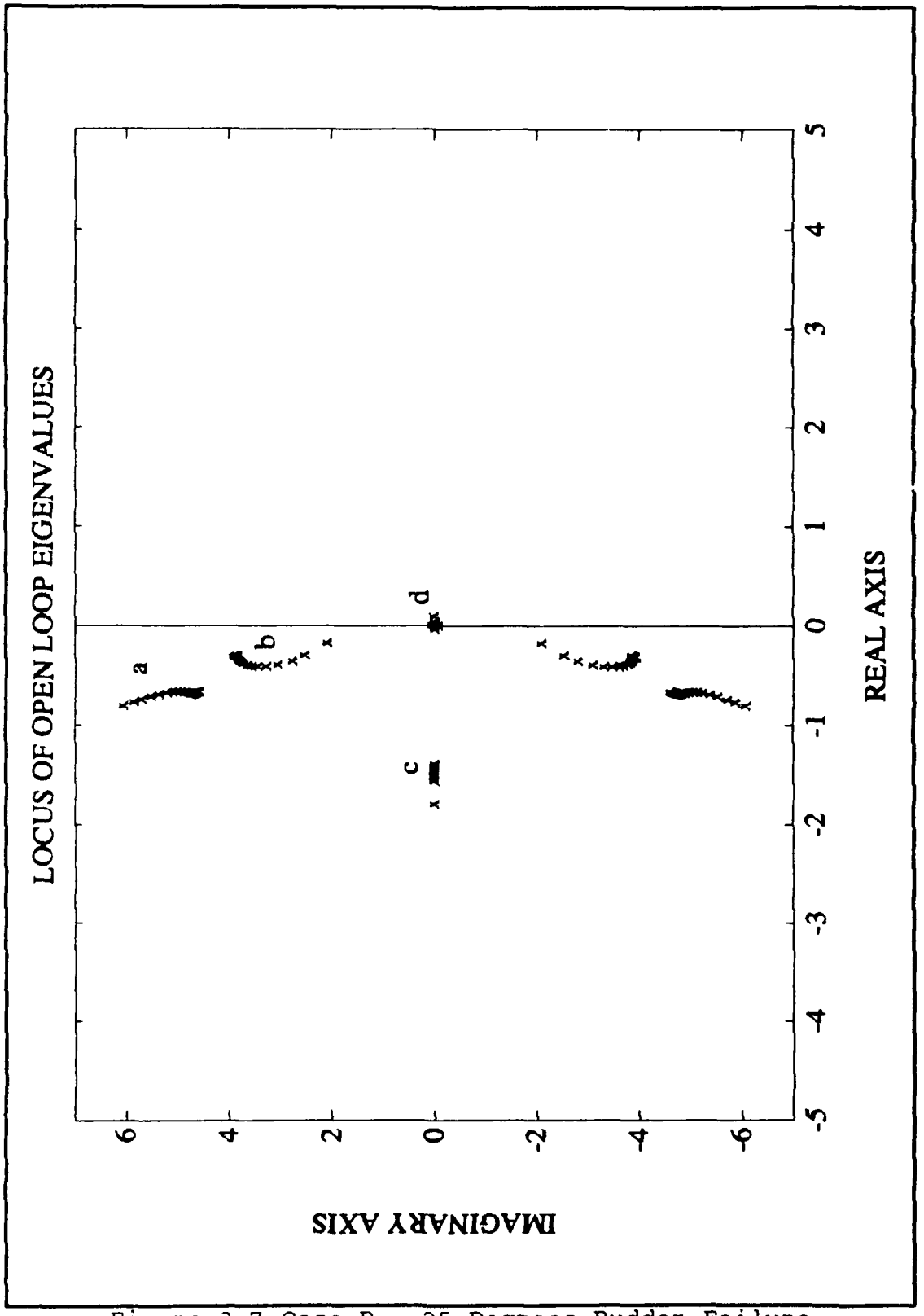

Figure 3-7 Case B -25 Degrees Rudder Failure

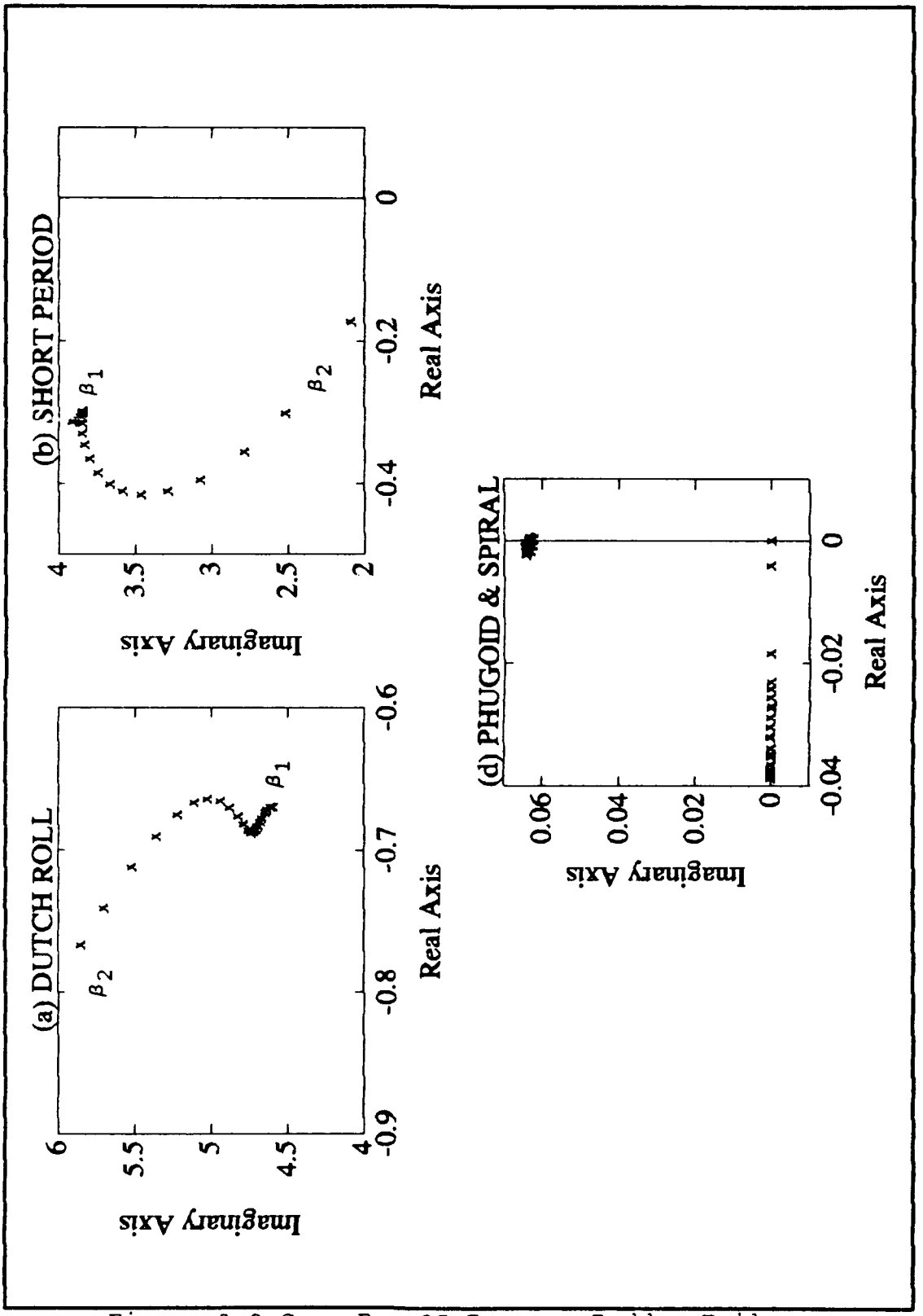

Figure 3-8 Case B -25 Degrees Rudder Failure

appropriate controller, it is possible to position the eigenvalues of the system to guarantee dynamically stability. Now the question that needs to be answered is: Does the present controller on the aircraft still adequate considering the damaged rudder? The next chapter will provide a means to answer this question.

Summary In this chapter, all the equations needed to analyze the dynamic stability of the open loop F-16 aircraft having sustained a rudder failure were derived and put into matrix form to facilitate the analysis. The results showed that the aircraft remains dynamically stable, but with lightly damped phugoid, short period and dutch roll modes. A rigorous analysis of the results is done in Chapter V.

IV. STATE SPACE MODEL DEVELOPMENT

Introduction

In order to investigate if the F-16 control system augments the aircraft dynamic stability for given trim conditions and specific rudder failures, a state space model of the aircraft flight control system was created. The aircraft plant derived in Chapter III is for different trim conditions, but at a specific speed and altitude. To be rigorous, a state space model would have to be developed for each trim condition, since the model is dependent on the trim velocity of the aircraft and α trim. For the range of trim conditions analyzed, the same control system model is used throughout the analysis.

Plant Matrix Development

In order to construct a state space representation of the F-16 control system, a flight condition must be selected. The control law diagram presented in the F-16 Software Mechanization Document [8] is linearized about the flight condition presented in Table 2-2. No pilot input are used, so all paths associated with pilots inputs can be ignored. Since the horizontal tail is used to command both pitch and roll rates, an effective flaperon deflection input

was determined [8]. The effective flaperon deflection is

$$\delta_{Feff} = \delta_F + .294\delta_{HT} \qquad (4\text{-}1)$$

where:

δ_{Feff} = *Effective Flaperon Deflection* (°)

δ_F = *FlaperonDeflection* (°)

δ_{HT} = *Horizontal Tail Deflection* (°)

This effective flaperon deflection was incorporated into the computer code to calculate the B matrix for both cases at the given trim conditions. The effective flaperon deflection is only used for the roll rate commands. Another modification is also made to the control law diagram. The load factor command is change to pitch rate command. The gain in the command path of the control law diagram has to be adjusted in order to convert load factor to a pitch rate command. This is done using the steady Z axis acceleration as shown in equation 4-2.

$$A_n = \frac{q\ V_0}{(\ 57.3\ )\ (\ 32.2\ )} \qquad (4\text{-}2)$$

where:

A_n = *normal acceleration at pilot station* (*g*)

q = *pitch rate* (°/*s*)

V_0 = *steady state forward velocity* (*ft/s*)

Figures 4-1 and 4-2 show the final configuration of the linearized control law for both the longitudinal and lateral axis. Since the aircraft has a failed rudder, the lateral axis still needs to be altered to represent it. This is done by removing all feedback paths that are input into the rudder. The final configuration of the linearized control law for the lateral directional axis is shown in Figure 4-3.

The state vector used to represent the aircraft is shown in equation 4-3.

$$X = [\, u \;\alpha\; \beta\; p\; q\; r\; \phi\; \theta\; \psi \,] \tag{4-3}$$

Since the commanded input is pitch rate instead of load factor, the outputs of the system available for feedback are α, q, and A_n. A_n is in units of g's. The expression for the normal load factor at the pilot station is

$$\begin{aligned} a_z &= a_{z_{cg}} - X_a \dot{q} \\ &= \dot{w} - qV_0 - X_a \dot{q} \end{aligned} \tag{4-4}$$

which can be transformed using small angle approximation into

$$A_n = [\, -V_0\, (\, \dot{\alpha} - q\,) + X_a \dot{q}\,] \left[\, \frac{1}{32.2} \,\right] \tag{4-5}$$

where X_a is the distance from the aircraft cg to the accelerometer located under the pilot's seat. For the F-16,

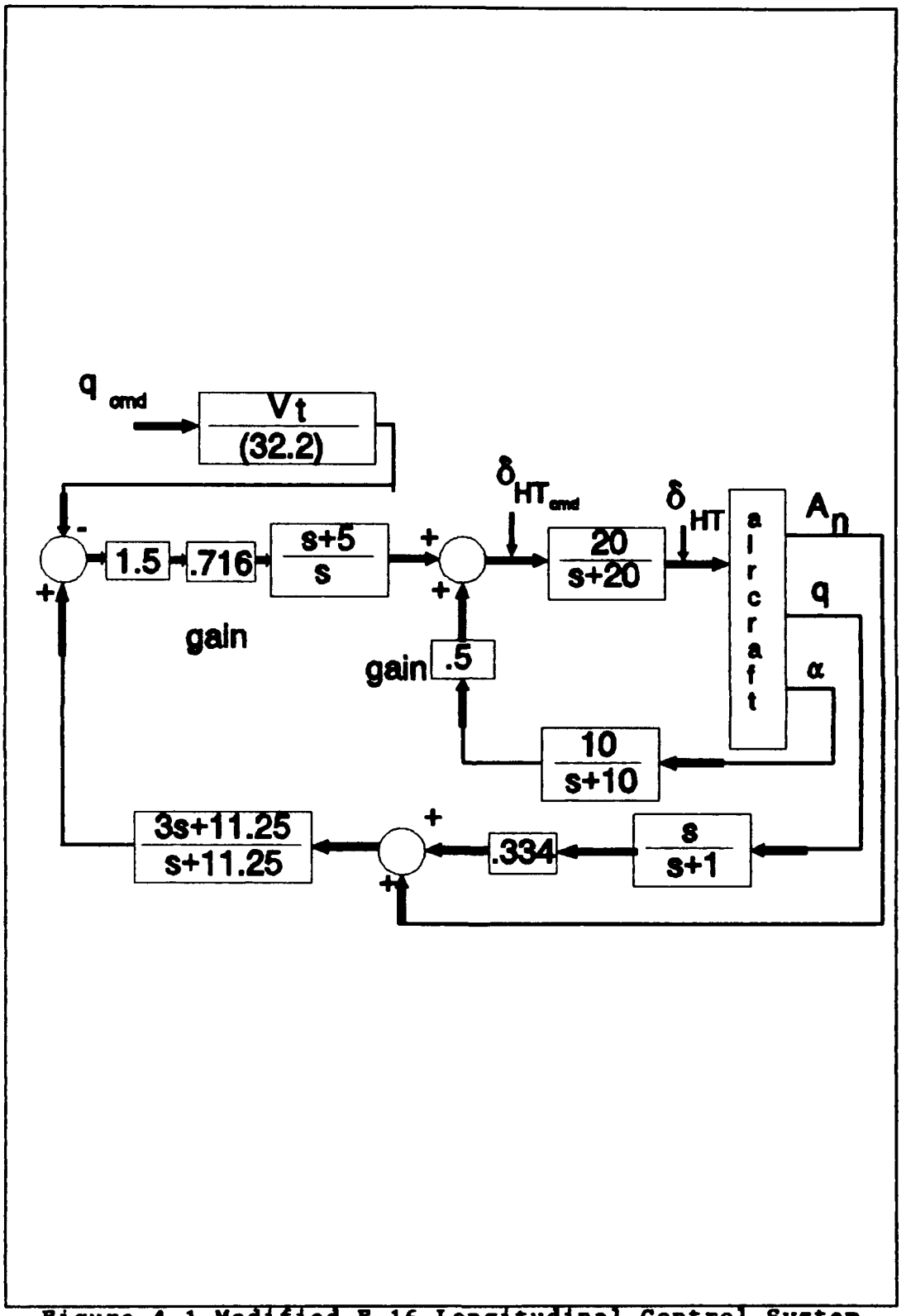

Figure 4-1 Modified F-16 Longitudinal Control System

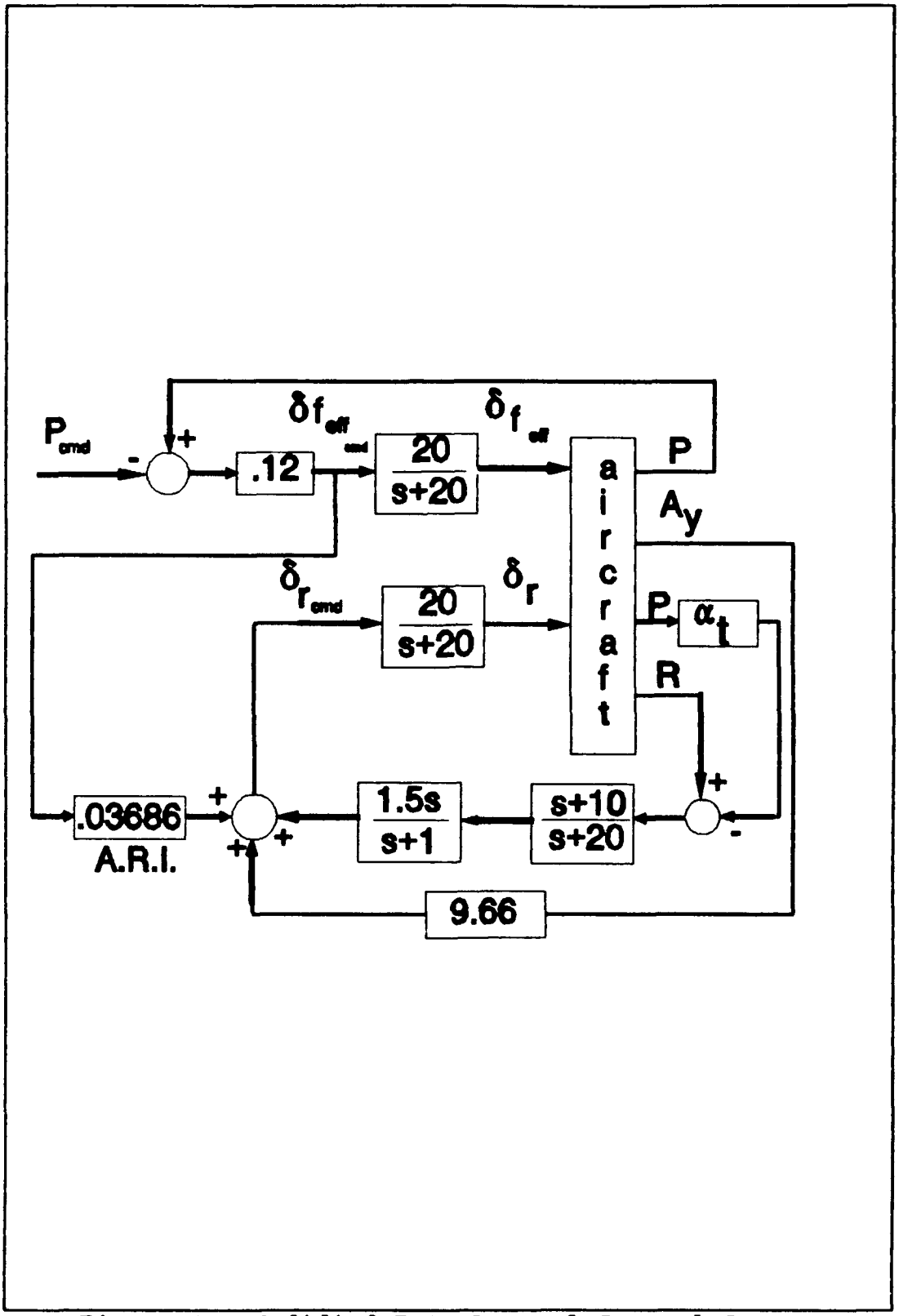

Figure 4-2 Modified F-16 Lateral Control System

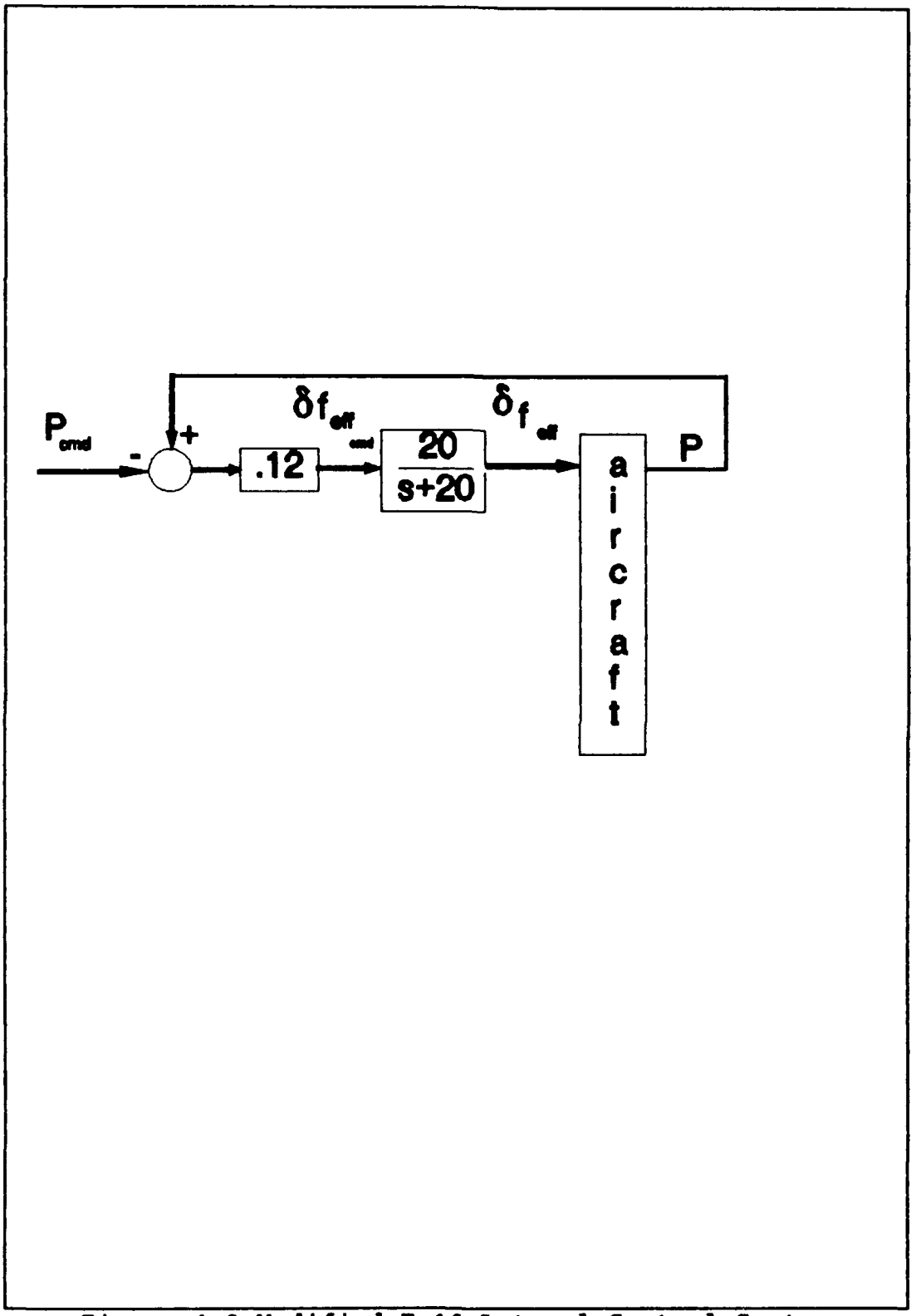

Figure 4-3 Modified F-16 Lateral Control System with a Failed Rudder

X_a is 14.0 feet. The next step is to build the measurement matrices, C and D, associated with the plant. Referring to figure 4-1, 4-3, and equation 4-5, the measurement matrices become:

$$[Y] = \begin{bmatrix} 0 & 1 & 0 & 0 & 0 & 0 & 0 & 0 & 0 \\ 0 & 0 & 0 & 1 & 0 & 0 & 0 & 0 & 0 \\ 0 & 0 & 0 & 0 & 1 & 0 & 0 & 0 & 0 \\ - & - & - & - & A_{n1} & - & - & - & - \end{bmatrix} [X] + \begin{bmatrix} 0 & 0 \\ 0 & 0 \\ 0 & 0 \\ - & A_{n2} \end{bmatrix} [\delta_i] \qquad (4\text{-}6)$$

where A_{n1} and A_{n2} are :

$$A_{n1} = \left(\frac{-V_0}{32.2}\right) a(2,i) + \left(\frac{X_a}{32.2}\right) a(5,i) - \left(\frac{-V_0}{32.2}\right) [0\ 0\ 0\ 0\ 1\ 0\ 0\ 0\ 0] \qquad (4\text{-}7)$$

$$A_{n2} = \left(\frac{-V_0}{32.2}\right) b(2,j) + \left(\frac{X_a}{32.2}\right) b(5,j)$$

with i = 1, 2, 3, ..., 9, j= 1, 2, and a(2,i), a(5,i), b(2,j), b(5,j) representing the second and fifth row of elements of the A and B matrix developed in Chapter III. Therefore the final open loop system can be represented by

$$\dot{X} = A X + B U \qquad (4\text{-}8a)$$

$$\underline{y} = C\,\underline{x} + D\,\underline{u} \qquad (4\text{-}8b)$$

In order to prevent implicit algebraic equations while deriving the closed loop system, the state vector, X, can be redefined by including the control deflection into the state and the actuator model into the input. This will then lead to

$$\dot{\underline{x}}' = A'\,\underline{x}' + B'\,\underline{u}' \qquad (4\text{-}8c)$$

$$\underline{y}' = C'\,\underline{x}' \qquad (4\text{-}8c)$$

where the D matrix is part of C'.

Controller Development

The feedback and feedforward paths shown in Figure 4-1 and 4-3 can be expressed as a matrix in the Laplace domain in terms of the aircraft inputs and outputs as

$$\begin{bmatrix} \delta_{HT} \\ \delta_{Feff} \end{bmatrix} = \begin{bmatrix} \dfrac{1.056(s+5)(3s+11.25)}{s(s+11.25)} & 0 \\ \dfrac{4.2}{(s+10)} & 0 \\ 0 & .12 \\ \dfrac{0.353(s+5)(3s+11.25)}{(s+1)(s+11.25)} & 0 \end{bmatrix}^T \begin{bmatrix} A_n \\ \alpha \\ p \\ q \end{bmatrix} + \begin{bmatrix} \dfrac{-20.99(s+5)}{s} & 0 \\ 0 & -0.12 \end{bmatrix} \begin{bmatrix} q_{cmd} \\ p_{cmd} \end{bmatrix} \qquad (4\text{-}9)$$

The transformation of the matrix from the Laplace domain to the time domain can be done by transforming each Laplacian element into a state space phase variable canonical form [13:210-215]. The transformation in this case was done using the command called tfm2ss of the control analysis computer program called Pro-Matlab, [10]. A minimum realization was also performed on the matrix to remove unnecessary states. The feedforward (subscript E) and feedback (subscript K) in the time domain are shown in equation 4-10a to 4-11b respectively.

$$\dot{\underline{x}}_E = A_E \underline{x}_E + B_E \underline{\delta}_{cmd} \qquad (4\text{-}10a)$$

$$\underline{y}_E = C_E \underline{x}_E + D_E \underline{\delta}_{cmd} = \underline{u}_2 \qquad (4\text{-}10b)$$

$$\dot{\underline{x}}_K = A_K \underline{x}_K + B_K \underline{y} \qquad (4\text{-}11a)$$

$$\underline{y}_K = C_K \underline{x}_K + D_K \underline{y} = \underline{u}_1 \qquad (4\text{-}11b)$$

where

$$\underline{\delta}_{cmd} = [\, q_{cmd} \; p_{cmd} \,]^T \qquad (4\text{-}12a)$$

and

$$\underline{u} = \underline{u}_1 + \underline{u}_2 \qquad (4\text{-}12b)$$

Closed Loop System Derivation

The F-16 utilizes negative input and positive feedback in its control law diagram, as shown in Figures 4-1 and 4-2. This is due to the sign convention which defines a positive deflection of the effective flaperon or the horizontal tail as being trailing edge down. Since the computer program used to get the closed loop state space representation uses negative feedback, the sign of the C and D matrix need to be changed. The block representation of the total system is shown in Figure 4-4. Using Eq (4-10a) through (4-12b), it is now possible to derive the closed loop model of the aircraft.

Substituting equation 4-8d into 4-11a and 4-11b gives

$$\dot{x}_K = A_K x_k + B_k C x' \qquad (4\text{-}13a)$$

$$u_1 = C_K + D_K C x' \qquad (4\text{-}13b)$$

Placing equation 4-12b into 4-8c and substituting 4-13a and 4-13b will lead to

$$\dot{x}' = (A' + B' D_K C') x + B' C_K x_K + B' D_K \delta_{cmd} \qquad (4\text{-}14)$$

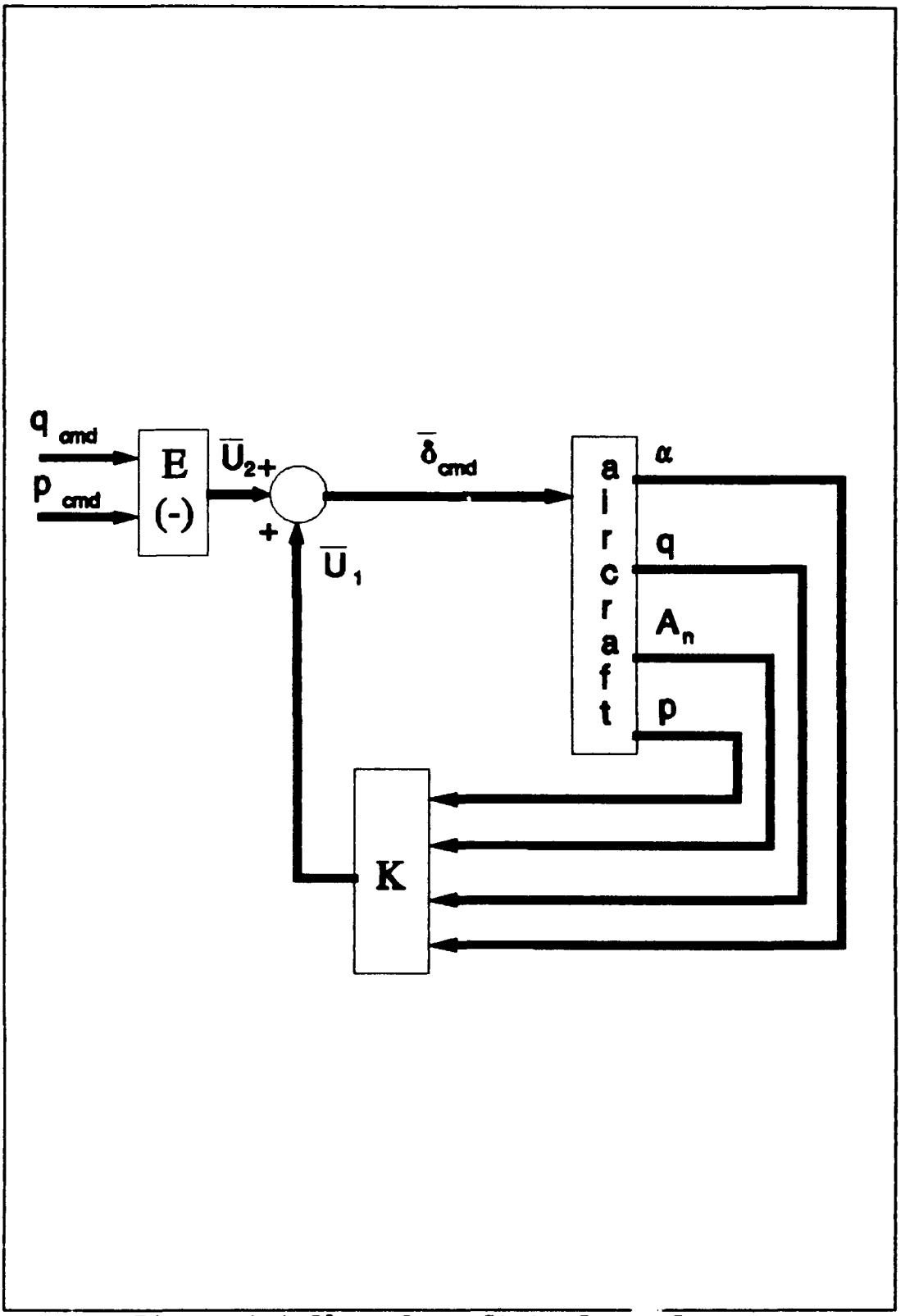

Figure 4-4 Close Loop State Space System

Combining equation 4-10a, 4-14, 4-8d, and 4-13a into matrix form yields

$$\begin{bmatrix} \dot{x}_E \\ \dot{x}' \\ \dot{x}_K \end{bmatrix} = \begin{bmatrix} A_E & 0 & 0 \\ B' C_E & A' + B' D_K C' & B' C_K \\ 0 & B_K C' & A_K \end{bmatrix} \begin{bmatrix} x_E \\ x' \\ x_K \end{bmatrix} + \begin{bmatrix} B_E \\ B' D_E \\ 0 \end{bmatrix} [\delta]_{cmd} \tag{4-15}$$

$$y = \begin{bmatrix} 0 & C' & 0 \end{bmatrix} \begin{bmatrix} x_E \\ x' \\ x_K \end{bmatrix} \tag{4-16}$$

Using Equation 4-15 and 4-16 it is now possible to determine the characteristics of the closed loop system. Appendix F shows an example of one open loop and closed loop systems for one trim condition of case B.

Summary

In this chapter the closed loop system was derived using a modified controller that takes into account the failed rudder. The eigenvalues can then be calculated for each case and failure. The open loop and closed loop eigenvalues can be compared to determine the effectiveness of the controller. Analysis of the results is performed in the following chapter.

V. DISCUSSION OF RESULTS

Introduction

In the previous chapter, the closed loop plant for the F-16 aircraft was derived considering a damaged rudder. The model is used to determine, for each rudder failure and trim condition, the closed loop eigenvalues of the system. A physical explanation is given on the behavior of the system and its implication on the aircraft dynamic stability.

Eigenvalues of the Closed Loop System

Using the controller developed in the previous chapter, the eigenvalues for each rudder failure and trim condition are calculated. Since the linearization of the equations of motion presented in Appendix D includes cross coupling derivatives and asymmetric trim condition, the results obtained from the closed loop system are dependent on the angle of attack (α), the sideslip angle (β), and the bank angle (Φ). Table 3-4 in Chapter III also describe Figures 5-1 to 5-8.

Longitudinal Motion

For case A, the closed loop eigenvalues for a rudder failure of 0 and -10 degrees are presented in Figures 5-1 and 5-2. The controller in this case does not significantly

change the location of the eigenvalues close to the imaginary axis.

If the rudder fails at zero degrees for Case B, Figures 5-3 and 5-4 show the migration of the eigenvalues from β_1= 0 degrees, Φ_1= 0 degrees, α_1= 3.17 degrees to β_2= -3.3 degrees, Φ_2= -5 degrees, α_2= .8 degrees. The phugoid complex conjugate eigenvalues remain very close to the origin (d), for both the open and closed loop system, since they depend primarily on aircraft velocity, which does not vary significantly. At various β, the closed loop phugoids become unstable with a natural frequency around 0.06 radians/second. This instability can easily be compensated by pilot. This is also true for rudder failure less than 0 degrees as seen in Figures 5-5 to 5-8.

The short period oscillations (b) in the open loop case presented in Figure 3-2 are lightly damped. By introducing the controller, their damping decrease where they become unstable for values of β between -2.17 and -1.28 degrees as shown on Figures 5-3 and 5-4. For rudder failure of -10 degrees the instability occurs for values of β between -2.66 and -0.7 degrees. As the aircraft moves away from a wings level trim condition, α decreases and the bank angle becomes less than zero degrees, which means the stability derivatives related to α are affected. Since the model uses fixed dynamic stability derivatives, the natural frequency will tend to decrease and the damping will eventually

increase (for β less than -2.17 degrees for a 0 degrees rudder failure) as the absolute value of the stability derivatives related to α decrease [6:309]. For a rudder failure of less than -20 degrees, the short period roots are pairing with the controller roots, and two distinct motions appear as shown on Figures 5-7 and 5-8. The sideslip angle (β) at which those motions occur is less than -7 degrees, which is outside the boundary defined earlier.

Lateral Motion

In Figure 4-3, the controller has lost the ability to feedback any signal to the rudder. This effect is seen in the dutch roll behavior in Figures 5-1 to 5-8. Compared to the open loop case, the controller basically decreases the dutch roll damping since it has lost the ability to feedback either roll rate or side acceleration to the rudder. Since feeding back the roll rate, in this case, decreased the time constant of the spiral, this also had the effect of decreasing the dutch roll damping. As β moves away from a zero degrees value, the real part of the dutch roll tends to stay stationary while the magnitude of the imaginary part increases. As β becomes smaller, the dutch roll natural frequency increases and its damping decreases.

The spiral root for the closed loop case couples with a controller root to create a pair of complex conjugate roots near the origin. As β decreases, the roots move away from

the origin and create a lateral short period oscillation before returning to the real axis. For rudder failures less than -10 degrees, the complex conjugate roots break on the real axis where they become real as seen on Figure 5-5.

The roll also couples with one of the controller roots. The effect encountered from that coupling is only apparent for rudder failure less than -10 degrees as seen on Figure 5-5. A complex conjugate root is formed, moving away from the origin, which produces a lateral short period oscillation. As β decreases, the roots break into the real axis for β less than -3.7 degrees.

For a rudder failure less than -20 degrees, the real roots located on the real axis couple to form a short period lateral oscillation.

For case A, closed loop system instability occurs for various values of β. This instability is generated by the phugoid root. This is not critical since the natural frequency of the phugoid (around .06 radians/second) is such that the pilot can easily compensate for it.

Discussion of Results

Even if the aircraft can be trimmed for specific rudder failure, the present controller modeled in Chapter IV puts restrictions on the dynamic stability of the aircraft. For the open loop system, the eigenvalues determined for both cases gave a stable system for β less than -6 degrees. Since

the controller loses the ability to use the rudder, the control laws are altered. With the present controller, case A is stable if it is assumed that the pilot can compensate for the phugoid instability generated. For case B, not taking into account the phugoid, the failure permitted with the present controller is as follows:

Case B, 0 degrees rudder failure: the aircraft is stable except for $-2.2 < \beta < -1.3$ degrees.

Case B, -10 degrees rudder failure: the aircraft is stable except for $-2.7 < \beta < -0.9$ degrees.

Case B, -20 degrees rudder failure: the aircraft is stable for $-6.0 < \beta < -3.3$ degrees.

Case B, -25 degrees rudder failure: the aircraft is stable for $-6.0 < \beta < -4.9$ degrees.

In Chapter IV, the concept of controllability was presented. For each trim condition, the open loop plant and input matrices were evaluated for controllability. All were controllable with the available input. Therefore, it would be possible to redesign the controller in order to prevent the instability of the closed loop system. One of the important factors would rest in the control power still remaining at specific trim condition.

Summary

For both cases, the phugoid introduced instability. Since the frequency of the phugoid is low, it was assumed that the pilot would be able to compensate. For case A, the trim regions for both rudder failure types were dynamically stable. For case B, specific trim areas within each rudder failure types are to be avoided. This was determined using the modified controller presented in figure 4-1 and 4-3. Reconfiguration of the control laws could be done to increase the trim envelope. The only limiting factor would be the control power still remaining after the aircraft is trimmed.

This analysis presented an appreciation of the different types of motion that might be encountered when the aircraft needs to be trimmed at different sideslip angles due to a rudder failure.

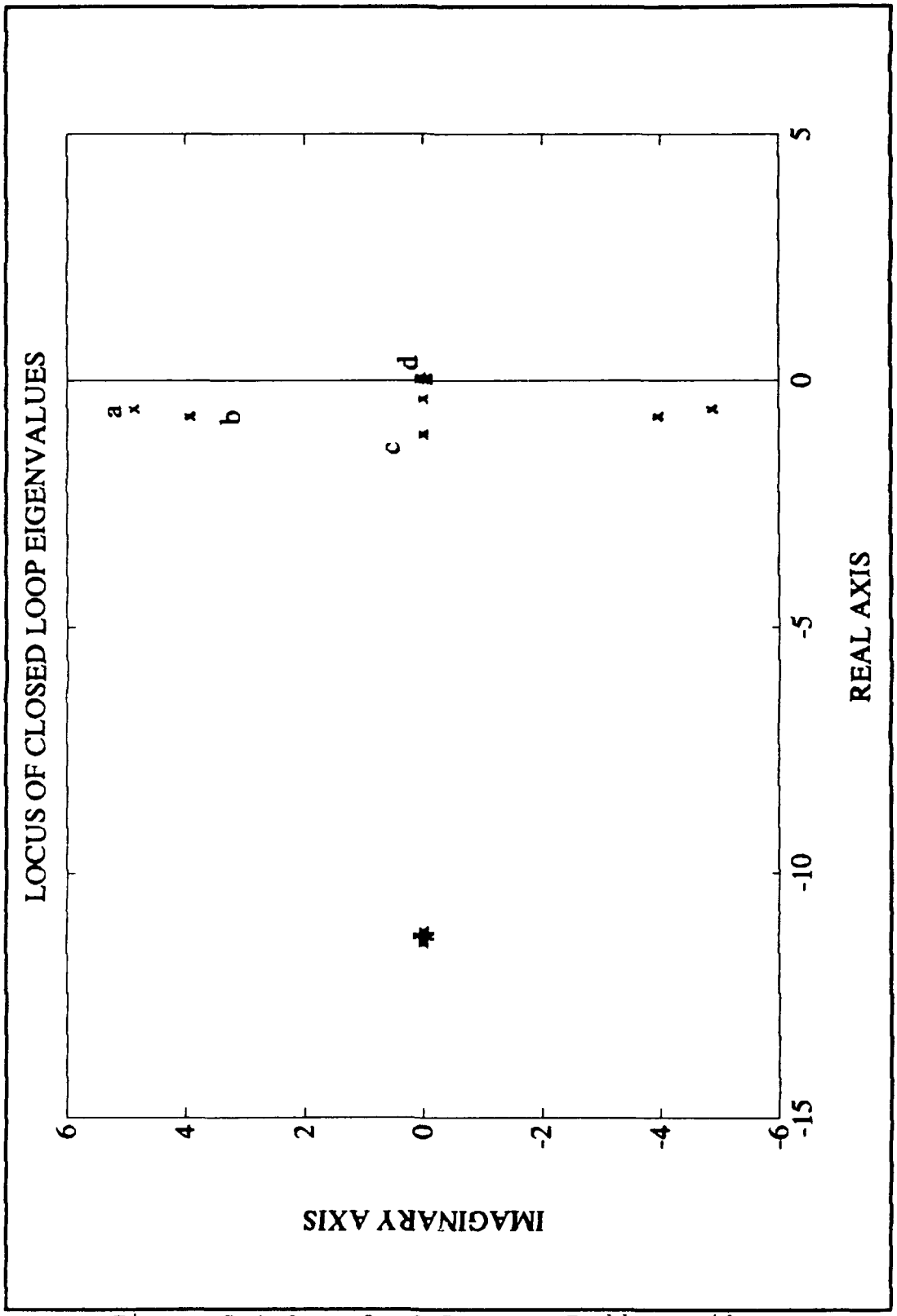

Figure 5-1 Case A 0 Degrees Rudder Failure

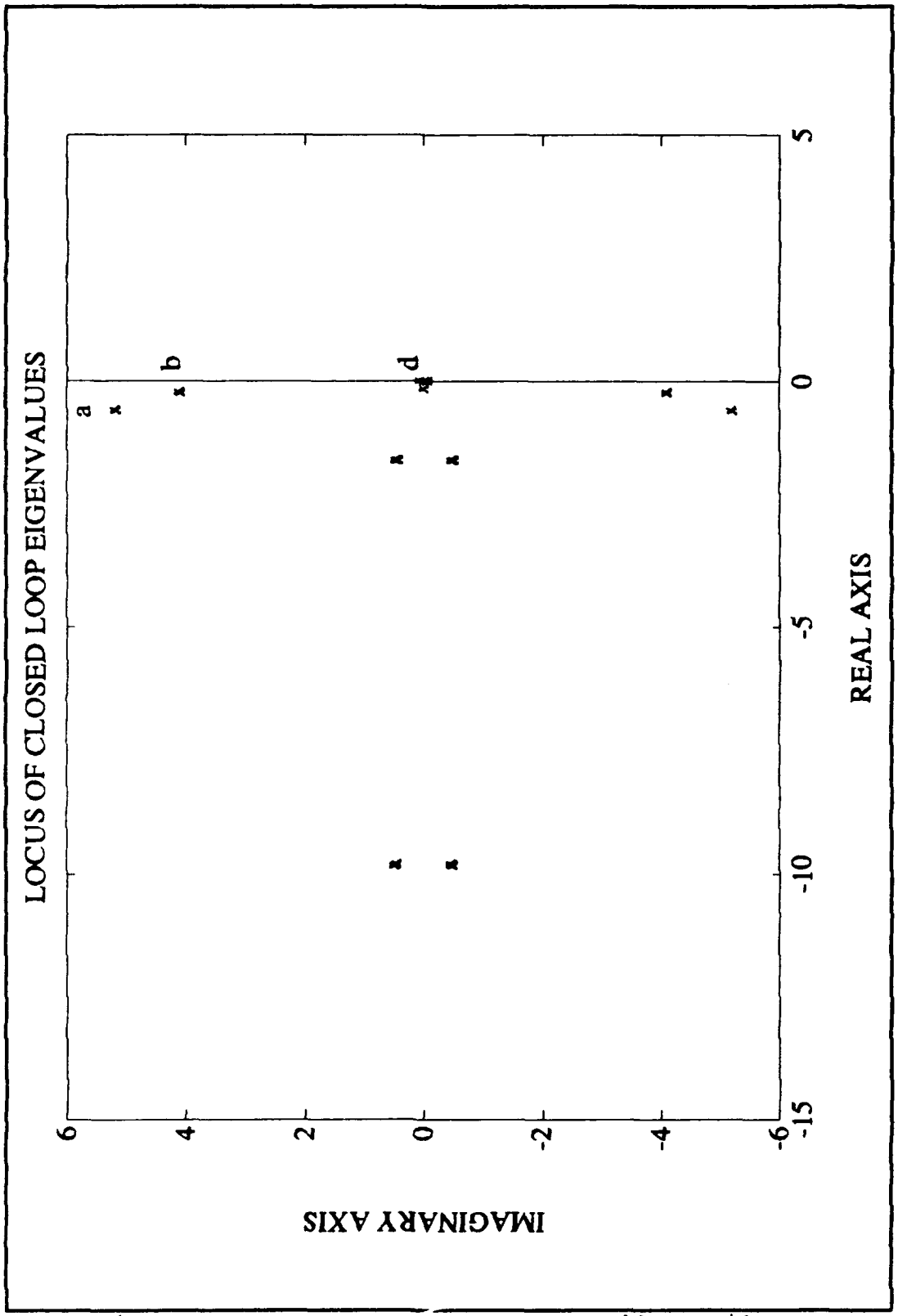

Figure 5-2 Case A -10 Degrees Rudder Failure

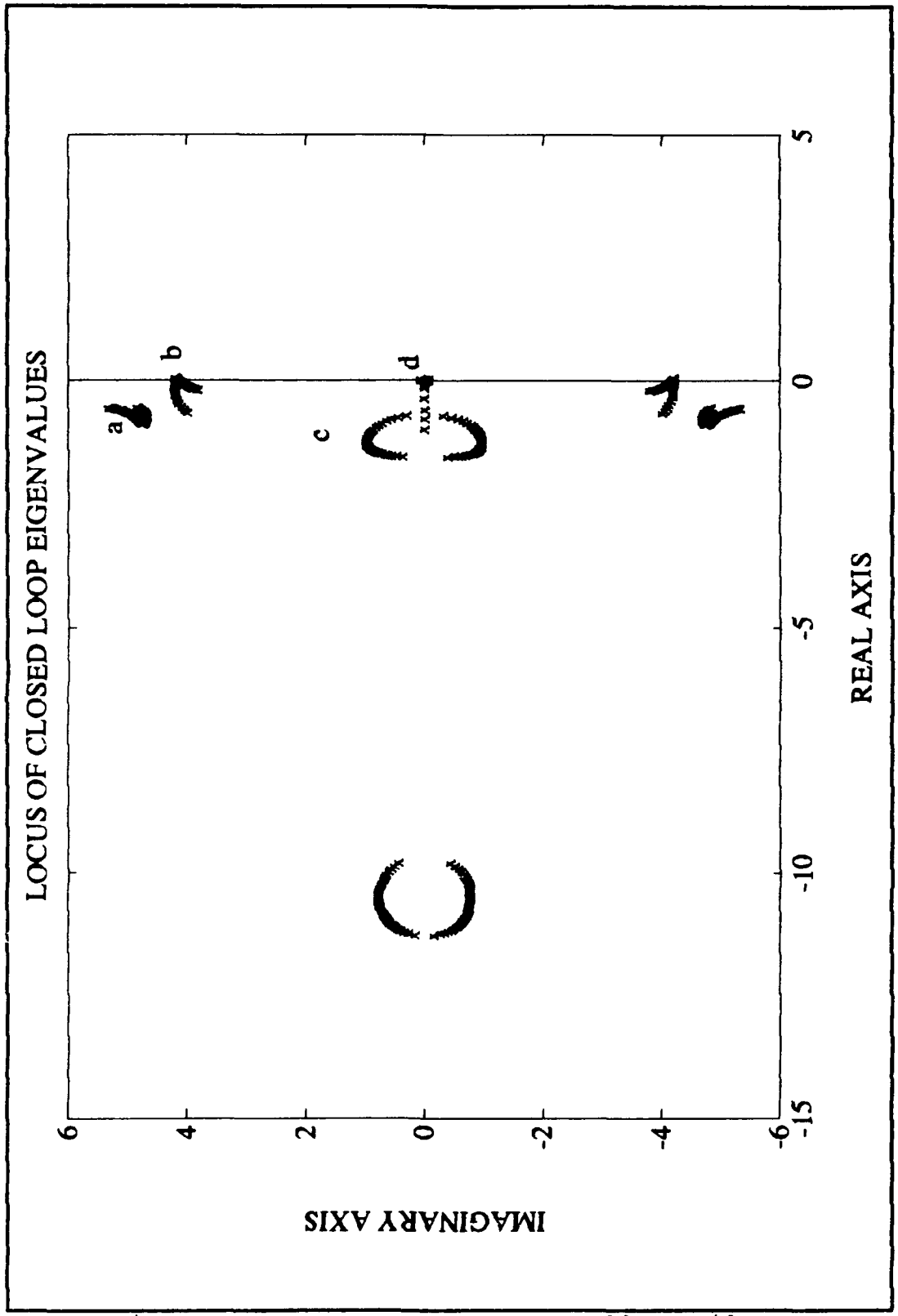

Figure 5-3 Case B 0 Degrees Rudder Failure

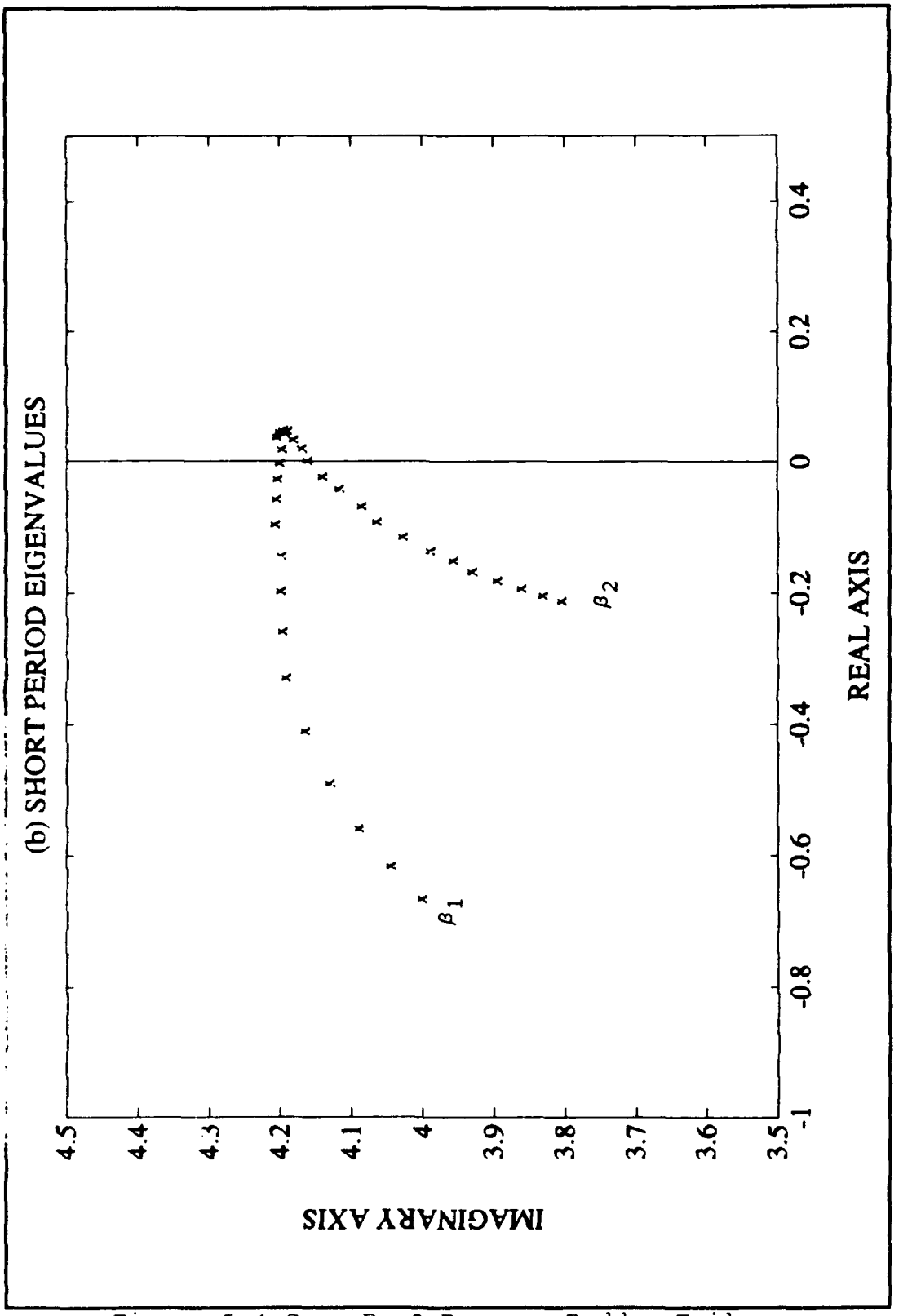

Figure 5-4 Case B 0 Degrees Rudder Failure

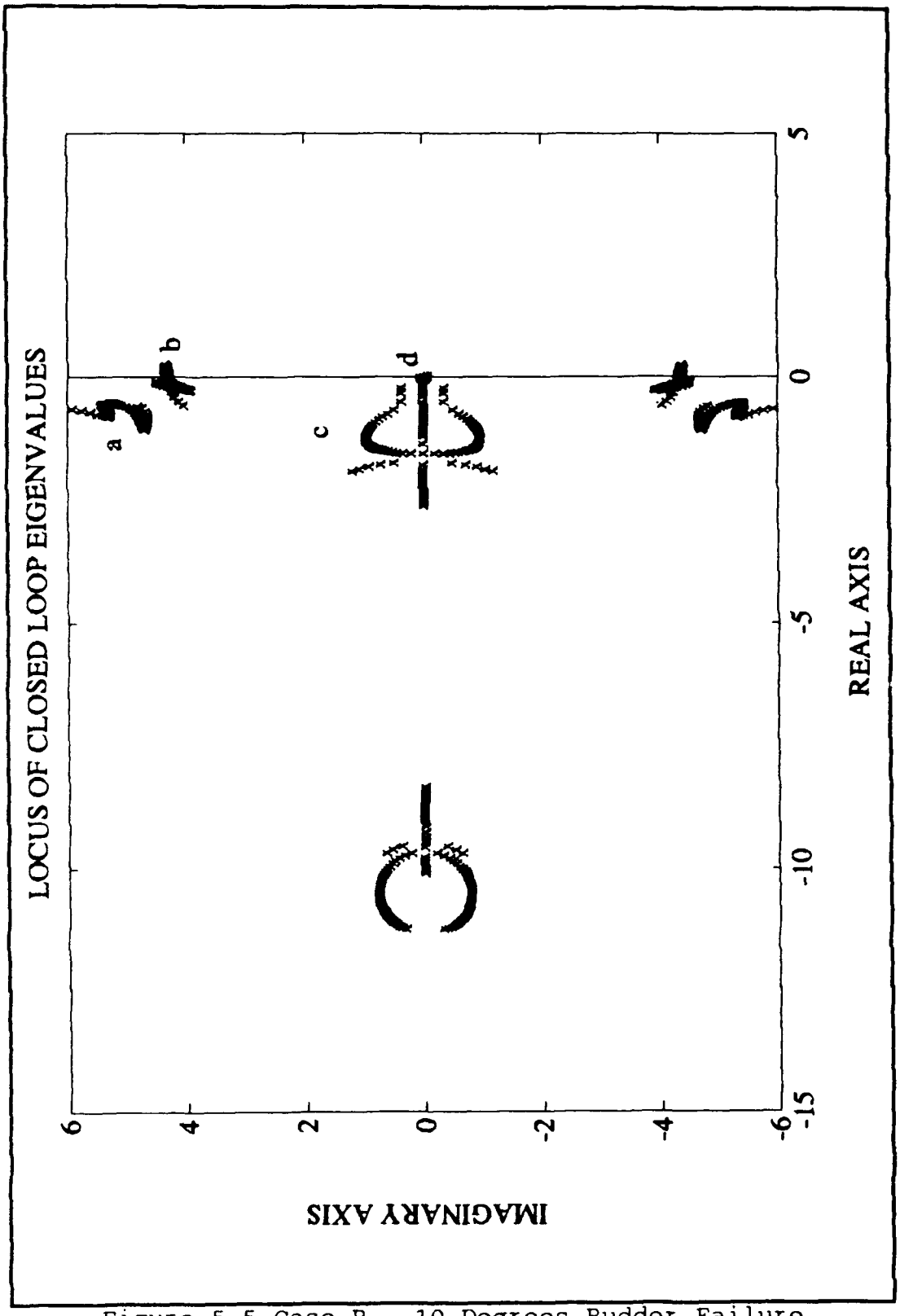

Figure 5-5 Case B -10 Degrees Rudder Failure

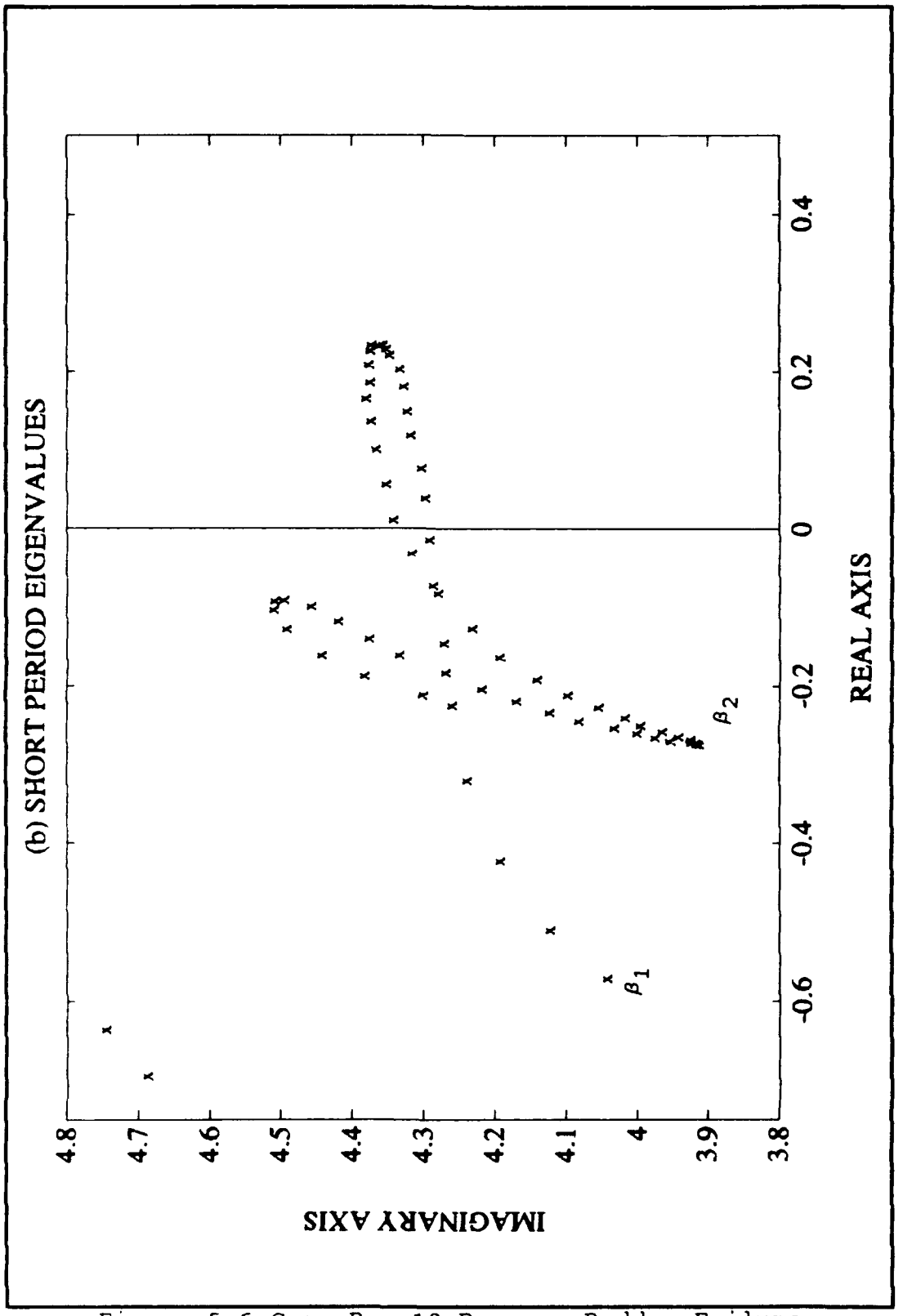

Figure 5-6 Case B -10 Degrees Rudder Failure

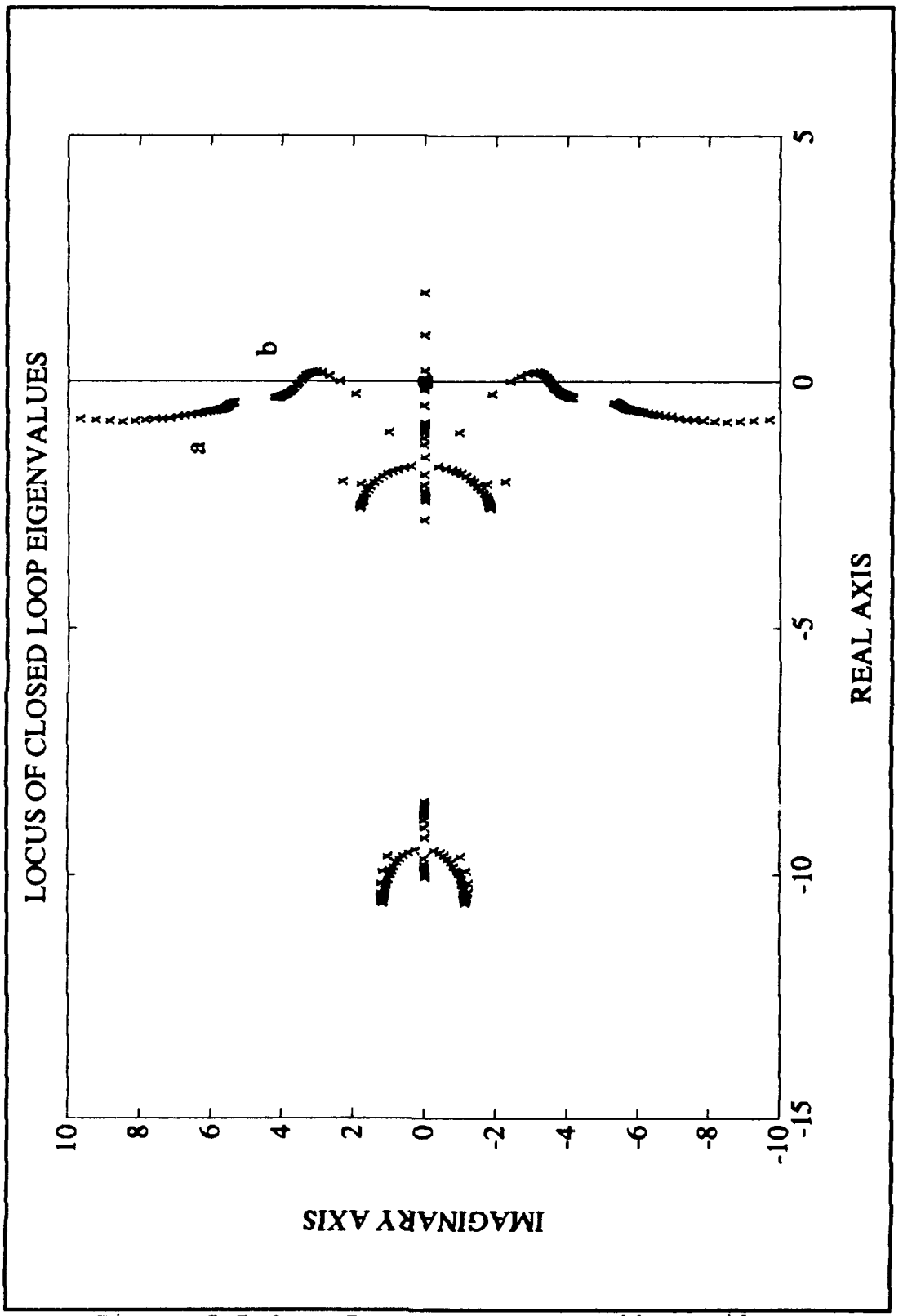

Figure 5-7 Case B -20 Degrees Rudder Failure

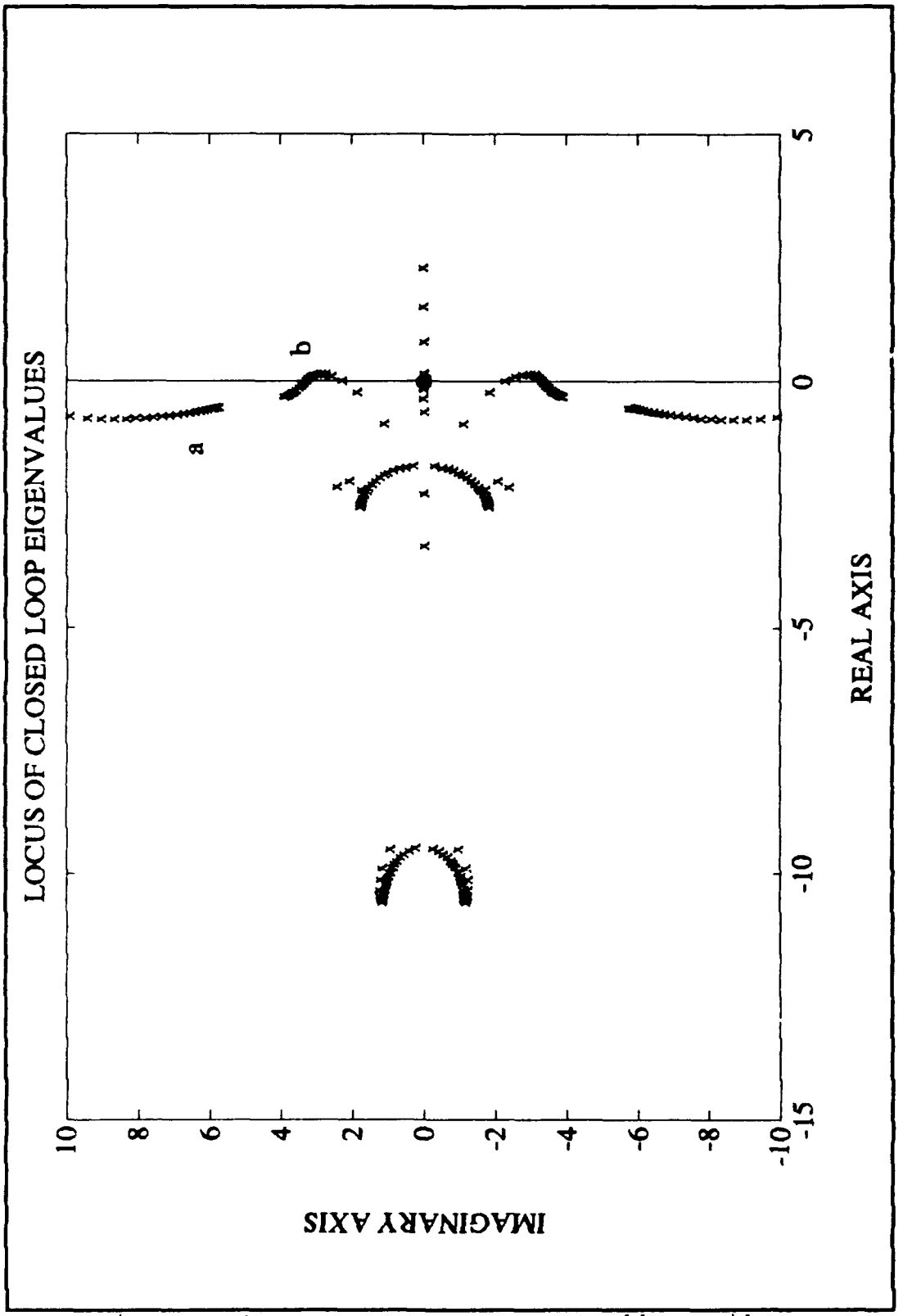

Figure 5-8 Case B -25 Degrees Rudder Failure

VI. CONCLUSIONS AND RECOMMANDATIONS

In Chapter I, it was stated that this research would investigate the dynamic stability characteristics of an aircraft which has sustained failure of a primary control surface. This analysis was done by using existing data to determine specific trim conditions and to evaluate the cross coupling derivatives to be included in a linearized aircraft model. A modified controller was then added to the aircraft model to evaluate the closed loop response of the system. Using the results of the closed loop dynamic characteristics, the trim regions were modified to represent the damaged aircraft. The following paragraphs provide a summary of the observations and conclusions of this research.

Trim Area

Equilibrium analyses was performed for two specific control implementations. The first used the actual control surface actuation scheme of the basic F-16 aircraft. The second permitted the horizontal tail aileron to deploy independently from the flaperon. The first case only allowed trim of the aircraft for a rudder failure between 0 and -10 degrees. The second case allowed trimming the aircraft for the worst case rudder failure analyzed (-25 degrees).

Plant Model

When the equilibrium areas were determined, they were used as input to the linearized equations of motion of the aircraft. The model included only cross coupled static stability derivatives. The aircraft plant matrices were produced. The eigenvalues of the plant were determined to evaluate the dynamic stability of the system for each trim condition. It was observed that the plant matrices were all dynamically stable for β less than -6 degrees at the given trim conditions. It was also noted that for all trim conditions, the system was controllable. Therefore, it is possible to improve the aircraft response even if it has sustained damage to its rudder.

Closed Loop System

The controller developed for the closed loop system took into consideration the damaged rudder. It was interesting to note that the controller was the limiting factor in this analysis since the closed loop system was dynamically unstable for some trim regions and rudder failures. The results also showed the coupling that took place when trimmed in an unsymmetrical orientation. As β decreases, the roll angle, Φ, decreases which introduces strong coupling between the lateral and longitudinal motion. This was observed by analyzing the eigenvalues of the closed

loop system. Satisfactory aircraft dynamic response would require restructuring the control laws since the present controller limits the aircraft.

Recommendation

During the course of this thesis, several areas of interest emerged which would provide better understanding of the problem of a control surface failure. They are:

1. The same analysis could be performed without using cross coupling stability derivatives. This would provide a baseline to evaluate their effect on the aircraft motion.
2. The inclusion of the cross coupling dynamic stability derivatives into the model would represent the plant more accurately.
3. Development of a new controller would also permit the aircraft to sustain damage to a primary control surface by using greater independence of each control.
4. Only rectilinear flight was analyzed in this research. Other flight conditions could also be analyzed to determine if there are preferred trajectories that could expand the trim envelope.

The first recommendation could easily be performed by removing the cross coupling stability derivatives from the actual plant model. This would permit the evaluation of the

impact of the different derivatives on the model.

The second recommendation would require the availability of the dynamic cross coupling derivatives. For the trim conditions evaluated in this thesis, it would be interesting to see if those cross coupling derivatives have a noticeable effect on the observed motion.

The third recommendation would imply the redesign of the aircraft control laws around the cases investigated, which is a major task since several trim condition were analyzed.

In the last recommendation, combinations of aircraft trajectories could also be evaluated together in order to achieve quasi-rectilinear flight.

APPENDIX A

F-16 Layout, Sign Conventions, and Axis Definitions

Figure A-1 shows a diagram of the general three-view layout of the F-16. Figure A-2 defines the aircraft axis systems, and the angles used to differentiate between them. Control surface deflection conventions are also shown since definitions for positive deflection are not universal. A graphical representation of the different axis system is also given.

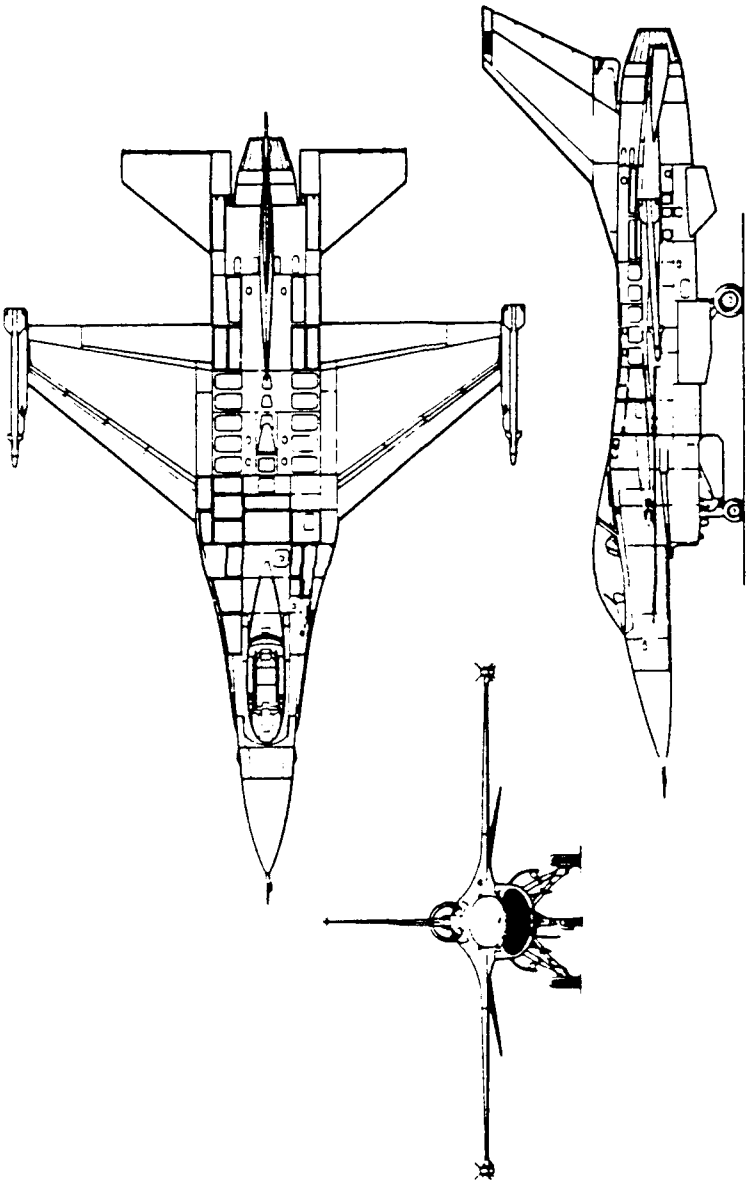

Figure A-1 F-16 Layout and General Arrangement

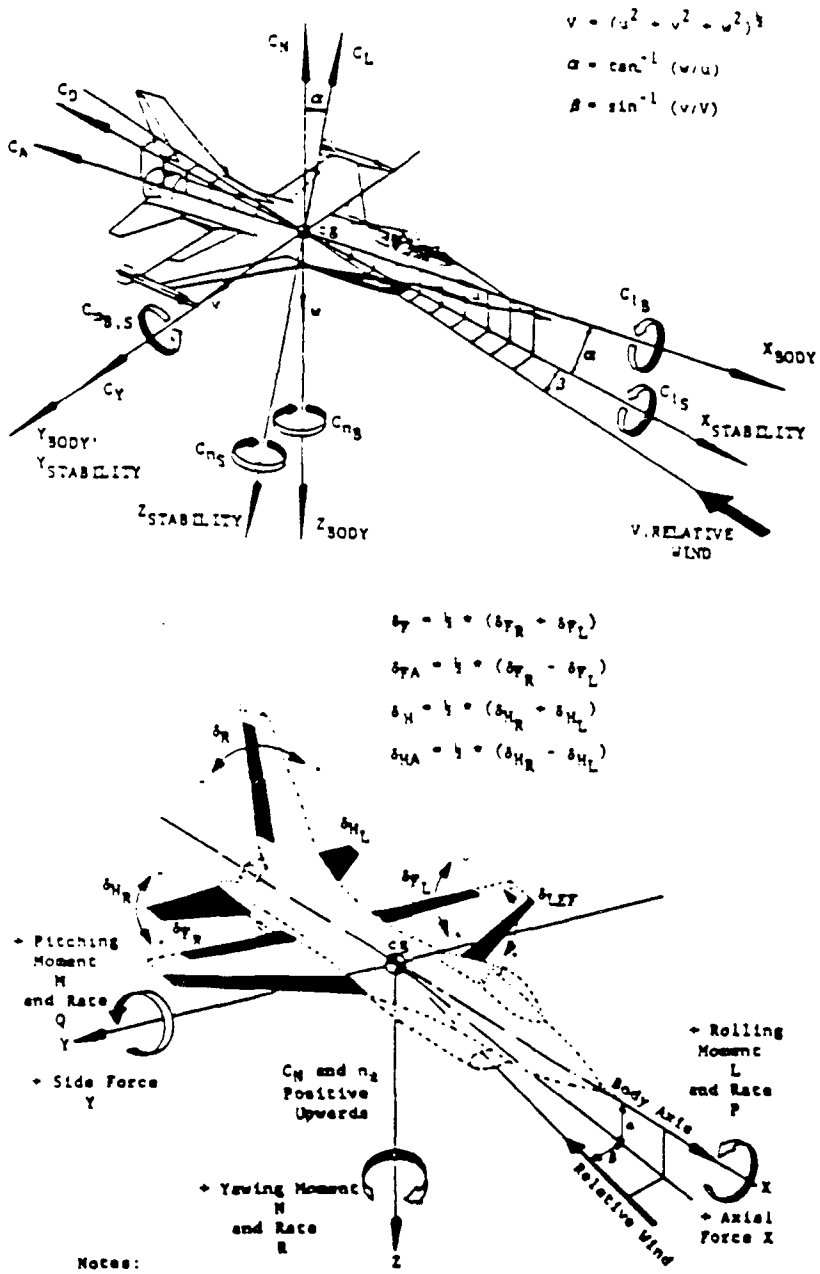

Notes:

(1) A positive control force produces a negative surface deflection and causes a positive moment about each axis.

(2) For each individual control surface, trailing-edge down (left) is positive.

(3) Leading-edge flap position is measured streamwise. All other positions are measured with respect to the hinge-line.

Figure A-2 Axis System and Sign Conventions

APPENDIX B

STATIC AIRCRAFT STABILITY DERIVATIVES

Included in this appendix are the functionnal forms of the F-16 static stability derivatives found by Zaiser [5]. The derivatives are used in the trim analysis and in the state-space model of the aircraft. Each set contain the following information:

1. The control surface, i.e. zero, left leading edge flap, etc.
2. The force or moment.
3. The correlation between the experimental data and its functional form.
4. The number of terms in the polynomial.

The columns of the data file contain the following information:

1. Number of the polynomial term
2. Power on the α term
3. Power on the β term
4. Power on the δ term
5. The coefficient associated with that term

```
zero
lift
0.99895786134833
8
 01    00    00    00 0.02425990
 02    00    01    00 0.01176668
 03    00    02    00 0.02273735
 04    00    03    00 -.00062970
 05    00    04    00 -.00059456
 06    01    00    00 0.07041496
 07    01    02    00 -.00001098
 08    02    00    00 -.00029655

zero
drag
0.99922396997176
12
 01    00    00    00 0.00989113
 02    00    01    00 0.00030617
 03    00    02    00 0.00082931
 04    00    03    00 -.00002382
 05    00    04    00 -.00002320
 06    01    00    00 -.00090749
 07    01    01    00 0.00017652
 08    01    02    00 0.00036501
 09    01    03    00 -.00001032
 10    01    04    00 -.00000963
 11    02    00    00 0.00114791
 12    02    01    00 0.00000162

zero
side
0.98699308975102
8
 01    00    00    00  .00000000
 02    00    01    00 -.01817564
 03    00    02    00 0.00011201
 04    00    03    00 -.00003593
 05    01    00    00 -.00007302
 06    02    00    00 0.00001572
 07    02    01    00 0.00000599
 08    03    00    00 -.00000196
```

```
zero
pitch
0.99941958860318
9
 01    00    00    00 0.00912623
 02    00    01    00 -.00372458
 03    00    02    00 -.00697840
 04    00    03    00 0.00019974
 05    00    04    00 0.00018126
 06    01    00    00 -.01944657
 07    01    01    00 -.00003131
 08    01    02    00 -.00001042
 09    02    00    00 -.00011202

zero
roll
0.97148373462692
12
 01    00    00    00 0.00000000
 02    00    01    00 -.00206500
 03    00    02    00 0.00002188
 04    00    03    00 0.00000592
 05    01    00    00 0.00003762
 06    01    01    00 -.00001006
 07    01    02    00 0.00000007
 08    01    03    00 0.00000037
 09    02    00    00 0.00000083
 10    02    01    00 0.00000072
 11    02    02    00 -.00000005
 12    02    03    00 0.00000003

zero
yaw
0.99450857443165
9
 01    00    00    00 0.00000000
 02    00    01    00 0.00598800
 03    00    02    00 -.00005049
 04    01    00    00 -.00008376
 05    01    01    00 0.00006041
 06    01    02    00 0.00000241
 07    02    00    00 -.00000379
 08    02    01    00  .00000559
 09    03    00    00 -.00000044

lie
lift
0.99911018902596
3
 01    00    00    01 -.00080409
 02    01    00    01 0.00000181
 03    00    01    01 -.00009354
```

```
lle
drag
0.99558264659623
3
 01    00    00    01 0.00023239
 02    01    00    01 0.00011567
 03    00    01    01 0.00001087

lle
side
0.99268840957863
3
 01    00    00    01 0.00003387
 02    01    00    01 -.00004212
 03    00    01    01 -.00003871

lle
pitch
0.99928094340029
3
 01    00    00    01 -.00017172
 02    01    00    01 -.00002018
 03    00    01    01 0.00004164

lle
roll
0.94950568502171
3
 01    00    00    01 -.00006718
 02    01    00    01 0.00001683
 03    00    01    01 -.00000630

lle
yaw
0.98693954647448
3
 01    00    00    01 -.00002596
 02    01    00    01 0.00001220
 03    00    01    01 0.00001053

rle
lift
0.99942437477478
3
 01    00    00    01 -.00092112
 02    01    00    01 0.00005393
 03    00    01    01 0.00006637
```

```
rle
drag
0.99902917949565
3
 01    00    00    01 0.00066338
 02    01    00    01 -.00009976
 03    00    01    01 0.00002005

rle
side
0.99129740157611
3
 01    00    00    01 -.00030801
 02    01    00    01 0.00007528
 03    00    01    01 -.00002878

rle
pitch
0.99947325104706
3
 01    00    00    01 -.00029839
 02    01    00    01 -.00001594
 03    00    01    01 -.00004731

rle
roll
0.92814744695374
3
 01    00    00    01 0.00012548
 02    01    00    01 -.00001585
 03    00    01    01 -.00000511

rle
yaw
0.98461215072914
3
 01    00    00    01 0.00017089
 02    01    00    01 -.00003002
 03    00    01    01 0.00001108

lfl
lift
0.99710493885523
3
 01    00    00    01 0.00808747
 02    01    00    01 -.00007270
 03    00    01    01 0.00016236
```

```
lfl
drag
0.99231474275174
3
 01    00    00    01 0.00004459
 02    01    00    01 0.00010485
 03    00    01    01 0.00002147

lfl
side
0.99121786830928
3
 01    00    00    01 0.00005379
 02    01    00    01 0.00002327
 03    00    01    01 -.00001908

lfl
pitch
0.99732533446253
3
 01    00    00    01 -.00220590
 02    01    00    01 -.00000686
 03    00    01    01 -.00014414

lfl
roll
0.94671363142610
3
 01    00    00    01 0.00124298
 02    01    00    01 -.00001534
 03    00    01    01 -.00000591

lfl
yaw
0.99067236168187
3
 01    00    00    01 0.00011910
 02    01    00    01 -.00002654
 03    00    01    01 0.00000969

rfl
lift
0.99710493885523
3
 01    00    00    01 0.00808747
 02    01    00    01 -.00007270
 03    00    01    01 -.00016236
```

```
rfl
drag
0.99231474275174
3
 01    00    00    01 0.00004459
 02    01    00    01 0.00010485
 03    00    01    01 -.00002147

rfl
side
0.99121786830928
3
 01    00    00    01 -.00005379
 02    01    00    01 -.00002327
 03    00    01    01 -.00001908

rfl
pitch
0.99732533446253
3
 01    00    00    01 -.00220590
 02    01    00    01 -.00000686
 03    00    01    01 0.00014414

rfl
roll
0.94671363142610
3
 01    00    00    01 -.00124298
 02    01    00    01 0.00001534
 03    00    01    01 -.00000591

rfl
yaw
0.99067236168187
3
 01    00    00    01 -.00011910
 02    01    00    01 0.00002654
 03    00    01    01 0.00000969

lht
lift
0.99875023115023
3
 01    00    00    01 0.00524917
 02    01    00    01 -.00001946
 03    00    01    01 0.00007021
```

```
lht
drag
0.98700590428333
3
 01    00    00    01 0.00023247
 02    01    00    01 0.00014775
 03    00    01    01 0.00001676

lht
side
0.99372908655258
3
 01    00    00    01 -.00098652
 02    01    00    01 0.00001164
 03    00    01    01 -.00001998

lht
pitch
0.99720293330100
3
 01    00    00    01 -.00712409
 02    01    00    01 0.00000701
 03    00    01    01 -.00009962

lht
roll
0.94875038542011
3
 01    00    00    01 0.00052168
 02    01    00    01 0.00000432
 03    00    01    01 0.00000226

lht
yaw
0.98483418189834
3
 01    00    00    01 0.00055888
 02    01    00    01 -.00002129
 03    00    01    01 0.00001092

rht
lift
0.99875023115023
3
 01    00    00    01 0.00524917
 02    01    00    01 -.00001946
 03    00    01    01 -.00007021
```

```
drag
drag
0.98700590428333
3
 01    00    00    01 0.00023247
 02    01    00    01 0.00014775
 03    00    01    01 -.00001676

rht
side
0.99372908655258
3
 01    00    00    01 0.00098652
 02    01    00    01 -.00001164
 03    00    01    01 -.00001998

rht
pitch
0.99720293330100
3
 01    00    00    01 -.00712409
 02    01    00    01 0.00000701
 03    00    01    01 0.00009962

rht
roll
0.94875038542011
3
 01    00    00    01 -.00052168
 02    01    00    01 -.00000432
 03    00    01    01 0.00000226

rht
yaw
0.98483418189834
3
 01    00    00    01 -.00055888
 02    01    00    01 0.00002129
 03    00    01    01 0.00001092

rud
lift
0.99903585130353
3
 01    00    00    01 -.00003361
 02    01    00    01 0.00000247
 03    00    01    01 0.00000177
```

```
rud
drag
0.97920031383825
3
 01    00    00    01 0.00022245
 02    01    00    01 -.00001533
 03    00    01    01 0.00002796

rud
side
0.99435063831380
3
 01    00    00    01 0.00334111
 02    01    00    01 0.00000440
 03    00    01    01 0.00000386

rud
pitch
0.99715538778147
3
 01    00    00    01 0.00000413
 02    01    00    01 -.00000019
 03    00    01    01 0.00003014

rud
roll
0.98420339634860
3
 01    00    00    01 0.00053189
 02    01    00    01 -.00004126
 03    00    01    01 0.00000001

rud
yaw
0.99464111708521
3
 01    00    00    01 -.00204024
 02    01    00    01 -.00000473
 03    00    01    01 -.00000257
```

APPENDIX C

Equilibrium Area Fortran Code Flow Chart

This Appendix contained the Flow Chart describing the Fortran code used to perform the investigation of the equilibrium area for case A and B. The Flow Chart is seen on Figures C-1 and C-2.

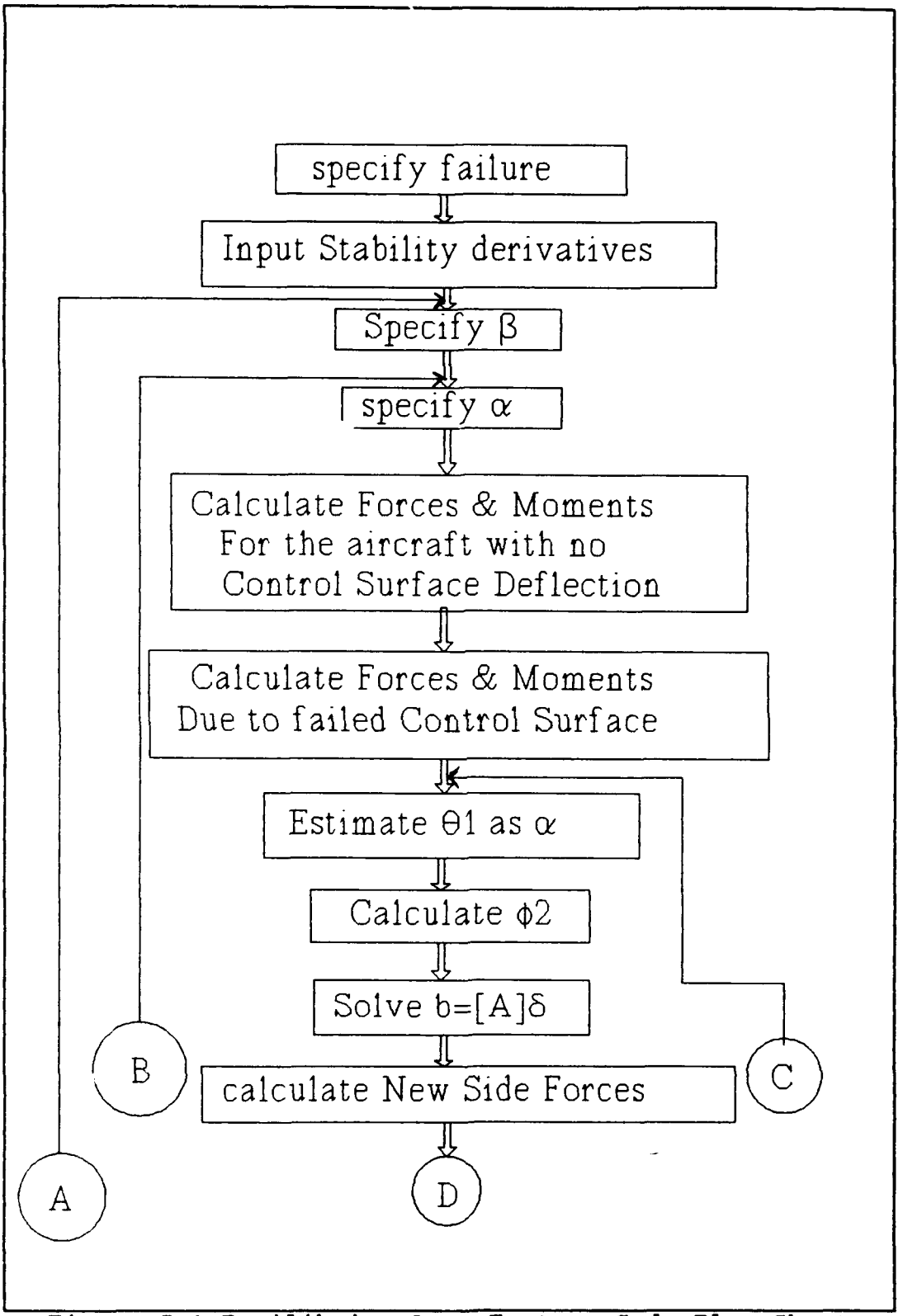

Figure C-1 Equilibrium Area Fortran Code Flow Chart

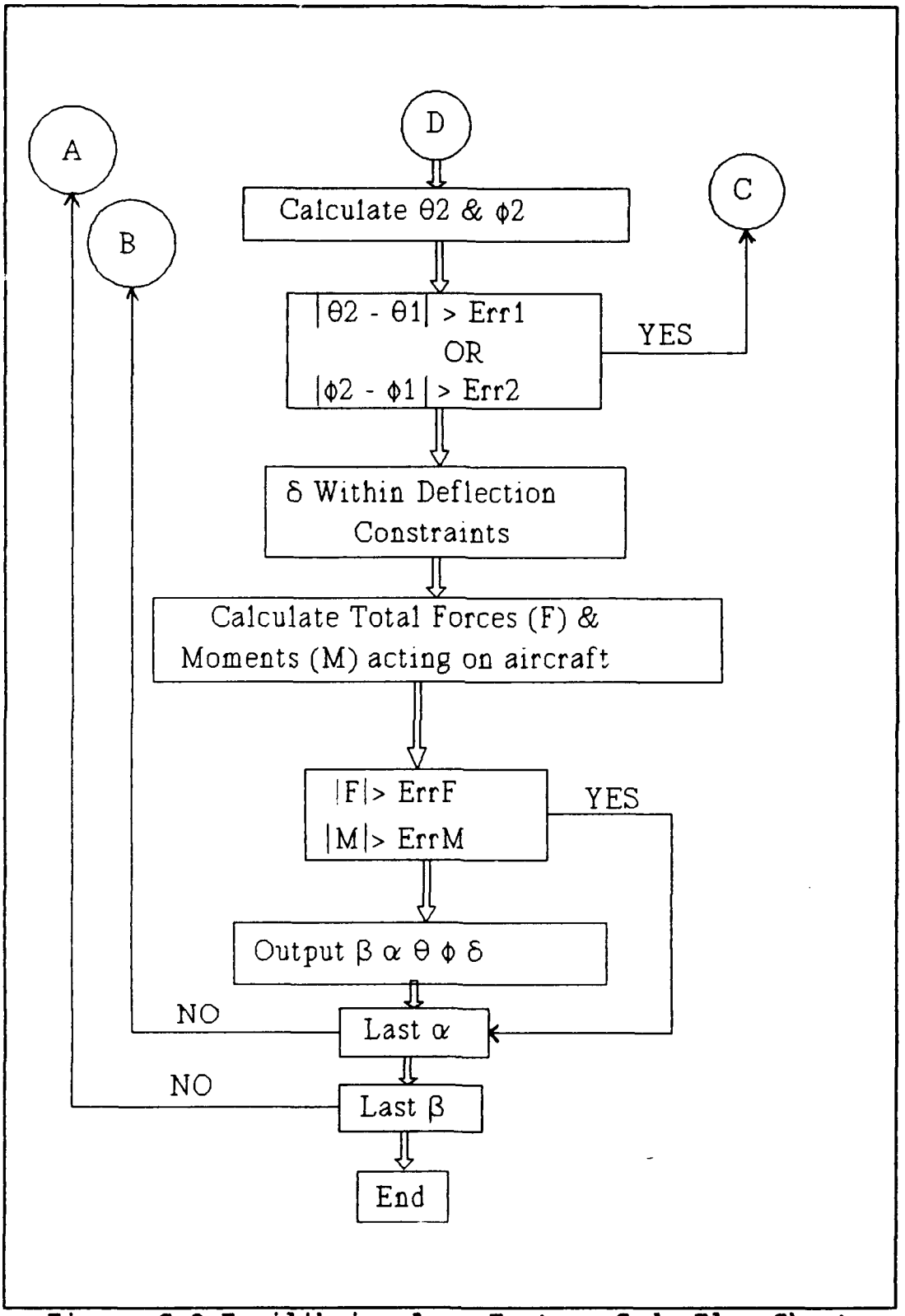

Figure C-2 Equilibrium Area Fortran Code Flow Chart

APPENDIX D

Linearized Equations of Motion

Introduction

In order to gain some insight into the nature of the dynamic stability characteristic of the damaged aircraft, it is necessary to derive the equations that governed the aircraft motion about some nominal condition. This Appendix will take the general equations of motion that are developed by McRuer [6:203-232], linearized them for a rectilinear flight condition, and expands the force and moment terms to include the effect of coupling that are generated by a non zero sideslip angle (β), and bank angle (Φ). The axis systems used in this appendix are the aircraft body axis system, and the stability axis system. A graphical representation of both axis system is shown in Figure A-2 of Appendix A.

Equations of motion

If the airframe is assumed to be a rigid body, the earth to be fixed in space, and the mass and mass distribution of the aircraft constant, the equations of motion, for an aircraft, in the body axis system are given by equation D-1. The kinematic equations that describe the aircraft attitude are given in equation D-2. All force terms

in equation D-1 incorporate the aerodynamic and the thrust forces. Assuming that the aircraft XZ plane is a plane of symmetry (I_{XY} and I_{YZ} equal zero) , equation D-1 can be simplified. The results is shown in equation D-3.

$$
\begin{aligned}
X &= m\,[\,\dot{U} + Q\,W - R\,V + g\sin\theta\,] \\
Y &= m\,[\,\dot{V} + R\,U - P\,W - g\cos\theta\sin\Phi\,] \\
Z &= m\,[\,\dot{W} + P\,V - Q\,U - g\cos\theta\cos\Phi\,] \\
L &= \dot{P}\,I_X + Q\,R\,(I_X - I_Y) - (P\,Q + \dot{R})\,I_{XZ} \\
&\quad + (P\,R - \dot{Q})\,I_{XY} - (Q^2 - R^2)\,I_{YZ} \\
M &= \dot{Q}\,I_Y + P\,R\,(I_X - I_Z) - (Q\,R + \dot{P})\,I_{XY} \\
&\quad + (P\,Q - \dot{R})\,I_{YZ} - (R^2 - P^2)\,I_{XZ} \\
N &= \dot{R}\,I_Z + P\,Q\,(I_Y - I_X) - (P\,R + \dot{Q})\,I_{YZ} \\
&\quad + (Q\,R - \dot{P})\,I_{XZ} - (P^2 - Q^2)\,I_{XY}
\end{aligned}
\qquad \text{(D-1)}
$$

$$
\begin{aligned}
\dot{\Phi} &= P + Q\tan\theta\sin\Phi + R\tan\theta\cos\Phi \\
\dot{\theta} &= Q\cos\Phi - R\sin\Phi \\
\dot{\Psi} &= R\left(\frac{\cos\Phi}{\cos\theta}\right) + Q\left(\frac{\sin\Phi}{\cos\theta}\right)
\end{aligned}
\qquad \text{(D-2)}
$$

$$
\begin{aligned}
X &= m\,[\,\dot{U} + Q\,W - R\,V + g\sin\theta\,] \\
Y &= m\,[\,\dot{V} + R\,U - P\,W - g\cos\theta\sin\Phi\,] \\
Z &= m\,[\,\dot{W} + P\,V - Q\,U - g\cos\theta\cos\Phi\,] \\
L &= \dot{P}\,I_X + Q\,R\,(I_X - I_Y) - (P\,Q + \dot{R})\,I_{XZ} \\
M &= \dot{Q}\,I_Y + P\,R\,(I_X - I_Z) - (R^2 - P^2)\,I_{XZ} \\
N &= \dot{R}\,I_Z + P\,Q\,(I_Y - I_X) + (Q\,R - \dot{P})\,I_{XZ}
\end{aligned}
\qquad \text{(D-3)}
$$

Linearized Equations of motion

Since equations D-2 and D-3 contain products of dependent variables, they need to be reduce to trackable form where the total motion can be represented by an average motion (trim condition symbolized by the subscript $_0$) representative of the operating condition, and a dynamic motion that account for small perturbations about the mean motion (symbolized by small letter). For a rectilinear flight, the average motion of the aircraft about it center of gravity will be zero as well as all acceleration terms. Assuming small perturbations about the trim condition, the linearized equations of motion can be written in the aircraft body axis system as

$$
\begin{aligned}
dX &= m\,(\,\dot{u} + W_0\, q - V_0\, r + g\,(\cos\theta_0)\,\theta\,) \\
dY &= m\,(\,\dot{v} + U_0\, r - W_0\, p - g\cos\theta_0 \cos\Phi_0\Phi \\
&\qquad + g\,(\sin\theta_0 \sin\Phi_0)\,\theta\,) \\
dZ &= m\,(\,\dot{w} + V_0\, p - U_0\, q + g\,(\cos\theta_0 \sin\Phi_0)\,\Phi \\
&\qquad + g\,(\sin\theta_0 \cos\Phi_0)\,\theta\,) \qquad \text{(D-4)} \\
dL &= \dot{p}\, I_X - \dot{r}\, I_{XZ} \\
dM &= \dot{q}\, I_Y \\
dN &= \dot{r}\, I_Z - \dot{p}\, I_{XZ}
\end{aligned}
$$

and the linearized kinematic equations as

$$\begin{aligned}
\dot{\Phi} &= p + q \tan\theta_0 \sin\Phi_0 + r \tan\theta_0 \cos\Phi_0 \\
\dot{\theta} &= q \cos\Phi_0 - r \sin\Phi_0 \\
\dot{\Psi} &= r \left(\frac{\cos\Phi_0}{\cos\theta_0} \right) + q \left(\frac{\sin\Phi_0}{\cos\theta_0} \right)
\end{aligned} \tag{D-5}$$

Assuming that the thrust vector is in line with the X body axis and balance all other trimmed forces, its contribution to the perturbed motion can be neglected [6:267]. Therefore, the dX, dY, dZ, dL, dM, dN are only perturbed aerodynamic forces that contribute to the dynamic of the aircraft. Using small angle approximation, it is possible to express v and w in term of β and α respectively. The resulting equation is shown below as

$$\begin{aligned}
\alpha &= \frac{w}{U_0} \quad \text{and} \quad \dot{\alpha} = \frac{\dot{w}}{U_0} \\
\beta &= \frac{v}{\sqrt{U_0^2 + W_0^2}} \quad \text{and} \quad \dot{\beta} = \frac{\dot{v}}{\sqrt{U_0^2 + W_0^2}}
\end{aligned} \tag{D-6}$$

Substituting equation D-6 into D-4 and rearranging such that the time derivative terms are on the left hand side of each equations will,lead to

$$\dot{u} = \left[\frac{dX}{m} - W_0 q + V_0 r - g(\cos\theta_0)\,\theta \right]$$

$$\dot{\beta} = \left(\frac{1}{(U_0^2 + W_0^2)} \right) \left[\frac{dY}{m} - U_0 r + W_0 p + g(\cos\theta_0 \cos\Phi_0)\,\Phi - g(\sin\theta_0 \sin\Phi_0)\,\theta \right]$$

$$\dot{\alpha} = \left(\frac{1}{U_0} \right) \left[\frac{dZ}{m} - V_0 p + U_0 q - g(\cos\theta_0 \sin\Phi_0)\,\Phi - g(\sin\theta_0 \cos\Phi_0)\,\theta \right]$$

$$\dot{p} = dL \left(\frac{I_Z}{I_X I_Z - I_{XZ}^2} \right) + dN \left(\frac{I_{XZ}}{I_X I_Z - I_{XZ}^2} \right) \qquad \text{(D-7)}$$

$$\dot{q} = \frac{dM}{I_Y}$$

$$\dot{r} = dL \left(\frac{I_{XZ}}{I_X I_Z - I_{XZ}^2} \right) + dN \left(\frac{I_X}{I_X I_Z - I_{XZ}^2} \right)$$

$$\dot{\Phi} = p + q(\tan\theta_0 \sin\Phi_0) + r(\tan\theta_0 \cos\Phi_0)$$

$$\dot{\theta} = q\cos\Phi_0 - r\sin\theta_0$$

$$\dot{\Psi} = q \left(\frac{\sin\Phi_0}{\cos\theta_0} \right) + r \left(\frac{\cos\Phi_0}{\cos\theta_0} \right)$$

The terms that need to be determined are the aerodynamic force and moment that are included in equation D-7.

Aerodynamic Forces and Moments

The representation of the aerodynamic forces and moments is usually made in the stability axis system

(subscript s). The aerodynamic forces and moments acting on the aircraft in the stability axis system are

$$
\begin{aligned}
X_S &= -Drag(D) = -\frac{1}{2}\,\rho\,V^2\,S\,C_D \\
Y_S &= Sideforce(Y) = -\frac{1}{2}\,\rho\,V^2\,S\,C_Y \\
Z_S &= -Lift(L) = -\frac{1}{2}\,\rho\,V^2\,S\,C_L \\
L_S &= RollingMoment = \frac{1}{2}\,\rho\,V^2\,S\,C_l \\
M_S &= PitchingMoment = \frac{1}{2}\,\rho\,V^2\,S\,C_m \\
N_S &= YawingMoment = \frac{1}{2}\,\rho\,V^2\,S\,C_n
\end{aligned}
\qquad \text{(D-8)}
$$

Since the equation of motions are written in the body axis system, the aerodynamic forces and moments need to be transformed into that axis system. The transformation matrix that puts the aerodynamic forces and moments into the body axis system is

$$
[\,B\,S\,] = \begin{bmatrix} \cos\alpha & 0 & \sin\alpha \\ 0 & 1 & 0 \\ -\sin\alpha & 0 & \cos\alpha \end{bmatrix} \qquad \text{(D-9)}
$$

Transforming the aerodynamic forces and moments in the body axis system will result in

$$
\begin{aligned}
X &= X_S \cos\alpha - Z_S \sin\alpha \\
&= \left(\frac{1}{2} \rho V^2 S \right) \left(- C_D \cos\alpha + C_L \sin\alpha \right) \\
Y &= Y_S \\
&= \frac{1}{2} \rho V^2 S C_Y \\
Z &= X_S \sin\alpha + Z_S \cos\alpha \\
&= \left(\frac{1}{2} \rho V^2 S \right) \left(- C_D \sin\alpha - C_L \cos\alpha \right) \\
L &= L_S \cos\alpha - N_S \sin\alpha \\
&= \left(\frac{1}{2} \rho V^2 S \right) \left(C_l \cos\alpha - C_n \sin\alpha \right) \\
M &= M_S \\
&= \frac{1}{2} \rho V^2 S C_m \\
N &= L_S \sin\alpha + N_S \cos\alpha \\
&= \left(\frac{1}{2} \rho V^2 S \right) \left(C_l \sin\alpha + C_n \cos\alpha \right)
\end{aligned}
\qquad \text{(D-10)}
$$

Equation D-10 can be expanded to determine its dependence with the perturbed motion. The expansion is done using a Tailor series expansion at a given trim condition.

The expansion is represented by

$$F = F_{\emptyset} + \left(\frac{\partial F}{\partial \Lambda_1}\right)|_{\emptyset}\lambda_1 + \left(\frac{\partial F}{\partial \Lambda_2}\right)|_{\emptyset}\lambda_2 + \ldots + \left(\frac{\partial F}{\partial \Lambda_n}\right)|_{\emptyset}\lambda_n$$
$$M = M_{\emptyset} + \left(\frac{\partial M}{\partial \Lambda_1}\right)|_{\emptyset}\lambda_1 + \left(\frac{\partial M}{\partial \Lambda_2}\right)|_{\emptyset}\lambda_2 + \ldots + \left(\frac{\partial M}{\partial \Lambda_n}\right)|_{\emptyset}\lambda_n \qquad \text{(D-11)}$$

where F represent the forces, M the moments, Λ the dependent variables, and λ the perturbation from the trim condition. The dependent variables in this case are

$$\Lambda = u, v, w, \dot{v}, \dot{w}, p, q, r, \delta \qquad \text{(D-12)}$$

where

$$u = V\cos\beta\cos\alpha$$
$$v = V\sin\beta \qquad \text{(D-13)}$$
$$w = V\cos\beta\sin\alpha$$

The higher order term have been eliminated from the expansion to keep the perturbed equations of motion linear. Taking only the derivative terms in equation D-11, it is possible to evaluate the dependence of each aerodynamic forces and moments in the body axis system with respect to the dependent variables. Since the aircraft can be trimmed at some angle α, β, and Φ, decoupling of the linearized equations of motion will not be possible.

Since the acceleration in the X body direction is in general negligible, the term was omitted. Using equation

D-11 to expand equation D-10 for each dependent variables, this will give the contribution of the forces and moments to the perturbed motion. Expanding the X contribution in the body axis system for the dependent variable u will give

$$\frac{\partial X}{\partial u} = X_U = -\frac{\partial D}{\partial u}\cos\alpha - D\frac{\partial \cos\alpha}{\partial u} + \frac{\partial L}{\partial u}\sin\alpha + L\frac{\partial \sin\alpha}{\partial u} \qquad \text{(D-14)}$$

where the derivative of each components of equation D-14 are

$$\frac{\partial \sin\alpha}{\partial u} = \frac{\partial \sin\alpha}{\partial \alpha}\frac{\partial \alpha}{\partial u} = -\cos\alpha\frac{\sin\alpha}{\sqrt{U_0^2 + W_0^2}}$$

$$\frac{\partial \cos\alpha}{\partial u} = \frac{\partial \cos\alpha}{\partial \alpha}\frac{\partial \alpha}{\partial u} = \frac{\sin^2\alpha}{\sqrt{U_0^2 + W_0^2}}$$

$$\frac{\partial D}{\partial u} = \rho S\left[\frac{1}{2}C_D\frac{\partial V^2}{\partial u} + \frac{1}{2}V^2\frac{\partial V}{\partial u}\frac{\partial C_D}{\partial V} + \frac{1}{2}V^2\frac{\partial C_D}{\partial \alpha}\frac{\partial \alpha}{\partial u} + \frac{1}{2}V^2\frac{\partial C_D}{\partial \beta}\frac{\partial \beta}{\partial u}\right]$$

$$= \frac{\bar{q}S}{V_0}\left\{2C_D\cos\beta_0\cos\alpha_0 + V_0\frac{\partial C_D}{\partial V}\cos\beta_0\cos\alpha_0 - V_0\frac{\partial C_D}{\partial \alpha}\frac{\sin\alpha_0}{\sqrt{U_0^2+W_0^2}} - V_0\frac{\partial C_D}{\partial \beta}\frac{\sin\beta_0\cos\beta_0\cos\alpha_0}{\sqrt{U_0^2+W_0^2}}\right\} \qquad \text{(D-15)}$$

$$\frac{\partial L}{\partial u} = \frac{\bar{q}S}{V_0}\left[2C_L\cos\beta_0\cos\alpha_0 + V_0\frac{\partial C_L}{\partial V}\cos\beta_0\cos\alpha_0 - V_0\frac{\partial C_L}{\partial \alpha}\frac{\sin\alpha_0}{\sqrt{U_0^2+W_0^2}} - V_0\frac{\partial C_L}{\partial \beta}\frac{\sin\beta_0\cos\beta_0\cos\alpha_0}{\sqrt{u_0^2+w_0^2}}\right]$$

and $\bar{q} = \frac{1}{2}\rho V_0^2$

Combining all the terms will result in

$$X_U = \frac{\bar{q} S}{V_0}\left[\left(\left(-2 C_D - C_{D_U}\right)\cos\beta_0 + V_0 \frac{\sin\beta_0 \cos\beta_0}{\sqrt{U_0^2+W_0^2}} C_{D_\beta}\right)\cos^2\alpha_0 - \left(\frac{V_0}{\sqrt{U_0^2 + W_0^2}}\left(\left(C_L - C_{D_\alpha}\right) + \sin\beta_0 \cos\beta_0 C_{L_\beta}\right) + \left(-2 C_L - C_{L_U}\right)\cos\beta_0\right)\sin\alpha_0 \cos\alpha_0 + \frac{V_0}{\sqrt{U_0^2 + W_0^2}}\left(-C_{L_\alpha} - C_D\right)\sin^2\alpha_0\right] \quad \text{(D-16)}$$

In equation D-16, the dimensional derivative, X_U is expressed in terms of the nondimensional stability derivatives. The definition of each nondimensional stability derivatives is well documented in McRuer [6:292-293].Also, the addition of the cross coupling stability derivative terms that can easily be related to the both longitudinal and lateral derivatives for definition. The only difference with McRuer development is the C_{iU} derivative which is define as

$$C_{i_U} = V_0 \frac{\partial C_i}{\partial V}$$

where i can represent lift, drag, side force, rolling moment, pitching moment, and yawing moment.

Similar derivation can be done for each forces with respect to each dependent variables to determine the

expression of each dimensional derivatives in terms of the nondimensional stability derivatives . This will result in the following equations

$$Y_U = \frac{\bar{q}\,S}{V_0}\left[\left(\left(-(-2\,C_Y - C_{Y_U}) - \frac{V_0 \sin\beta_0 \cos\beta_0}{\sqrt{U_0^2 + W_0^2}}\,C_{Y_\beta}\right)\cos\alpha_0 - \left(\frac{V_0}{\sqrt{U_0^2 + W_0^2}}\,C_{Y_\alpha}\right)\sin\alpha_0\right]\right. \tag{D-17}$$

$$Z_U = \frac{\bar{q}\,S}{V_0}\left[\left(\left((-2\,C_L - C_{L_U})\cos\beta_0 + V_0\,\frac{\sin\beta_0 \cos\beta_0}{\sqrt{U_0^2+W_0^2}}\,C_{L_\beta}\right)\cos^2\alpha_0 - \left(\frac{V_0}{\sqrt{U_0^2 + W_0^2}}\left((C_L - C_{D_\alpha}) - \sin\beta_0 \cos\beta_0\,C_{D_\beta}\right)\right.\right.\right.$$
$$\left.\left.\left. - (-2\,C_D - C_{D_U})\cos\beta_0\right)\sin\alpha_0 \cos\alpha_0 - \frac{V_0}{\sqrt{U_0^2 + W_0^2}}\,(C_L - C_{D_\alpha})\sin^2\alpha_0\right]\right. \tag{D-18}$$

$$X_V = \frac{\bar{q}\,S}{V_0}\left[\left(\left(-2\,C_D - C_{D_U}\right)\sin\beta_0 - \frac{V_0 \cos^2\beta_0}{\sqrt{U_0^2 + W_0^2}}\,C_{D_\beta}\right)\cos\alpha_0 - \left(\left(-2\,C_L - C_{L_U}\right)\sin\beta_0 - \frac{V_0 \cos^2\beta_0}{\sqrt{U_0^2 + W_0^2}}\,C_{L_\beta}\right)\sin\alpha_0\right] \tag{D-19}$$

$$Y_V = \frac{\bar{q}\,S}{V_0}\left[-\left(-2\,C_Y - C_{Y_U} \right)\sin\beta_0 + \frac{V_0\cos^2\beta_0}{\sqrt{U_0^2 + W_0^2}}\,C_{Y_\beta} \right] \tag{D-20}$$

$$Z_V = \frac{\bar{q}\,S}{V_0}\left[\left(-2\,C_D - C_{D_U} \right)\sin\beta_0 - \frac{V_0\cos^2\beta_0}{\sqrt{U_0^2 + W_0^2}}\,C_{D_\beta}\right)\sin\alpha_0 + \left(-2\,C_L - C_{L_U} \right)\sin\beta_0 - \frac{V_0\cos^2\beta_0}{\sqrt{U_0^2 + W_0^2}}\,C_{L_\beta}\right)\cos\alpha_0\Bigg] \tag{D-21}$$

$$X_W = \frac{\bar{q}\,S}{V_0}\left[\frac{V_0}{\sqrt{U_0^2 + W_0^2}}\left(C_L - C_{D_\alpha} \right)\cos^2\alpha_0 + \Big(\left(-2\,C_D - C_{D_U} \right)\cos\beta_0 - \frac{V_0}{\sqrt{U_0^2 + W_0^2}}\left(-C_{L_\alpha} - C_D \right) + \frac{V_0\sin\beta_0\cos\beta_0}{\sqrt{U_0^2 + W_0^2}}\,C_{D_\beta}\Big)\sin\alpha_0\cos\alpha_0 + \left(-\left(-2\,C_L - C_{L_U} \right)\cos\beta_0 - \frac{V_0\sin\beta_0\cos\beta_0}{\sqrt{U_0^2 + W_0^2}}\,C_{L_\beta}\right)\sin^2\alpha_0\Bigg] \tag{D-22}$$

$$Y_W = \frac{\bar{q}\,S}{V_0}\left[\left(-\left(-2\,C_Y - C_{Y_U} \right)\cos\beta_0 - \frac{V_0\sin\beta_0\cos\beta_0}{\sqrt{U_0^2 + W_0^2}}\,C_{Y_\beta}\right)\sin\alpha_0 + \left(\frac{V_0}{\sqrt{U_0^2 + W_0^2}}\,C_{Y_\alpha}\right)\cos\alpha_0\Bigg] \tag{D-23}$$

$$Z_W = \frac{\bar{q}\,S}{V_0}\left[\frac{V_0}{\sqrt{U_0^2 + W_0^2}}\left(-C_{L_\alpha} - C_D\right)\cos^2\alpha_0 + \left(\left(-2\,C_L - C_{L_q}\right)\cos\beta_0 + \frac{V_0}{\sqrt{U_0^2 + W_0^2}}\left(C_L - C_{D_\alpha}\right) + \frac{V_0 \sin\beta_0 \cos\beta_0}{\sqrt{U_0^2 + W_0^2}} C_{L_\beta}\right)\sin\alpha_0 \cos\alpha_0 + \left(\left(-2\,C_D - C_{D_q}\right)\cos\beta_0 + \frac{V_0 \sin\beta_0 \cos\beta_0}{\sqrt{U_0^2 + W_0^2}} C_{D_\beta}\right)\sin^2\alpha_0\right] \tag{D-24}$$

$$X_{\dot{V}} = \frac{\bar{q}\,S\,b}{2\,V_0}\left[\frac{\cos^2\beta_0}{\sqrt{U_0^2 + W_0^2}}\left(-C_{D_\beta}\cos\alpha_0 + C_{L_\beta}\sin\alpha_0\right)\right] \tag{D-25}$$

$$Y_{\dot{V}} = \frac{\bar{q}\,S\,b}{2\,V_0}\left[\frac{\cos^2\beta_0}{\sqrt{U_0^2 + W_0^2}} C_{Y_\beta}\right] \tag{D-26}$$

$$Z_{\dot{V}} = \frac{\bar{q}\,S\,b}{2\,V_0}\left[\frac{\cos^2\beta_0}{\sqrt{U_0^2 + W_0^2}}\left(-C_{D_\beta}\sin\alpha_0 - C_{L_\beta}\cos\alpha_0\right)\right] \tag{D-27}$$

$$X_{\dot{W}} = \frac{\bar{q}\,S}{2\,V_0}\left[\frac{c}{\sqrt{U_0^2 + W_0^2}}\left(-C_{D_\alpha}\cos^2\alpha_0 + C_{L_\alpha}\cos\alpha_0\sin\alpha_0\right) + \frac{\sin\beta_0\cos\beta_0\,b}{\sqrt{U_0^2 + W_0^2}}\left(C_{D_\beta}\sin\alpha_0\cos\alpha_0 - C_{L_\beta}\sin^2\alpha_0\right)\right] \tag{D-28}$$

$$Y_{\dot{W}} = \frac{\bar{q}\,S}{2\,V_0}\left[\frac{1}{\sqrt{U_0^2 + W_0^2}}\left(c\,C_{Y_\alpha}\cos\alpha_0 - b\sin\beta_0\cos\beta_0\,C_{Y_\beta}\sin\alpha_0\right)\right] \tag{D-29}$$

$$Z_{\dot{w}} = \frac{\bar{q}\,S}{2\,V_0}\left[\frac{c}{\sqrt{U_0^2 + W_0^2}}\left(-C_{L_{\dot{\alpha}}}\cos^2\alpha_0 - C_{D_{\dot{\alpha}}}\sin\alpha_0\cos\alpha_0\right)\right. \tag{D-30}$$
$$\left. + \frac{\sin\beta_0\cos\beta_0\, b}{\sqrt{U_0^2 + W_0^2}}\left(C_{L_{\dot{\beta}}}\sin\alpha_0\cos\alpha_0 - C_{D_{\dot{\beta}}}\sin^2\alpha_0\right)\right]$$

$$X_q = \frac{\bar{q}\,S\,c}{2\,V_0}\left[-C_{D_q}\cos\alpha_0 + C_{L_q}\sin\alpha_0\right] \tag{D-31}$$

$$Y_q = \frac{\bar{q}\,S\,c}{2\,V_0}\,C_{Y_q} \tag{D-32}$$

$$Z_q = \frac{\bar{q}\,S\,c}{2\,V_0}\left[-C_{D_q}\sin\alpha_0 - C_{L_q}\cos\alpha_0\right] \tag{D-33}$$

$$X_p = \frac{\bar{q}\,S\,b}{2\,V_0}\left[-C_{D_p}\cos\alpha_0 + C_{L_p}\sin\alpha_0\right] \tag{D-34}$$

$$Y_p = \frac{\bar{q}\,S\,b}{2\,V_0}\,C_{Y_p} \tag{D-35}$$

$$Z_p = \frac{\bar{q}\,S\,b}{2\,V_0}\left[-C_{D_p}\sin\alpha_0 - C_{L_p}\cos\alpha_0\right] \tag{D-36}$$

$$X_r = \frac{\bar{q}\,S\,b}{2\,V_0}\left[-C_{D_r}\cos\alpha_0 + C_{L_r}\sin\alpha_0\right] \tag{D-37}$$

$$Y_r = \frac{\bar{q}\ S\ b}{2\ V_0}\ C_{Y_r} \tag{D-38}$$

$$Z_r = \frac{\bar{q}\ S\ b}{2\ V_0}\left[\ -C_{D_r}\ \sin\alpha_0 - C_{L_r}\ \cos\alpha_0\ \right] \tag{D-39}$$

$$X_{\delta_i} = \bar{q}\ S\left(\ -\ C_{D_{\delta_i}}\ \cos\alpha_0 + C_{L_{\delta_i}}\ \sin\alpha_0\ \right) \tag{D-40}$$

$$Y_{\delta_i} = \bar{q}\ S\ C_{Y_{\delta_i}} \tag{D-41}$$

$$Z_{\delta_i} = \bar{q}\ S\left(\ -\ C_{D_{\delta_i}}\ \sin\alpha_0 - C_{L_{\delta_i}}\ \cos\alpha_0\ \right) \tag{D-42}$$

Expanding the moments contribution with respect to each dependent variables will lead to

$$L_U = \frac{\bar{q}\ S\ b}{2\ V_0}\left[\left(\left(\ 2\ C_1 + C_{l_U}\ \right)\cos\beta_0 - V_0\ \frac{\sin\beta_0\ \cos\beta_0}{\sqrt{U_0^2+W_0^2}}\ C_{l_\beta}\ \right)\cos^2\alpha_0\right.$$
$$+\left(\frac{V_0}{\sqrt{U_0^2+W_0^2}}\left(\left(\ C_n - C_{n_\alpha}\ \right) + \sin\beta_0\ \cos\beta_0\ C_{n_\beta}\ \right)\right.$$
$$\left.+\left(\ -2\ C_n - C_{n_U}\ \right)\cos\beta_0\right)\sin\alpha_0\ \cos\alpha_0$$
$$\left.-\frac{V_0}{\sqrt{U_0^2+W_0^2}}\left(\ -\ C_{n_\alpha} - C_1\ \right)\sin^2\alpha_0\right] \tag{D-43}$$

$$M_U = \frac{\bar{q}\, S\, c}{2\, V_0} \left[\left(\left(2\, C_m + C_{m_U} \right) - \frac{V_0 \sin\beta_0 \cos\beta_0}{\sqrt{U_0^2 + W_0^2}}\, C_{m_\beta} \right) \cos\alpha_0 - \left(\frac{V_0}{\sqrt{U_0^2 + W_0^2}}\, C_{m_q} \right) \sin\alpha_0 \right] \tag{D-44}$$

$$N_U = \frac{\bar{q}\, S\, b}{2\, V_0} \left[\left(\left(2\, C_n + C_{n_U} \right) \cos\beta_0 - V_0 \frac{\sin\beta_0 \cos\beta_0}{\sqrt{U_0^2 + W_0^2}}\, C_{n_\beta} \right) \cos^2\alpha_0 - \left(\frac{V_0}{\sqrt{U_0^2 + W_0^2}} \left(\left(-C_l - C_{n_q} \right) - \sin\beta_0 \cos\beta_0\, C_{l_\beta} \right) - \left(-2\, C_l - C_{l_U} \right) \cos\beta_0 \right) \sin\alpha_0 \cos\alpha_0 + \frac{V_0}{\sqrt{U_0^2 + W_0^2}} \left(C_n - C_{l_q} \right) \sin^2\alpha_0 \right] \tag{D-45}$$

$$L_V = \frac{\bar{q}\, S\, b}{2\, V_0} \left[\left(\left(2\, C_l + C_{l_U} \right) \sin\beta_0 - \frac{V_0 \cos^2\beta_0}{\sqrt{U_0^2 + W_0^2}}\, C_{l_\beta} \right) \cos\alpha_0 + \left(\left(-2\, C_n - C_{n_U} \right) \sin\beta_0 - \frac{V_0 \cos^2\beta_0}{\sqrt{U_0^2 + W_0^2}}\, C_{n_\beta} \right) \sin\alpha_0 \right] \tag{D-46}$$

$$M_V = \frac{\bar{q}\, S\, c}{2\, V_0} \left[\left(2\, C_m + C_{m_U} \right) \sin\beta_0 + \frac{V_0 \cos^2\beta_0}{\sqrt{U_0^2 + W_0^2}}\, C_{m_\beta} \right] \tag{D-47}$$

$$N_V = \frac{\bar{q}\, S\, b}{2\, V_0}\left[\left[\left(\, 2\, C_l + C_{l_U}\,\right)\sin\beta_0 - \frac{V_0\cos^2\beta_0}{\sqrt{U_0^2 + W_0^2}}\, C_{l_\beta}\right]\sin\alpha_0 - \left[\left(\, -2\, C_n - C_{n_U}\,\right)\sin\beta_0 - \frac{V_0\cos^2\beta_0}{\sqrt{U_0^2 + W_0^2}}\, C_{n_\beta}\right]\cos\alpha_0\right] \tag{D-48}$$

$$L_W = \frac{\bar{q}\, S\, b}{V_0}\left[\frac{-\,V_0}{\sqrt{U_0^2 + W_0^2}}\left(\, C_n - C_{l_\alpha}\,\right)\cos^2\alpha_0 - \left[\left(\, -2\, C_l - C_{l_U}\,\right)\cos\beta_0 - \frac{V_0}{\sqrt{U_0^2 + W_0^2}}\left(\, -\, C_{n_\alpha} - C_l\,\right) + \frac{V_0\sin\beta_0\cos\beta_0}{\sqrt{U_0^2 + W_0^2}}\, C_{l_\beta}\right]\sin\alpha_0\cos\alpha_0 + \left[\left(\, -2\, C_n - C_{n_U}\,\right)\cos\beta_0 + \frac{V_0\sin\beta_0\cos\beta_0}{\sqrt{U_0^2 + W_0^2}}\, C_{n_\beta}\right]\sin^2\alpha_0\right] \tag{D-49}$$

$$M_W = \frac{\bar{q}\, S\, c}{V_0}\left[\left[\left(\, 2\, C_m + C_{m_U}\,\right)\cos\beta_0 - \frac{V_0\sin\beta_0\cos\beta_0}{\sqrt{U_0^2 + W_0^2}}\, C_{m_\beta}\right]\sin\alpha_0 + \left[\frac{V_0}{\sqrt{U_0^2 + W_0^2}}\, C_{m_\alpha}\right]\cos\alpha_0\right] \tag{D-50}$$

$$L_V = \frac{\bar{q}\, S\, b^2}{2\, V_0}\left[\frac{\cos^2\beta_0}{\sqrt{U_0^2 + W_0^2}}\left(\, C_{l_\beta}\cos\alpha_0 - C_{n_\beta}\sin\alpha_0\,\right)\right] \tag{D-52}$$

$$M_V = \frac{\bar{q}\, S\, b\, c}{2\, V_0}\left[\frac{\cos^2\beta_0}{\sqrt{U_0^2 + W_0^2}}\, C_{m_\beta}\right] \tag{D-53}$$

$$N_W = \frac{\bar{q}\,S\,b}{V_0}\left[\frac{-V_0}{\sqrt{U_0^2 + W_0^2}}\left(-C_{n_{\dot{\alpha}}} - C_l\right)\cos^2\alpha_0 - \left(\left(-2\,C_n - C_{n_{\bar{U}}}\right)\cos\beta_0 + \frac{V_0}{\sqrt{U_0^2 + W_0^2}}\left(C_n - C_{l_{\dot{\alpha}}}\right) + \frac{V_0\,\sin\beta_0\,\cos\beta_0}{\sqrt{U_0^2 + W_0^2}}\,C_{n_\beta}\right)\sin\alpha_0\,\cos\alpha_0 - \left(\left(-2\,C_l - C_{l_{\bar{U}}}\right)\cos\beta_0 + \frac{V_0\,\sin\beta_0\,\cos\beta_0}{\sqrt{U_0^2 + W_0^2}}\,C_{l_\beta}\right)\sin^2\alpha_0\right] \tag{D-51}$$

$$N_{\dot{V}} = \frac{\bar{q}\,S\,b^2}{2\,V_0}\left[\frac{\cos^2\beta_0}{\sqrt{U_0^2 + W_0^2}}\left(C_{l_\beta}\,\sin\alpha_0 + C_{n_\beta}\,\cos\alpha_0\right)\right] \tag{D-54}$$

$$L_{\dot{W}} = \frac{\bar{q}\,S\,b}{2\,V_0}\left[\frac{c}{\sqrt{U_0^2 + W_0^2}}\left(C_{l_{\dot{\alpha}}}\cos^2\alpha_0 - C_{n_{\dot{\alpha}}}\,\cos\alpha_0\,\sin\alpha_0\right) + \frac{\sin\beta_0\,\cos\beta_0\,b}{\sqrt{U_0^2 + W_0^2}}\left(-C_{l_\beta}\,\sin\alpha_0\,\cos\alpha_0 + C_{n_\beta}\,\sin^2\alpha_0\right)\right] \tag{D-55}$$

$$M_{\dot{W}} = \frac{\bar{q}\,S\,c}{2\,V_0}\left[\frac{1}{\sqrt{U_0^2 + W_0^2}}\left(c\,C_{m_{\dot{\alpha}}}\,\cos\alpha_0 - b\,\sin\beta_0\,\cos\beta_0\,C_{m_\beta}\,\sin\alpha_0\right)\right] \tag{D-56}$$

$$N_{\dot{W}} = \frac{\bar{q}\,S\,b}{2\,V_0}\left[\frac{c}{\sqrt{U_0^2 + W_0^2}}\left(C_{n_{\dot{\alpha}}}\cos^2\alpha_0 + C_{l_{\dot{\alpha}}}\,\sin\alpha_0\,\cos\alpha_0\right) - \frac{\sin\beta_0\,\cos\beta_0\,b}{\sqrt{U_0^2 + W_0^2}}\left(C_{n_\beta}\,\sin\alpha_0\,\cos\alpha_0 - C_{l_\beta}\,\sin^2\alpha_0\right)\right] \tag{D-57}$$

$$L_q = \frac{\bar{q}\ S\ c\ b}{2\ V_0} \left[C_{l_q} \cos\alpha_0 - C_{n_q} \sin\alpha_0 \right]$$

(D-58)

$$M_q = \frac{\bar{q}\ S\ c^2}{2\ V_0} C_{m_q}$$

(D-59)

$$N_q = \frac{\bar{q}\ S\ c\ b}{2\ V_0} \left[C_{l_q} \sin\alpha_0 + C_{n_q} \cos\alpha_0 \right]$$

(D-60)

$$L_p = \frac{\bar{q}\ S\ b^2}{2\ V_0} \left[C_{l_p} \cos\alpha_0 - C_{n_p} \sin\alpha_0 \right]$$

(D-61)

$$M_p = \frac{\bar{q}\ S\ b\ c}{2\ V_0} C_{m_p}$$

(D-62)

$$N_p = \frac{\bar{q}\ S\ b^2}{2\ V_0} \left[C_{l_p} \sin\alpha_0 + C_{n_p} \cos\alpha_0 \right]$$

(D-63)

$$L_r = \frac{\bar{q}\ S\ b^2}{2\ V_0} \left[C_{l_r} \cos\alpha_0 - C_{n_r} \sin\alpha_0 \right]$$

(D-64)

$$M_r = \frac{\bar{q}\ S\ b\ c}{2\ V_0} C_{m_r}$$

(D-65)

$$N_r = \frac{\bar{q}\, S\, b^2}{2\, V_0} \left[C_{l_r} \sin\alpha_0 + C_{n_r} \cos\alpha_0 \right]$$

(D-66)

$$L_{\delta_i} = \bar{q}\, S\, b \left(C_{l_{\delta_i}} \cos\alpha_0 - C_{n_{\delta_i}} \sin\alpha_0 \right)$$

(D-67)

$$M_{\delta_i} = \bar{q}\, S\, C\, C_{m_{\delta_i}}$$

(D-68)

$$N_{\delta_i} = \bar{q}\, S\, b \left(C_{l_{\delta_i}} \sin\alpha_0 + C_{n_{\delta_i}} \cos\alpha_0 \right)$$

(D-69)

Using equations D-16 to D-69, it is possible to determine the contribution of the total perturbed force and moment which is

$$d\,X = X_U\, u + X_V\, v + X_W\, w + X_{\dot{V}}\, \dot{v} + X_{\dot{W}}\, \dot{w} + X_p\, p + X_q\, q + X_r\, r + X_{\delta_i}\, \delta_i$$

(D-70)

$$d\,Y = Y_U\, u + Y_V\, v + Y_W\, w + Y_{\dot{V}}\, \dot{v} + Y_{\dot{W}}\, \dot{w} + Y_p\, p + Y_q\, q + Y_r\, r + Y_{\delta_i}\, \delta_i$$

(D-71)

It is now possible to replace equations D-70 to D-75

$$d\,Z = Z_U\,u + Z_V\,v + Z_W\,w + Z_{\dot{V}}\,\dot{v} + Z_{\dot{W}}\,\dot{w} + Z_p\,p + Z_q\,q + Z_r\,r + Z_{\delta_i}\,\delta_i \tag{D-72}$$

$$d\,L = L_U\,u + L_V\,v + L_W\,w + L_{\dot{V}}\,\dot{v} + L_{\dot{W}}\,\dot{w} + L_p\,p + L_q\,q + L_r\,r + L_{\delta_i}\,\delta_i \tag{D-73}$$

$$d\,M = M_U\,u + M_V\,v + M_W\,w + M_{\dot{V}}\,\dot{v} + M_{\dot{W}}\,\dot{w} + M_p\,p + M_q\,q + M_r\,r + M_{\delta_i}\,\delta_i \tag{D-74}$$

$$d\,N = N_U\,u + N_V\,v + N_W\,w + N_{\dot{V}}\,\dot{v} + N_{\dot{W}}\,\dot{w} + N_p\,p + N_q\,q + N_r\,r + N_{\delta_i}\,\delta_i \tag{D-75}$$

into D-7 to get the total motion of the aircraft about a trim condition which can be represented by

$$\dot{\underline{x}} = A\,\underline{x} + B\,\underline{u} \tag{D-76}$$

where

$$\underline{x} = [\,u \;\; \alpha \;\; \beta \;\; p \;\; q \;\; r \;\; \Phi \;\; \theta \;\; \Psi\,]^T$$

$$\underline{u} = [\,\delta_1 \;\; \delta_2 \;\; \ldots \;\; \delta_n\,]^T \tag{D-77}$$

and δ_n represent specific control surfaces that can be controlled by the pilot.

Summary

In this Appendix, the linearized equations of motion for an aircraft were derived. They were used in the computer code of Appendix E to get the F-16 plant and control variables matrices to evaluate the dynamic stability of the aircraft.

APPENDIX E

State Space Derivation Fortran Code

This appendix describes the computer code used to convert the stability derivatives for an aircraft at a specific trim condition into a state space representation of the form

$$\dot{x} = A x + B u \qquad \text{(E-1)}$$

where A is the plant matrix, B is the control matrix, x is the state, and u the control. Aircraft-specific data need to be entered into the program as well as its stability derivatives. Cross-coupling dynamic stability can be entered into the code. Figure E-1 is a symplified flow chart representation of the code.

If more than one trim condition is input into the program, the output for the A matrices is a file where each matrix occupied a 10x9 space. Each 10x9 space is subdivided as follows:

a. the first line describe the aircraft attitude (β, α, Φ, θ, zeros)

b. the remaining 9x9 space represents the plant matrix

The output for the B matrix occupied a 10x2 space. The first line contains β and α, and the remaining 9x2 space is the control variables matrix B.

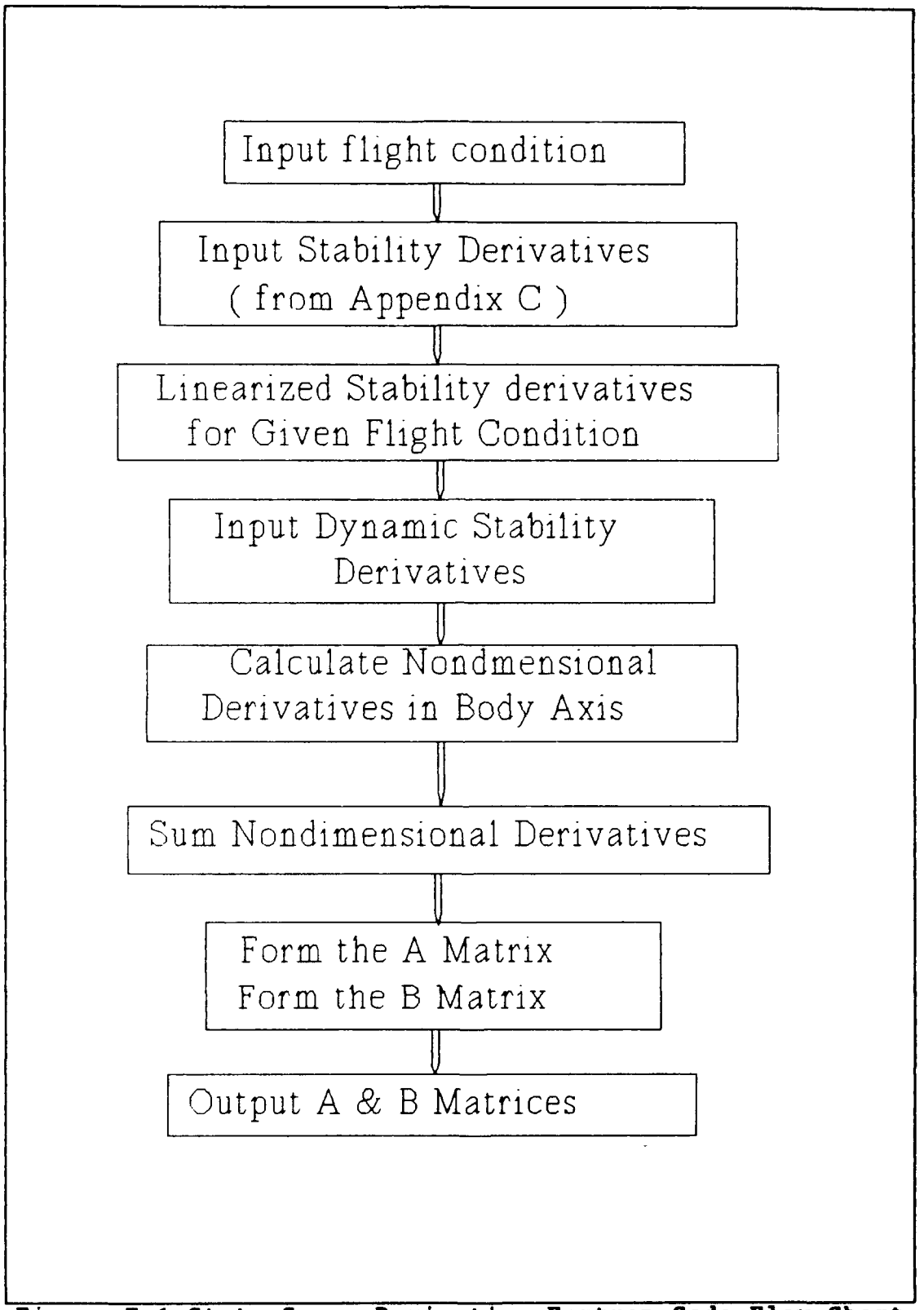

Figure E-1 State Space Derivation Fortran Code Flow Chart

APPENDIX F

CLOSED LOOP SYSTEM EXAMPLE

This Appendix contains an example of the derivation of the closed loop system eigenvalues for case B.

The aircraft states are:

$$x = [\, u \;\; \alpha \;\; \beta \;\; p \;\; q \;\; r \;\; \phi \;\; \theta \;\; \psi \;\; \delta_{Feff} \;\; \delta_{HT} \,]^T$$

$$u = \begin{bmatrix} \delta_{Feff} \\ \delta_{HT} \end{bmatrix}_{cmd} \qquad \text{(F-1)}$$

The open loop state space matrices are represented by

$$\dot{x} = A\,x + B\,u$$
$$y = C\,x + D\,u \qquad \text{(F-2)}$$

where A is the plant matrix, B the control input matrix, and C and D are the measurement matrices associated with each state or control. Matrices A and B were developed using the linearized equations of motion of Appendix D and the computer code developed of Appendix E. Matrices C and D were determined using equation 4-6 to 4-8c. The matrices are presented on the following page.

A =

Columns 1 through 6

```
-1.3100e-003   1.7500e+001   1.0900e+001  -8.6500e-004  -3.6200e+001  -9.2300e+000
-5.7800e-005  -8.1600e-001   2.9000e-001   1.3800e-002   9.9800e-001             0
-2.4000e-006  -1.4700e-003  -2.1300e-001   5.4500e-002             0  -9.9600e-001
-1.0000e-003   2.9500e+000  -3.7000e+001  -1.4400e+000             0   2.1800e-001
 1.9300e-003  -2.1600e+001   7.6500e+000  -1.7100e-003  -5.5100e-001             0
 3.3100e-004  -3.1500e-001   1.4800e+001  -1.4100e-003             0  -4.7300e-001
            0             0             0   1.0000e+000             0             0
            0             0             0             0   1.0000e+000   1.4500e-002
            0             0             0             0  -1.4500e-002             0
            0             0             0             0             0             0
            0             0             0             0             0             0
```

Columns 7 through 11

```
-4.3600e-005  -3.2100e+001             0  -1.9800e-001  -7.2900e+000
 6.9700e-004  -2.6200e-003             0  -3.5700e-003   8.8700e-004
 4.8000e-002   3.7900e-005             0  -2.0300e-003   3.9300e-004
            0             0             0   1.2100e+000  -4.1800e-002
-8.6400e-005   3.2500e-004             0  -2.8900e-001   4.7100e-002
            0             0             0   5.1700e-001  -4.4200e-002
            0             0             0             0             0
            0             0             0             0             0
            0             0             0             0             0
            0             0             0  -2.0000e+001             0
            0             0             0             0  -2.0000e+001
```

B =

```
     0     0
     0     0
     0     0
     0     0
     0     0
     0     0
     0     0
     0     0
     0     0
    20     0
     0    20
```

D =

```
     0     0
     0     0
     0     0
     0     0
```

C =

Columns 1 through 6

```
            0   1.0000e+000             0             0             0             0
            0             0             0   1.0000e+000             0             0
            0             0             0             0   1.0000e+000             0
 1.9748e-003   6.7476e+000  -2.4095e+000  -2.7288e-001  -1.9893e-001             0
```

Columns 7 through 11

```
            0             0             0             0             0
            0             0             0             0             0
            0             0             0             0             0
-1.3783e-002   5.1808e-002             0  -5.4622e-002   2.8838e-003
```

The state space system that represents the feedback paths (Figure 4-4) is written in the same form as equation F-2 with the matrices A_K, B_K, C_K, D_K. The original system had several states that could be removed. The results are:

A_k =

```
-7.3497e+000  4.7151e+000 -2.1075e+000 -2.9966e+000
 3.8161e+000 -3.6699e+000 -1.0872e+000  8.1433e-001
-7.6241e-016  7.0566e-001 -1.2343e+001 -5.1952e+000
 1.3395e-016 -1.1561e-016  2.6901e+000  1.1121e+000
```

B_k =

```
 3.0575e-002  4.6053e-002            0  6.0851e-003
-3.0824e-003 -3.1984e-002            0 -8.6013e-003
 7.0122e-002 -2.0804e-002            0  2.5616e-002
-9.4972e-003  5.0364e-003            0 -4.4444e-003
```

C_k =

```
-1.2270e-014  1.0676e-014 -1.9959e-014 -8.3393e+002
           0             0             0             0
```

D_k =

```
-3.1680e+000             0             0 -1.0589e+000
           0             0 -1.2000e-001             0
```

Assuming that no inputs are feed forward , both systems can be combined together using equations 4-15 and 4-16 , to form the closed loop model of the aircraft. The results are shown on the following pages using the representation of equation F-2 with the matrices A_{CL}, B_{CL}, C_{CL}, D_{CL} to represent the close loop system.

A_{CL} =

Columns 1 through 6

```
-1.3100e-003  1.7500e+001  1.0900e+001 -8.6500e-004 -3.6200e+001 -9.2300e+000
-5.7800e-005 -8.1600e-001  2.9000e-001  1.3800e-002  9.9800e-001             0
-2.4000e-006 -1.4700e-003 -2.1300e-001  5.4500e-002             0 -9.9600e-001
-1.0000e-003  2.9500e+000 -3.7000e+001 -1.4400e+000             0  2.1800e-001
 1.9300e-003 -2.1600e+001  7.6500e+000 -1.7100e-003 -5.5100e-001             0
 3.3100e-004 -3.1500e-001  1.4800e+001 -1.4100e-003             0 -4.7300e-001
           0             0             0  1.0000e+000             0             0
           0             0             0             0  1.0000e+000  1.4500e-002
           0             0             0             0 -1.4500e-002             0
 4.1824e-002  2.0627e+002 -5.1031e+001 -5.7794e+000 -4.2131e+000             0
           0             0             0             0  2.4000e+000             0
 1.2017e-005  7.1635e-002 -1.4662e-002  4.4392e-002 -1.2105e-003             0
-1.6986e-005 -6.1120e-002  2.0725e-002 -2.9636e-002  1.7110e-003             0
 5.0587e-005  2.4297e-001 -6.1722e-002 -2.7794e-002 -5.0958e-003             0
-8.7767e-006 -3.9486e-002  1.0709e-002  6.2492e-003  8.8411e-004             0
```

Columns 7 through 12

```
-4.3600e-005 -3.2100e+001             0 -1.9800e-001 -7.2900e+000             0
 6.9700e-004 -2.6200e-003             0 -3.5700e-003  8.8700e-004             0
 4.8000e-002  3.7900e-005             0 -2.0300e-003  3.9300e-004             0
           0             0             0  1.2100e+000 -4.1800e-002             0
-8.6400e-005  3.2500e-004             0 -2.8900e-001  4.7100e-002             0
           0             0             0  5.1700e-001 -4.4200e-002             0
           0             0             0             0             0             0
           0             0             0             0             0             0
           0             0             0             0             0             0
-2.9190e-001  1.0972e+000             0 -2.1157e+001  6.1076e-002  2.4539e-013
           0             0             0             0 -2.0000e+001             0
-8.3869e-005  3.1526e-004             0 -3.3238e-004  1.7548e-005 -7.3497e+000
 1.1855e-004 -4.4562e-004             0  4.6982e-004 -2.4804e-005  3.8161e+000
-3.5306e-004  1.3271e-003             0 -1.3992e-003  7.3872e-005 -7.6241e-016
 6.1255e-005 -2.3026e-004             0  2.4276e-004 -1.2817e-005  1.3395e-016
```

Columns 13 through 15

```
           0             0             0
           0             0             0
           0             0             0
           0             0             0
           0             0             0
           0             0             0
           0             0             0
           0             0             0
           0             0             0
-2.1352e-013  3.9918e-013  1.6679e+004
           0             0             0
 4.7151e+000 -2.1075e+000 -2.9966e+000
-3.6699e+000 -1.0872e+000  8.1433e-001
 7.0566e-001 -1.2343e+001 -5.1952e+000
-1.1561e-016  2.6901e+000  1.1121e+000
```

B_{CL} =

```
     0     0
     0     0
     0     0
     0     0
     0     0
     0     0
     0     0
     0     0
     0     0
    20     0
     0    20
     0     0
     0     0
     0     0
     0     0
```

C_{CL} =

Columns 1 through 6

```
         0  1.0000e+000            0            0            0            0
         0            0            0  1.0000e+000            0            0
         0            0            0            0  1.0000e+000            0
 1.9748e-003  6.7476e+000 -2.4095e+000 -2.7288e-001 -1.9893e-001            0
```

Columns 7 through 12

```
         0            0            0            0            0            0
         0            0            0            0            0            0
         0            0            0            0            0            0
-1.3783e-002  5.1808e-002            0 -5.4622e-002  2.8838e-003            0
```

Columns 13 through 15

```
         0            0            0
         0            0            0
         0            0            0
         0            0            0
```

D_{CL} =

```
     0     0
     0     0
     0     0
     0     0
```

The eigenvalues, or poles, of the open loop plant are:

```
                0
-6.6025e-001+ 4.7020e+000i
-6.6025e-001- 4.7020e+000i
-3.7151e-001+ 4.0162e+000i
-3.7151e-001- 4.0162e+000i
-1.3977e+000
-2.2807e-003+ 6.4055e-002i
-2.2807e-003- 6.4055e-002i
-2.8505e-002
-2.0000e+001
-2.0000e+001
```

The eigenvalues of the closed loop system are given by

```
                0
-2.0781e+001
-2.0001e+001
-1.1034e+001+ 5.9130e-001i
-1.1034e+001- 5.9130e-001i
-8.5100e-001+ 4.6972e+000i
-8.5100e-001- 4.6972e+000i
-1.4483e-001+ 4.1989e+000i
-1.4483e-001- 4.1989e+000i
-9.5788e-001+ 8.1864e-001i
-9.5788e-001- 8.1864e-001i
-4.2502e-003+ 5.9495e-002i
-4.2502e-003- 5.9495e-002i
 8.5586e-003
-1.4456e-001
```

And the transmission zeros of the close loop system are

```
-1.1250e+001- 5.1020e-016i
-1.0000e+001+ 1.0214e-016i
-1.0000e+000
-7.5158e-008
 9.1738e-017
```

BIBLIOGRAPHY

1. Rubertus, Duane P. " Self-Repairing Flight Control System Overview," IEEE NAECON, 1280-1286 (1983).

2. Eslinger, Robert A. Multivariable Control Law Design for the AFTI/F-16 With a Failed Control Surface. MS Thesis, AFIT/GE/ENG/84D-28. School of Engineering, Air Force Institute of Technology (AU), Wright-Patterson AFB, OH, December 1974.

3. Weiss, J., Eterno, J., Grunberg, D., Looze, D. "Investigation of an Automatic Trim Algorithm for Restructurable Aircraft Control," IEEE NAECON, 400-406 (1986).

4. Turhal, First Lieutenant Y. Ertugrul. Turkish Air Force. Investigation of F-16 Control Failures and Optimal Setting of Functional Controls. MS Thesis, AFIT/GAE/ENG/86D-19. School of Engineering, Air Force Institute of Technology (AU), Wright-Patterson AFB, OH, December 1986.

5. Zaiser, Stephen M. Stability Characteristics of a Combat Aircraft with Control Surface Failure. MS Thesis, AFIT/GAE/ENY/89D-42. School of Engineering, Air Force Institute of Technology (AU), Wright-Patterson AFB, OH, December 1989.

6. McRuer, Duane, Ashkenas, Irving, and Graham, Dunstan. Aircraft Dynamics and Automatic Control. Princeton, New Jersey: Princeton University Press, 1973.

7. Etkin, Bernard. Dynamic of Atmospheric Flight. New York: John Wiley and Sons Inc., 1972.

8. F-16 Software Mechanization Document. General Dynamics Document # 16ZC037A. General Dynamics, Fort Worth Division, Forth Worth, TX, 1988.

9. Press, William H. et. al. Numerical Recipes. Cambridge University Press, New York, 1986.

10. Moler, Cleve, Little, John, and Bangert, Steve. Pro-Matlab for VAX/VMS Computer. The Math Works, Inc., South Natick, MA, August 1988.

11. Ridgely, D. Brett and Banda, S. Siva. Introduction to Robust Multivariable Control. Report # AFWAL-TR-85-3102. Flight Dynamic Laboratory, Wright-Patterson AFB, OH, February 1986.

12. Orlik-Rukemann, K.J. Techniques for Dynamic Stability Testing in Wind Tunnels. AGARD CP-235, 1978.

13. Bice, Gregory W. Development of an Automatic Ground Collision Avoidance System Using Digital Terrain Database. MS Thesis, AFIT/GAE/ENY/89D-03. School of Engineering, Air Force Institute of Technology, Wright-Patterson AFB, OH, December 1889.

VITA

Captain Marc Roy [redacted]. In 1977 he joined the Canadian Forces and in 1978 he was accepted to the Royal Military College (RMC) in Kingston, Ontario, Canada, where he major in mechanical engineering. In May 1982 he graduated from RMC and received a Bachelors of Science degree. His first assignment was at the Defence Research Establishment in Valcartier where he worked on armament related projects. In 1986 he was transferred to the National Defence Headquarter in Ottawa. He worked a year as a Life Cycle Maintenance Manager on conventional Air-to-Ground weapons. His last two years in Ottawa, He worked on International Cooperative Development Projects related to the Family of Weapon Memorandum of Understanding and the Modular Standoff Weapon project. In May 1989, he reported to the Air Force Institute of Technology at Wright-Patterson AFB where he began a Master degree in Engineering .

[redacted]

REPORT DOCUMENTATION PAGE

Form Approved
OMB No. 0704-0188

1. AGENCY USE ONLY (Leave blank)	2. REPORT DATE	3. REPORT TYPE AND DATES COVERED
	December 1990	Master Thesis

4. TITLE AND SUBTITLE

DYNAMIC ANALYSIS OF A COMBAT AIRCRAFT WITH CONTROL SURFACE FAILURE

5. FUNDING NUMBERS

6. AUTHOR(S)

Marc Roy, Captain, Canadian Forces

7. PERFORMING ORGANIZATION NAME(S) AND ADDRESS(ES)

Air Force Institute of Technology,
WPAFB, OH, 45433-6583

8. PERFORMING ORGANIZATION REPORT NUMBER

AFIT/GAE/ENY/90D-24

9. SPONSORING/MONITORING AGENCY NAME(S) AND ADDRESS(ES)

10. SPONSORING/MONITORING AGENCY REPORT NUMBER

11. SUPPLEMENTARY NOTES

12a. DISTRIBUTION/AVAILABILITY STATEMENT

Approved for Public Release: Distribution unlimited

12b. DISTRIBUTION CODE

13. ABSTRACT (Maximum 200 words)

In this thesis, an investigation was performed to analyze the dynamic stability characteristic of an aircraft which has sustained damage to a primary control surface. The analysis was performed using the existing functional form of actual wind tunnel data taken on a F-16 model. Two control schemes are used for trimming an F-16 that has sustained damaged to its rudder.

The investigation was conducted for one flight condition representative of the aircraft at cruise speed. Region in α/β space where trim can be achieved was selected as input into a linearized aircraft model. This model took into account the failed control surface. The eigenvalues of the open and closed loop models were analyzed to determine the region in α/β space where the aircraft was dynamically stable. The migration of the eigenvalues for several trim conditions was also investigated to gain some insight on the aircraft behavior while in an unsymmetrical orientation.

14. SUBJECT TERMS	15. NUMBER OF PAGES
Aircraft, Aircraft Dynamic, Control, Failure, Control Surface Failure, Stability and Control	132
	16. PRICE CODE

17. SECURITY CLASSIFICATION OF REPORT	18. SECURITY CLASSIFICATION OF THIS PAGE	19. SECURITY CLASSIFICATION OF ABSTRACT	20. LIMITATION OF ABSTRACT